SAPIENZA
UNIVERSITÀ DI ROMA

PhD course in
Biochemistry

ULB UNIVERSITÉ LIBRE DE BRUXELLES

PhD course in
Sciences agronomiques et ingénierie biologique

Impact of β-hexachlorocyclohexane on human cellular biochemistry and environmental remediation strategies.

PhD candidate:

Elisabetta Rubini
XXXIII cycle

PhD tutors:

Prof. Fabio Altieri

Prof. David Cannella

Supervisor:

Prof. Margherita Eufemi

Triennium 2017-2020

PhD coordinator: Prof. Stefano Gianni

Index

1. Organochlorine pesticides (OCPs)

1.1. Introduction.

Environmental pollution represents one of the most pressing problems in industrialized countries and in recent years has raised concerns and doubts also from the scientific perspective. A growing number of epidemiological observational studies, carried out on population at risk, correlated the exposure to environmental chemicals with the incidence of several pathological conditions, ranging from metabolic to cardiological and reproductive diseases, until the development of cancers[1]. These evidences have made more urgent the need for further investigations on the biological mechanism at the basis of pollutants' toxicity.

In particular, the review statistics show that 40% of all pesticides are organochlorines (OCPs)[2], constituting a substantial source of contamination all over the world. The evaluation of the impact of these chemicals on human health draw a lot of attention in the scientific community. OCPs belong to a large class of organic compounds catalogued by the Stockholm Convention as "POPs" (Persistent Organic Pollutants). The list of banned chemicals includes dioxins and their derivatives, hexachlorocyclohexane, polychlorinated biphenyls, and aldrin, whereas many other similar substances are subjected to restrictions[3].

OCPs have a related chemical structure, showing chlorine-substituted aliphatic or aromatic rings; their hazardousness is mostly due to shared physicochemical properties such as lipophilia and energetic stability, responsible for the high environmental persistence and bioaccumulation potential of these molecules. Table 1 summarizes the principal compounds representative of OCPs and their features, comprising the biochemical effects on human health[4].

Chemical Name	Structure	Use	Environmental persistence	Biochemical effects on human health	Physical properties
Dieldrin $C_{12}H_8Cl_6O$		Insecticide	Half life: 9 months	Neurotoxic, reproductive, developmental, immunological, genotoxic, tumorigenic effects, nausea, vomiting, muscle twitching and aplastic anaemia (USEPA 2003)	Melting point: 177°C Boiling point: 330°C H_2O solubility: 0.195 mg/mL at 25°C
DDT $C_{14}H_9Cl_5$		Acaricide Insecticide	Half life: 2-15 years	Prickling sensation of the mouth, nausea, dizziness, confusion, headache, lethargy, incoordination, vomiting, fatigue, tremors in the extremities, anorexia, anaemia, muscular weakness, hyperexcitability, anxiety, and nervous tension (Klaassen, 1996)	Melting point: 109°C Boiling point: 260°C H_2O solubility: 25 µg/L at 25°C
Dicofol $C_{14}H_9Cl_5O$		Acaricide	Half life: 60 days	Nausea, dizziness, weakness and vomiting from ingestion or respiratory exposure, skin irritation or rash from dermal exposure, hyperactivity, headache, nausea, vomiting, unusual sensations and fatigue (Rohm and Haas Company).	Melting point: 79°C Boiling point: 193°C H_2O solubility: 0.8 mg/L at 25°C
Endosulfan $C_9H_6Cl_6O_3S$		Insecticide	Half life: 150 days	Decreases the white blood cell count and macrophage migration, adverse effects on humoral and cell-mediated immune system. Affects semen quality, sperm count, spermatogonial cells, sperm morphology and other defects in male sex hormones DNA damage and mutation (Singh *et al.*, 2007; Susan & Sania, 1999)	Melting point: 209°C Boiling point: decomposes H_2O solubility: 0.33 mg/mL at 25°C
Lindane $C_6H_6Cl_6$		Acaricide Insecticide Rodenticide	Half life: 15 months	Damage human liver, kidney, neural and immune systems, and induces birth defects cancer, cause neurotoxicity, reproductive toxicity and hepatotoxicity (Bano & Bhatt, 2010; Vijaya Padma *et al.*, 2011)	Melting point: 112°C Boiling point: 323°C H_2O solubility: 7.3 mg/L at 25°C
Polychlorinated Biphenyls (PCB)	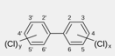	Insecticide Plasticizer	Half life: months to years	Neurological disorders and short term memory, mutagenic effects by interfering with hormones in the body, sexual, skeletal, and mental development issues (Winneke, G, 2011)	Melting point: 25-306°C Boiling point: 285-456°C H_2O solubility: 0.0012-4830 µg/L at 25°C

Table 1. Major organochlorine pesticides, their chemical structures, common uses, environmental persistence, biochemical effects and physical properties. Adapted from *Jayaraj R. et al, 2016.*

1.2. OCPs toxicology

The overuse or misuse of pesticides is adversely affecting both environmental and human health: in fact, only a small percentage of these compounds (0.3%) goes into the target, while the rest goes somewhere else[5]. Many pesticides have been identified as endocrine-disrupting chemicals (ECDs)[6]. A recent report commissioned by the European Parliament's Committee on Petitions (PETI), and also taken up by *The Lancet Oncology*[7], entitled "*Endocrine Disruptors: from Scientific Evidence to Human Health Protection*"[8] noted that EDCs have been linked to several cancers, including breast, prostate, vaginal, and thyroid cancers[9-10- 11].

1.2.1. Endocrine Disruption.

Due to their physical characteristics and chemical structure, EDCs can mimic or block the transcriptional activation elicited by naturally circulating hormones, thus inducing an imbalance in intracellular homeostasis.

Steroid hormones are a large class of lipophilic molecules that act on a variety of target sites and closely regulate many physiological functions. In particular, sexual and reproductive development is closely regulated by androgens, oestrogens, and progestins[12]. Upon secretion, hormones blood levels increase by several orders of magnitude and then rapidly return to the basal concentration when the stimulus stops. Hormones have a short half-life in human body and after having served their biological purposes are inactivated by enzymatic systems. Increasing or decreasing steroid metabolism could contribute to the negative effects of EDC[13]. Steroid Hormone Receptors (SHR) function as hormone dependent nuclear transcription factors. Upon entering the cell by passive diffusion, the hormone (H) binds the receptor, which is subsequently released from heat shock proteins, and translocates to the nucleus. There, the receptor undergoes dimerization, binds specific DNA sequences, called Hormone Responsive Elements or HREs, and recruits a number of coregulators that facilitate gene transcription[14].

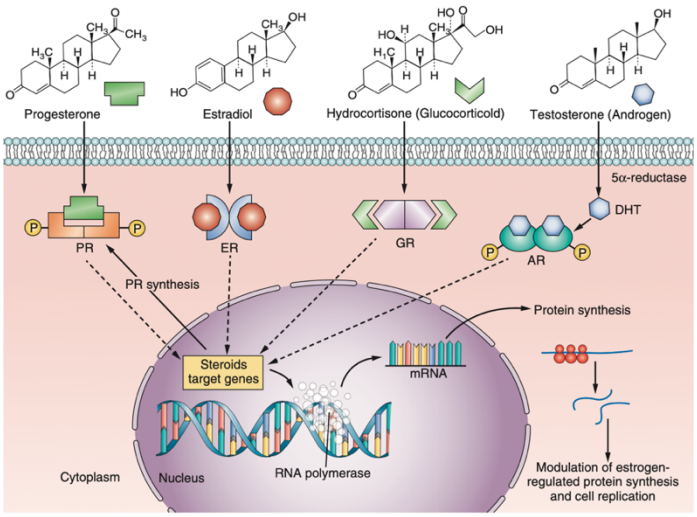

Figure 1. Schematic diagram of signal transduction pathways for clones of steroid hormones and their effects on protein-regulated synthesis and cellular replication.

Figure 2 outlines the key characteristics of ECDs, according to *La Merril et al.*[15]; these parameters represent the functional properties of agents that alter hormones action and comprise the major mechanisms by which the endocrine system can be disrupted.

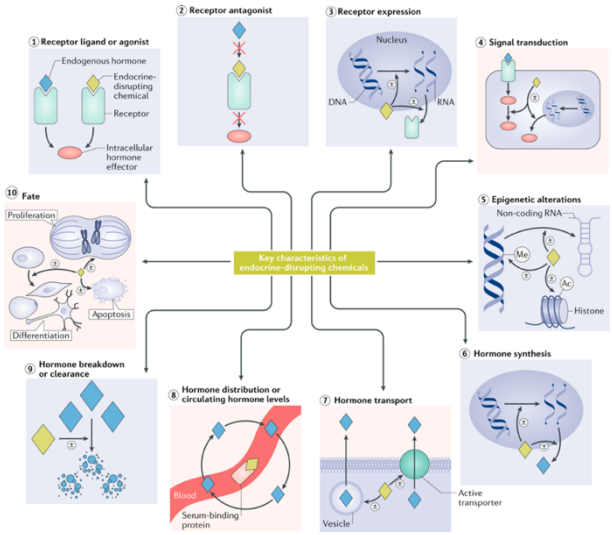

Figure 2. Key characteristics of endocrine-disrupting chemicals.

1.2.2. Activation of AhR pathway.

Exogenous substances that come into contact with the human body are referred to as xenobiotics, which bring together a wide range of non-physiological and structural divergent chemicals including organochlorine pollutants. Without a metabolic transformation, xenobiotics would reach a toxic concentration; for this reason, the organism has developed different detoxification mechanisms resulting in the induction of metabolizing enzymes. Organochlorine pollutants may bind and modulate several endocrine receptors, one for all the Aryl Hydrocarbon Receptor (AhR)[16]. AhR is considered the xenobiotic sensor *par excellence* but is also a converging point for many physiological intracellular processes[17]. From a biochemical point of view, AhR is a cell nuclear receptor that acts as ligand-activated transcription factor involved in the recognition and metabolism of xenobiotics, leading to the activation of cytochrome P450 enzymes needed for their clearance from the body[18]. In its inactive state, AhR is complexed with the 90 kDa heat shock protein AhR-interacting protein (AIP), p23 and SRC. This chaperone complex keeps AhR in the cytosol, preventing its proteasomal degradation and keeping it in a high-affinity state for its ligands. Upon agonist binding, AhR and some components of the chaperone complex translocate to the nucleus, where AhR binds DNA-responsive elements to control gene expression. After exerting its function, AhR is addressed to the ubiquitin-proteasome system and is degraded [19](figure 3).

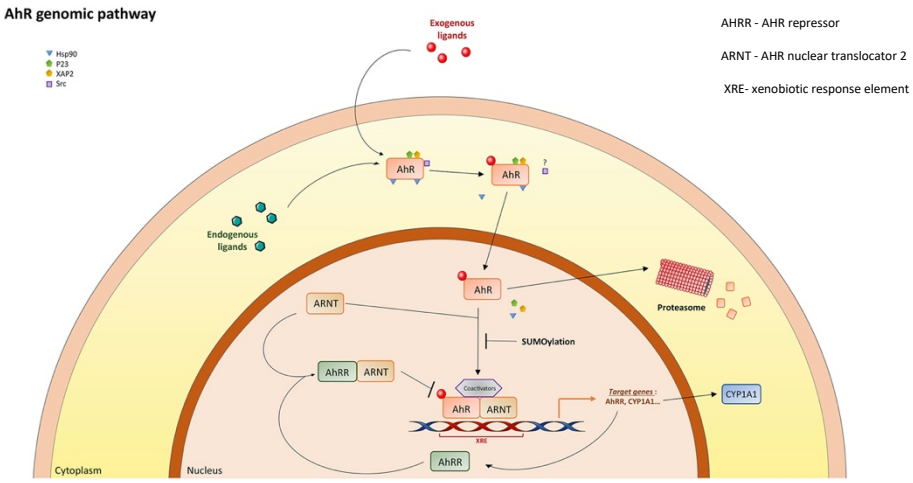

Figure 3. AhR activation pathway.

1.2.3. Oxidative stress and mitochondrial dysfunction.

There are other reported mechanisms linking pesticides exposure to chronic diseases, such as mitochondrial dysfunction and oxidative stress induction.

A particular subgroup of ECDs, referred as metabolism-disrupting chemical (MDC), can specifically affect energy homeostasis. Mitochondria are best known as the powerhouse of the cell for their crucial role in the oxidative phosphorylation and energy conversion, but these organelles are also involved in other intracellular events such as hormones secretion, generation of reactive oxygen species and cell death. Numerous studies have reported that MDC-induced mitochondrial dysfunction is characterized by perturbations in mitochondrial bioenergetics, biogenesis and dynamics, activation of the mitochondrial pathway of apoptosis and excessive ROS production. ROS are physiologically formed in cells as a consequence of both oxidative biochemical reactions and external factors, but, when overproduced, they can become harmful. There is substantial evidence that environmental pollution induces oxidative stress via increased intracellular steady-state levels of ROS such as

$O_2^{\bullet -}$ and H_2O_2 and, under these conditions, the endogenous antioxidants may be unable to encounter ROS formation. This situation may cause cellular damage by peroxidation of membrane lipids, inactivation of enzymes, cross-linking and breakdown of DNA [20-21].

1.3. OCPs activation pathways.

Several signalling pathways underlie the toxic effects of organochlorine pesticides, involving the regulation of cell growth, survival, proliferation, migration, invasion, apoptosis, and anticancer drug resistance[22]. For some of the most popular OCPs (i.e. TCDD, lindane, PCBs, bisphenol A, dieldrin) the *Comparative Toxicogenomic Database* (http://ctdbase.org), which provides information about the exposure effects of a wide range of chemicals integrated with functional and pathway data, reveals common intracellular transduction cascades mediated by several different proteins, included STAT3.

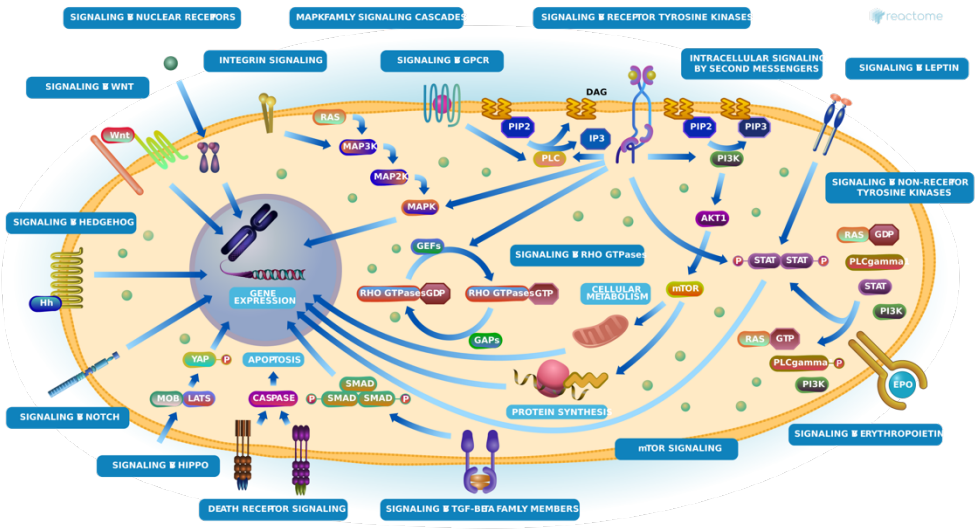

Figure 4. The intracellular signalling network involved in organochlorines-induced responses.

2. Signal Transducer and Activator of Transcription 3 (STAT3)

2.1. The STAT protein family.

The STAT (Signal Transducer and Activator of Transcriptions) protein family is a group of ubiquitously expressed intracellular transcription factors involved in the regulation of a variety of critical functions such as cell differentiation, proliferation, apoptosis, angiogenesis, metastasis, and immune responses[23]. Seven STAT members have been identified - STAT1, STAT2, STAT3, STAT4, STAT5A, STAT5B, and STAT6 - and multiple isoforms have also been found. STATs can be generally activated by a series of extracellular signalling molecules (i.e. cytokines, growth factors, hormones) and they can modulate the transcription of responsive genes, leading to downstream phenotypic effects. Despite their functional differences, all seven STAT proteins share common structural elements (figure 5).

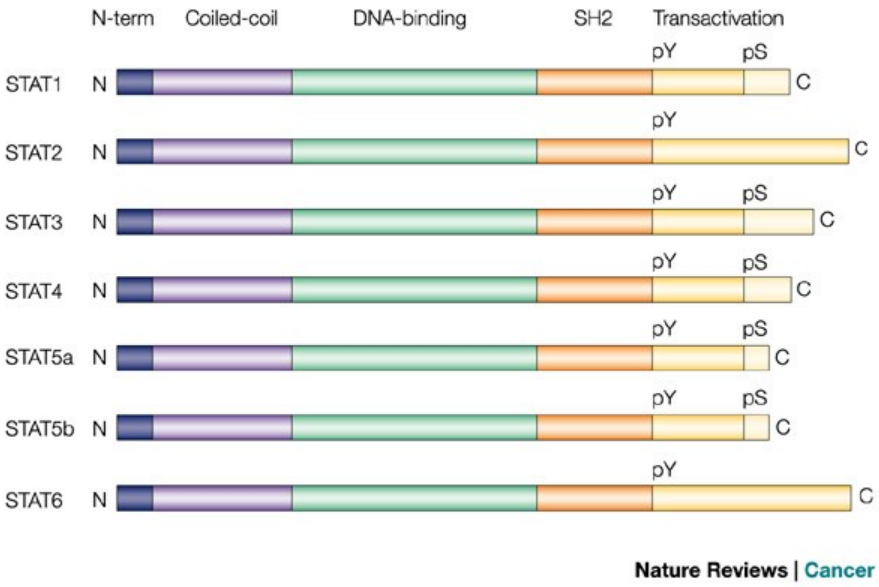

Figure 5. STAT family domains architecture

Stat2 and Stat6 proteins consist of approximately 850 amino acid residues, whereas the other five members are 750-800 amino acids in length.

Each STAT protein includes several conserved domains that contribute to protein biological behavior:

- The *N-terminal* protein-protein interaction domain (PPID) mediates interaction between neighboring STAT proteins (or other coregulatory proteins) and contributes to cooperative binding of STAT dimers on DNA, leading to the formation of stabilized tetramers;
- The *DNA binding domain* is involved in DNA binding, recruitment of coactivators, and the transcription of STAT target genes;
- The *Src-homology 2 (SH2) domain* is necessary for STATs dimerization and their recruitment to phosphorylated receptors. In fact, differences in STAT SH2 domains determine the selectivity for the target receptors;
- A critical tyrosine residue is located near the SH2 domain and is required for SH-phosphotyrosine interaction between monomeric STATs to form dimers;
- The *C-terminal* transcriptional activation domain (TAD) is involved in the communication with transcriptional complexes. In addition, the carboxy-terminal domain contains a site of serine phosphorylation (pS) that enhances transcriptional activity in some STATs [24-25-26].

As STATs regulate fundamental biological processes in normal cells, their alteration has a deep biological impact on intracellular homeostasis. In particular, STAT3 has been frequently reported constitutively overexpressed and/or hyperactivated in a variety of tumor types[27], suggesting its essential contribution to the malignancies.

2.1.1. STAT3 activation.

Like other STATs proteins, STAT3 is a latent cytoplasmic transcription factor that translocate into the nucleus upon cytokines or growth factors stimulation. Following the interaction between a ligand and its receptor, STAT3 is activated through the phosphorylation at the critical tyrosine residue 705 that triggers STAT3 dimerization via the reciprocal phosphotyrosine-SH2 interactions. Then, dimeric STAT3 translocates into the nucleus where regulates the transcription of responsive target genes[28].

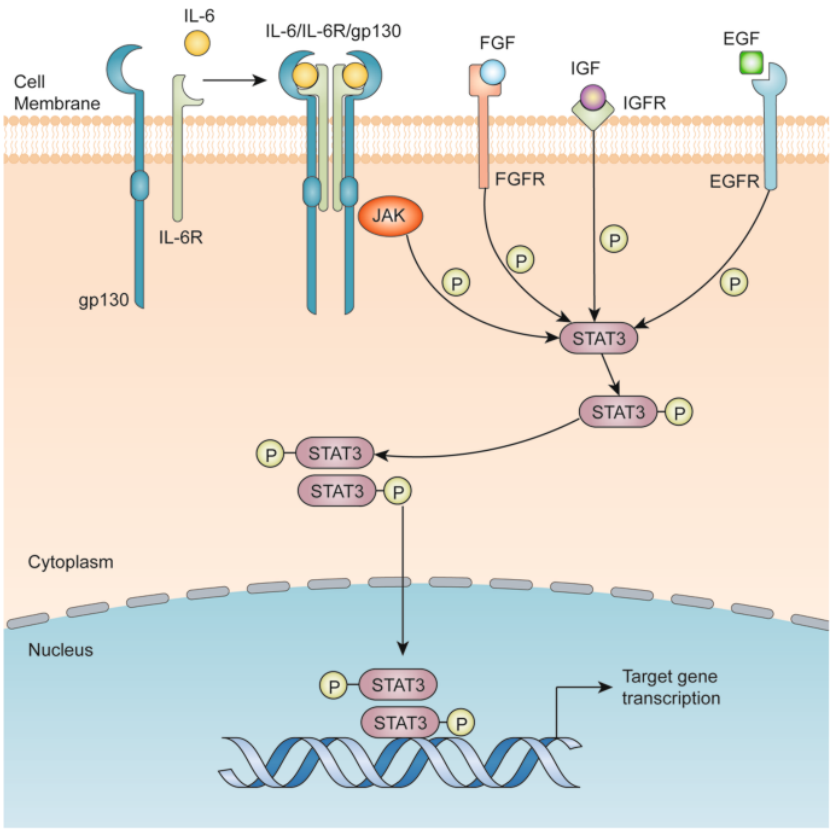

Figure 6. General schematic representation of STAT3 canonical activation.

Activation of STAT3 through the phosphorylation at Y705 residue is referred to as STAT3 canonical pathway and can be mediated by multiple upstream inputs. There are receptors present on plasma membrane, like gp130 receptor, that lacks intrinsic tyrosine kinase activity and recruits cytoplasmic kinases like JAK family including JAK1, JAK2, JAK3 and TYK2. On the other hand, there are receptors like EGFR, PDGFR, Her2, FGFR, VEGFR, IGFR and HGFR with intrinsic tyrosine kinase activity that itself phosphorylates Y705 residue and induces STAT3 activation. Apart from receptors present on plasma membrane there are cytoplasmic kinases also that can activate STAT3 signaling like Bcr-Abl fusion protein, Src kinase family and Bone Marrow X-linked (BMX) kinase. Multiple ligands like cytokines (IL6, LIF, OSM, L-10, and IL-11) and growth factors (EGF, PDGF and CSF-1) are known to stimulate STAT3 signaling[29].

2.1.2. STAT3 non-canonical activation.

Besides its well-described canonical signaling, STAT3 can be subjected to the phosphorylation at the serine residue 727, located in the carboxy-terminal transcriptional activation domain, responsible for STAT3 functions independent of the canonical phosphorylation at Y705. In particular, pS^{727}STAT3 seems to be essential for important mitochondrial activities and is required for the optimal transcriptional induction of a subset of target genes [30]. Specifically, mitochondrial STAT3 was shown to preserve optimal ETC activity, increase membrane polarization and ATP production, and enhance the activity of lactate dehydrogenase, probably by interacting with ETC complexes I and II [31]. The Ser^{727} phosphorylation is a more-complex regulated

modification because different activation signals lead to serine phosphorylation by different kinases, including ERK1, ERK2, p38, JNK and MAP kinases. Ser[727]phosphorylation at the transactivating domain is considered a secondary event after Y705 phosphorylation and is required for the maximal transcriptional activity of STAT3[32].

2.1.3. STAT3 alternative post-translational modifications.

Post-translational modifications (PTMs) come in various forms and a single type of PTM can be responsible for very different biological functions, depending on the modification site and the context of the signaling pathway. Chemical modifications are reversible and can include the addition of functional groups (as phosphorylation, acetylation) or redox-based modifications (as S-glutathionylation). Phosphorylation is one of the most common and studied PTMs and constitutes an extremely important regulation mechanism in several cellular processes, as many enzymes and receptors are activated and deactivated via phosphorylation/dephosphorylation determined by the interplay of specific kinases and phosphatases[33]. Protein acetylation has a prevalence and significance that rival those of phosphorylation; it is involved in crucial intracellular phenomena and can govern relevant protein properties such as enzymatic activity, localization, stability, or interactions with other molecules[34] . Instead, the redox-sensitive proteome can be post-translationally modified through disulfide linkages between the tripeptide glutathione and cysteine residues within proteins, primarily promoted by oxidative stress[35]. PTMs can function as sensors, allowing cells to quickly and dynamically adapt to changes in environmental conditions. STAT3 can be decorated with many PTMs that are able to modulate its functions. In response to cytokines and growth factors signaling, STAT3 can be acetylated (Ac) on multiple lysine (K)

residues by the CBP/p300 histone acetyltransferase; in particular, K685 acetylation is important for the formation of STAT3 dimer and transcription enhancement at certain genes, perhaps independent of tyrosine phosphorylation[36]. Then, STAT3 can become glutathionylated on multiple cysteine residues, impairing its transcriptional activity, either under conditions of oxidative stress or downstream of IL-6 signaling, which can raise reactive oxygen species (ROS) levels[37].

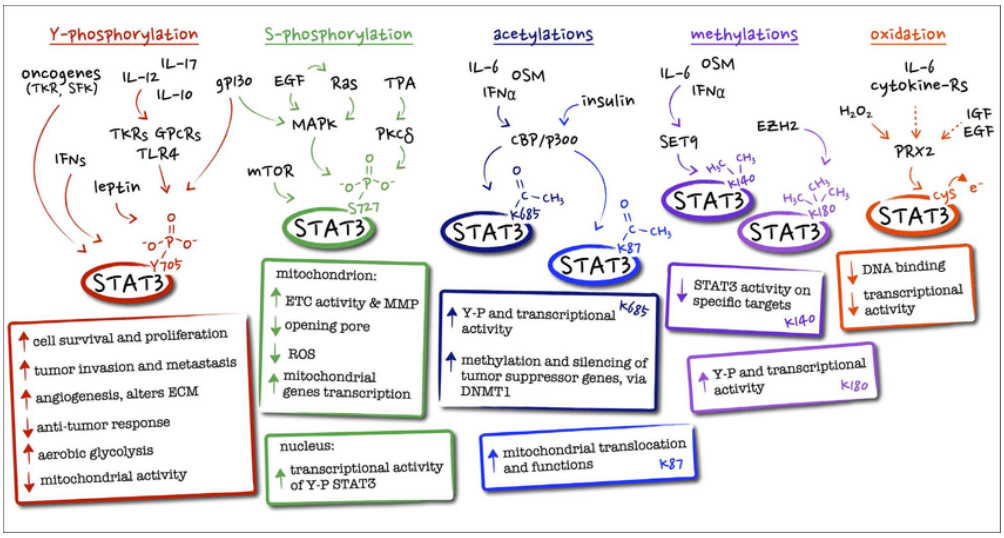

Figure 7. An overview of STAT3 post-translational modifications pattern.

2.2. STAT3 and cancer.

STAT3 is a converging point for many intracellular signaling pathways and an-ever growing number of publications demonstrated its constitutive hyperactivation in nearly every human cancer (neck, brain, breast, liver, lung, kidney, pancreas, prostate, ovary cancer, and multiple myeloma, as well as acute myeloid leukemia)[38]. Accumulating evidence support the critical role of STAT3 in malignant transformation and carcinogenesis. In fact, constitutive STAT3 activation is required for cellular processes that include proliferation, survival, inflammation, invasion, metastasis and angiogenesis, all supporting tumor initiation and progression toward a more aggressive phenotype [39].

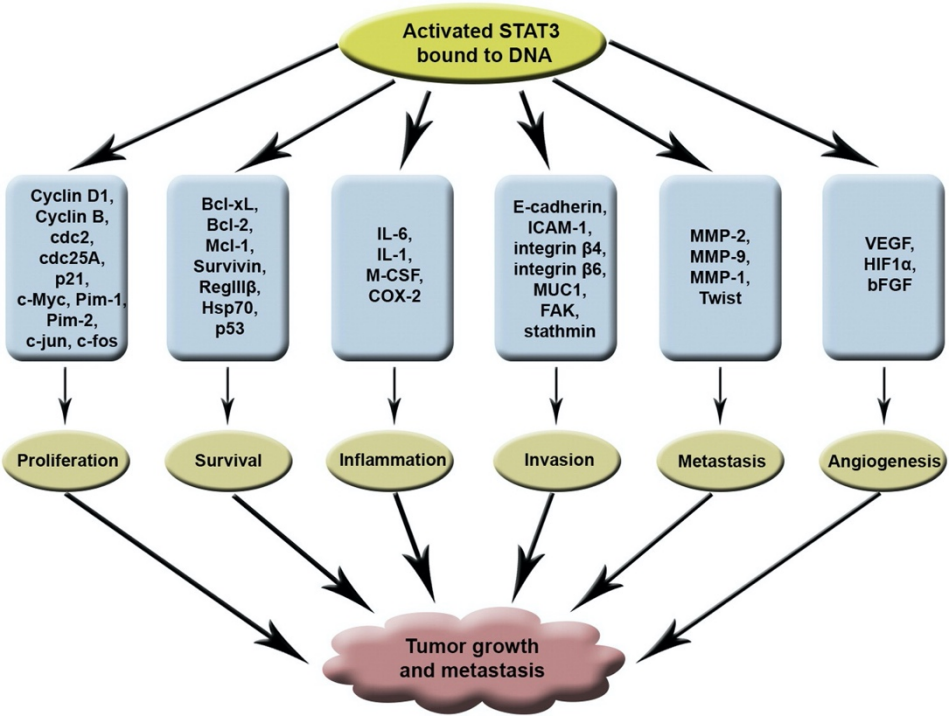

Figure 8. STAT3 roles in tumor progression.

2.3. STAT3 and energy metabolism.

STAT3 is a pleiotropic protein and, in addition to its canonical functions, has been reported to be a master regulator of energy metabolism in both its nuclear and mitochondrial form. In particular, STAT3 activation appears to participate, together with PKM2 (pyruvate kinase isoform 2) and HIF-1α (Hypoxia-inducible factor 1α), in the positive feedback loop which is involved in the Warburg Effect[40]. This loop enhances aerobic glycolysis and proliferation: oxygen deprivation or oncogenes, up-regulating HIF-1α and increasing HIF-1α activity, lead to increased levels of the pyruvate kinase PKM2 isoform; in turn, this enhances HIF-1α transcriptional activity and directly phosphorylates STAT3; closing the loop, activated STAT3 up-regulates HIF-1α expression[41].

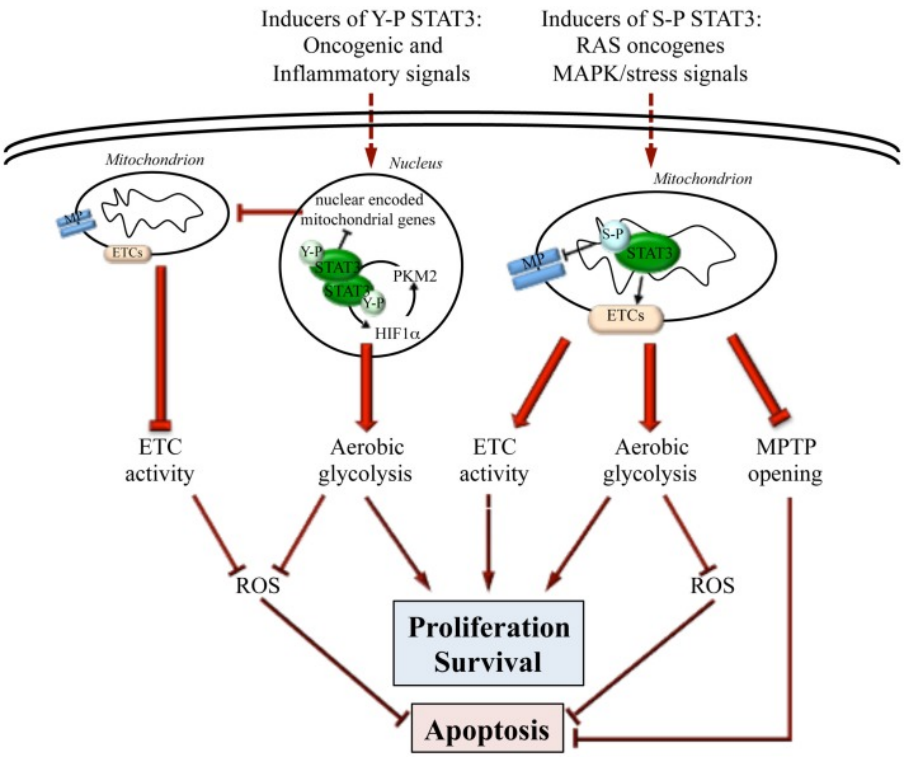

Figure 9. STAT3 involvement in cellular energy metabolism.

3. Hexachlorocyclohexane

3.1. Physicochemical properties.

Hexachlorocyclohexane (HCH) is a chlorinated cyclic saturated hydrocarbon extensively used as a commercial pesticide starting from the late 1940s.

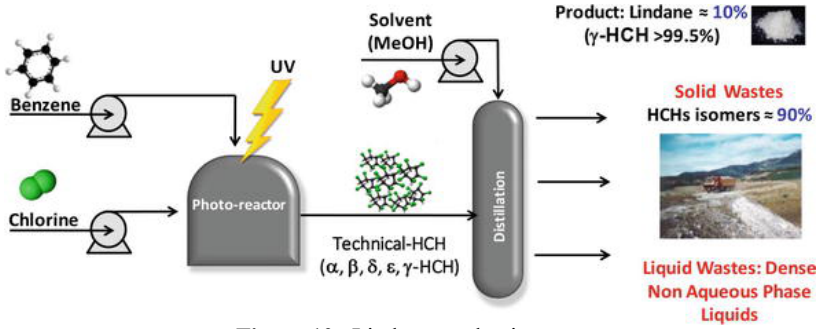

Figure 10. Lindane production process

Hexachlorocyclohexane is almost universally synthetized through the photochlorination of benzene, resulting in a mixture of isomers (α,β, γ, δ, ε) that structurally differ in the axial and equatorial orientation of the chlorine atoms with respect to the cyclohexane carbon ring (figure 11).

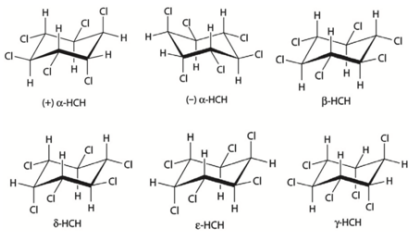

Property	α-HCH	β-HCH	γ-HCH	δ-HCH
Conformation	aaeeee	eeeeee	aaaeee	aeeeee
Molecular weight	290.83	290.83	290.83	290.83
Melting point	159–160°C	314–315°C	112.5°C	141–142°C
Boiling point	288°C	60°C	323.4°C	60°C
Water solubility	2.03 ppm	0.2 ppm	7.4 ppm	15.7 ppm
Solubility in organic solvents (per 100 g)				
Ethanol	1.8 g	1.1 g	6.4 g	24.4 g
Ether	6.2 g	1.8 g	20.8 g	35.4 g
Benzene	–	1.9 g	28.9 g	41.4 g

Figure 11 and **Table 2.** Chemical structure of HCH isomers and physicochemical properties. Boiling points for β- and δ- HCH were measured at 0.5 mmHg and 0.36 mmHg respectively.

The raw product from the chlorination of benzene contains about 14% γ- HCH and 86% of inactive isomers, i.e. α: 65-70%, β: 7-10%, γ: 14-15%, δ: approximately 7%, ε: 1-2%, and 1-2% other components. Among these

isomers, only γ-HCH has specific insecticidal properties and it is possible to extract and purify the active γ-HCH. If the purity is more than 90% in terms of γ-HCH, it is to referred as Lindane[42]. The different HCH isomers and their physicochemical properties are shown in figure 6 and table 2.

3.2. Production and environmental impact.

The production and application of lindane during the last 7 decades have resulted in environmental contamination at global scale. For each tonne of lindane 8–12 tonnes of waste HCH isomers were produced, and the production of approximately 600,000 t of lindane has therefore led to 4.8 to 7.2 million tonnes of HCH/POPs waste. These waste isomers were mostly buried in uncontrolled dumps at many sites around the world[43] ; the stockpiles and the large contaminated sites can be categorized as “mega-sites”.

Figure 12. Map of countries with HCH legacy problems

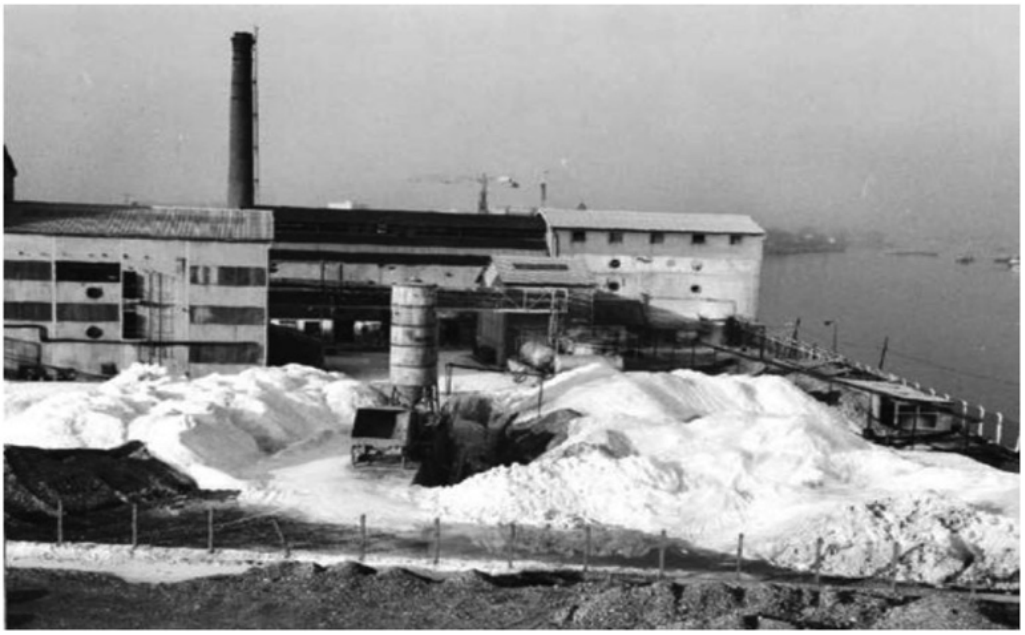

Figure 13. HCH residuals in France.

Considering the magnitude of the problem, α-, β-, and γ-HCH were banned in several countries, including Italy (Regulation EC No 850/2004), and were designated as Persistent Organic Pollutants in the Stockholm Convention in May 2009 [44-45].

Compared to other HCH isomers, β-HCH has stronger lipophilic properties and is most stable from the physical and metabolic point of view due to the equatorial position of all the six chlorine atoms in the chair cyclohexane conformation; this stability is reflected in the environmental and biological persistence of this isomer.

3.3. Hexachlorocyclohexane in Italy.

The company SNIA-BDP (Società di Navigazione Italo Americana Bombrini Parodi Delfino) located in Colleferro, a town in the south of Rome, the Central Italy, was the only lindane manufacturer in Italy since the 50's. In 2005, during a random national survey on chemical contamination of raw cow's milk, products from farms located in the rural area of Valle del Sacco, Colleferro, were found to be polluted with β-HCH as a result of the illegal disposal of chemical waste produced by the close industrial conglomerate[46]. Considering the contamination of the food chain, an epidemiological investigation on the population at risk in three towns (Colleferro, Gavignano, Segni) near to the offending site was established in 2006 and is still ongoing (VEGA 2016)[47]. Results of the survey demonstrated high β-HCH serum levels among the 690 subjects participating in the surveillance program, with a β-HCH amount below the limit of quantification observed only in seven people; in addition, β-HCH serum concentration increases with age particularly in patients with more than 50 years, and becomes even higher among people over 70 years[48].

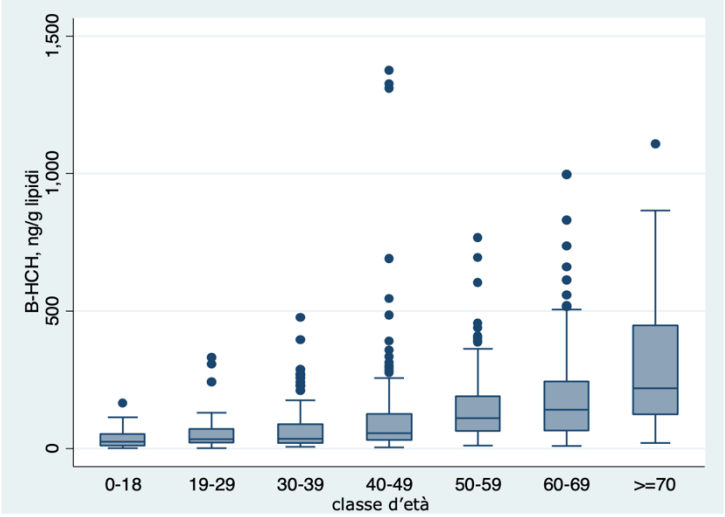

Figure 14. Box-blot for β-HCH serum levels (ng/g of lipids) by age groups

4. Remediation strategies for environmental contamination

4.1. Environmental remediation: an overview.

The modernization in productive technologies, together with an increase of the agricultural sector, is reflected by an excessive use of pesticides and fertilizers to satisfy the requirements of an ever-growing world population[49] .

According to the World Health Organization (WHO), 23% of all global deaths are linked to environmental pollution, amounting to roughly 12.6 million deaths a year[50]; this scenario makes more urgent the need to select appropriate remediation approaches based on a careful analysis of physical, chemical and biological factors affecting each contaminated site.

Environmental remediation is defined as the process of removing contaminants from soil, surface and groundwater in order to preserve living systems and the environment against further deterioration for a sustainable future[51]. The remediation is generally carried out on soil or water media and may be conducted separately or together, depending on the type and extent of the pollution.

4.1.1. Environmental remediation technologies.

The presence in the soil and groundwater of contaminants in concentrations far over the tolerance threshold represents a high potential health as well as ecological risk. For this reason, the optimization of different remediation methodologies could offer a valid tool to clean up polluted sites in relation to the characteristics of the environmental media. In broad terms, technical principles for remediation can be divided into physical, chemical and biological processes. These techniques may be applied in the contaminated area (*in situ*), or by removing the soil from the contaminated area, treating it in a specific treatment complex, and restoring the treated soil to its original place

(*ex situ*). The primary action approach for contaminated sites is the containment technique, consisting in the use of barriers in order to avoid the migration of the pollutants to neighboring soil and to inhibit the flow of clean water through the contaminated area. Containment is achieved by the installation of low-permeable or impermeable cutoff walls that minimize the risk for further contamination[52].

Biological techniques are based on the bioremediation principle that involves the use of microorganism (i.e. bacteria, fungi) for the removal and/or degradation of hazardous chemicals from various environmental media. Microorganisms used in decontamination purposes have often the capability to degrade almost all organic contaminants; the transformation of these substances, in fact, provide the microorganisms with both carbon atoms and electrons, which are beneficial for their own growth and reproduction[53]. Another promising method among biological techniques is the phytoremediation, an *in situ* and clean procedure based on the use of some species of plants with the ability to accumulate or degrade specific organic pollutants. Phytoremediation and bioremediation cannot be viewed separately, since plants constantly interact with microorganism that sometimes establish close associations or symbiotic relationships [54].

A hybrid remediation tool between chemical and biological remediation technologies is constituted by biosurfactants. In general, surfactants are amphipathic compounds that have a hydrophobic moiety directed towards the surface and a hydrophilic portion orientated towards the solution. These amphiphilic molecules can reduce the surface tension at air/water or oil/water interfaces. Surfactants produced by microorganisms are extracellular metabolites referred to as biosurfactants and their biotechnological properties allow their application in the environmental field for xenobiotic

biodegradation and bioremediation[55] (i.e. Deep Horizon oil spill remediation Corexit 9500s – DOSS)[56]. New ecofriendly biosurfactants with the advantage of owning biodegradable or biological-derived dispersant molecules have recently been developed (i.e. rhamnolipid, sophorolipid, and surfactin)[57]. These biosurfactants are in general less harmful, if not harmless at all, to the environment: in fact, they can be degraded immediately after their applications, being less persistent contrary to DOSS in Corexit[58].

And last but not least, chemical methods are employed to remediate the contaminating substances that have been hoarded in the soil by adding chemicals or solvents into the polluted site in order to convert them into less toxic and less harmful products[59].

4.1.2. Bioremediation vs Chemical remediation.

The success of a remediation process requires an optimized development and selection of strategies capable of responding to the specific conditions of the polluted sites. However, each technology has advantages and disadvantages, making it necessary to synergistically integrate different approaches, such as the chemical and the biological one [60].

Chemical methods can offer a cost-effective and fast remediation compared to slow bioremediation process, but sometimes their use can compromise the quality of the environmental media, thus limiting their large-scale application. On the other hand, biological remediation has been reported as an efficient approach with long-term attenuation benefits but is usually unable to quickly remove highly persistent and toxic pollutants. In addition, the microbial degradation is limited to environments where specialized microbial populations are competitive[61-62]. In light of these considerations, the

combination of different methods could be beneficial to achieve a higher removal efficiency and to address the limitation of each technique.

4.2. Hexachlorocyclohexane environmental degrading approaches.

Several technologies have been investigated as potential remediation solutions for hexachlorocyclohexane contaminated sites, but the characteristics and stability of this molecule enhance its resistance towards degradation, making each effort quite challenging. This imposes the need to develop efficient large-scale systems to achieve proper HCH breakdown strategies.

The microbial degradation of HCH is attracting increasing attention and an ever-growing number of studies reported potential microorganisms for the efficient bioremediation of HCH-polluted environments, in particular for the γ-isomer [63]. The key reaction during microbial degradation of halogenated compounds is the removal of the halogen atom, i.e., dehalogenation of the organic halogen. During this step, the halogen atoms, usually responsible for the toxicity of this molecule, are most commonly replaced by a hydrogen or a hydroxyl group. Halogen removal reduces both recalcitrance to biodegradation and the risk of forming toxic intermediates during subsequent metabolic steps. Lindane can be biodegraded under both aerobic and anaerobic conditions, but it is generally mineralized only under aerobic conditions [64-65].

The aerobic degradation pathway of lindane summarized in figure 15 was extensively studied in *Sphingobium japonicum* UT26 [66]. In this pathway, lindane is converted to 1,2,4-trichlorobenzene (1,2,4-TCB), 2,5-dichlorophenol (2,5-DCP), and 2,5-dichlorohydroquinone (2,5-DCHQ) by the enzymatic activities of dehydrochlorinase (LinA), halidohydrolase (LinB), and dehydrogenase (LinC). The degradation of lindane to 2,5-DCHQ is referred to as an upstream pathway, which is further metabolized through the downstream

pathway 2,5-DCHQ is converted to β-ketoadipate by reductive dechlorinase (LinD), ring-cleavage dioxygenase (LinE), and maleylacetate reductase (LinF). Researchers documented β-ketoadipate as a marker metabolite for the degradation of compounds containing aromatic rings. The intermediate β-ketoadipate is further converted to succinyl-coenzyme A (CoA) and acetyl-CoA by succinyl-CoA: 3-oxoadipate CoA transferase (LinGH) and β-ketoadipyl CoA thiolase (LinJ). Both these compounds are metabolized in the tricarboxylic acid (TCA) cycle. In addition, other studies reported that lindane can be metabolized by microorganisms to produce pentachlorocyclohexene (PCCH), 3,4,5,6-tetrachloro-1-cyclohexene (TCCH), pentachlorobenzene (PCB), or trichlorobenzene (TCB) [67].

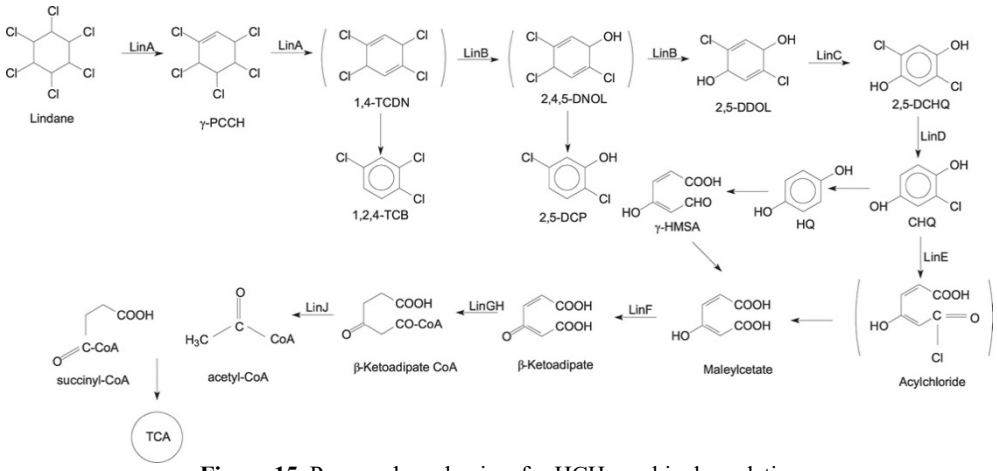

Figure 15. Proposed mechanism for HCH aerobic degradation.

Bacteria have been found to be capable of bioremediating HCH through chemical and physical interactions that lead to structural changes or complete degradation of the target molecule. A wide range of bacteria were reported to degrade lindane at different rates and a number of lindane-degrading bacteria strains have been identified and screened[68]. Fungal biodegradation is also considered an environment friendly approach for the detoxification of POPs.

Fungi, in fact, possess non-specific extracellular enzymatic systems, which include lignin peroxidases, manganese peroxidases and laccases, that can catalyze several reactions toward a wide range of substrates[69]. In particular, laccases are blue multicopper oxidases constitutively expressed in many plants and fungi and are involved in the catabolism of organic pollutants. These enzymes, in fact, are able to catalyze the oxidation of diphenols and aromatic amines by removing an electron and a proton from a hydroxyl group [70]. As regards the physicochemical techniques, some traditional approaches, such as coagulation, flocculation, membrane separation or adsorption on activated carbon, only do a phase transfer of the pollutant. A modern oxidation technology like the photo-Fenton process has been applied for the degradation of several classes of pesticides and refractory compounds. Generally, Fenton's process involves application of iron salts and hydrogen peroxide to produce hydroxyl radicals. This reaction is spontaneous and can occur with or without the influence of light[71].

4.3. Fenton's Reactions.

Among the oxidative technologies, one of the best known and most developed is the Fenton's reaction. This chemical process was reported for the first time in 1894 by the French scientist H.J. Fenton, who discovered the oxidizing potential of Fe^{2+}/H_2O_2 systems at pH 2-3. Under the activation of Fe^{2+}, medium containing hydrogen peroxide (H_2O_2) can produce reactive hydroxyl radicals (•OH) with a strong electron-capturing ability, allowing them to attack most organic groups without selectivity[72]. The Fenton's reaction is expressed by:

$$Fe^{2+} + H_2O_2 \rightarrow Fe^{3+} + \bullet OH + OH^-$$

It has many advantages such as high performance, simplicity (operated at room temperature and atmospheric pressure for substrates oxidation, no energy input is required as a catalyst or to activate H_2O_2) and non-toxicity[73].

However, Fenton's reaction still has some disadvantages including high operating costs, limited optimum pH range (pH~3), large volume of iron sludge produced, and difficulties in recycling the homogeneous catalyst (Fe^{2+})[74]. In order to overcome these practical limitations, research efforts have been focused on finding suitable catalysts other than iron to generate •OH from H_2O_2. In this regard, Fenton-like systems were developed by substituting the iron with other metals at a low oxidation state. In terms of its reactivity toward H_2O_2, copper shows very similar redox properties to those of iron, with the non-negligible difference that Cu^{2+}/H_2O_2 Fenton-like system reaches the maximum efficiency over a broader pH range (near-neutral or neutral) compared to the Fe^{2+}/H_2O_2, which works only under acidic conditions [75-76]. The reaction of the copper-dependent •OH production is reported:

$$Cu^{2+} + H_2O_2 \rightarrow Cu^{+} + \bullet OH + OH^{-}$$

Another extensively used Fenton's process is the so-called Photo-Fenton, in which the combination of H_2O_2, together with iron and UV radiation, boosts the production of more hydroxyl radicals, thus enhancing the degradation rate of substrates. The use of solar irradiation has opened a high application potential for large-scale solar photochemical installations and specific reviews on this topic have been published[77].

4.3.1. Fenton's Reaction applied to the removal of hexachlorocyclohexane.

Over the last decades, Fenton's reaction has emerged as a valid environmental remediation technology and has been successfully applied for the degradation of several classes of pesticides and persistent chemicals[78-79-80].

Taking into consideration the potential of Fenton's reaction, some studies focused on the application of Fe^{2+}/H_2O_2 based oxidation systems for the breakdown of the insecticide γ-HCH.

Begum et al[81] reported the complete dechlorination of lindane with the formation of 1-hexene using Fenton's reagent (Fe^{2+}/H_2O_2) in aqueous phase at pH= 3. The proposed degradation pathway is showed below:

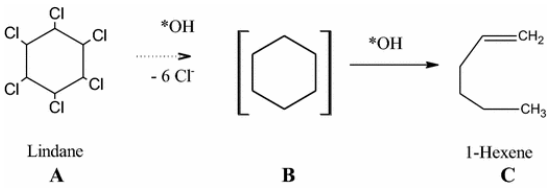

Nitoi et al[71] evaluated the oxidation efficiency of UV/Fe^{2+}/H_2O_2 systems on lindane degradation, suggesting the following photooxidation process:

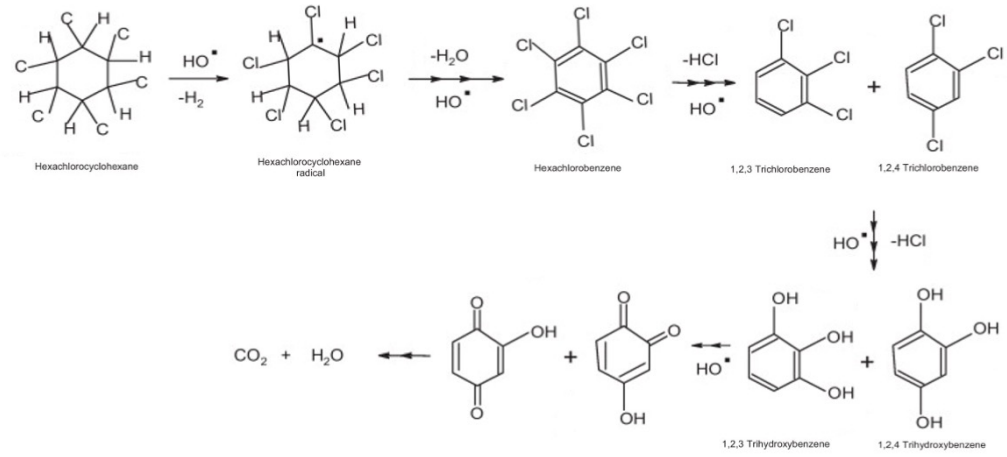

Figure 16. Mechanism for lindane degradation proposed by *Nitoi et al*. Lindane is progressively dechlorinated until its breakdown to CO_2 and H_2O_2, passing through intermediates with less chlorine atoms. Reaction intermediates were identified by GC.

5. Research Aims

The presented work was carried out on two parallel research lines in order to achieve a more comprehensive overview on β-HCH, which is one of the most widespread and, at the same time, poorly studied among organochlorine pesticides. For this reason, it appears to be absolutely essential to deepen the knowledge of β-HCH biological impact starting with the possible triggering of signaling pathways crucial for intracellular homeostasis. β-HCH can be absorbed by humans through contamination of the food chain and it is then bioaccumulated in adipose tissue (10 to 30 times higher than isomer γ), with a slow elimination time from the body (5 times lower than other isomers)[82]; on the basis of its characteristics, β-HCH is suspected to be harmful to humans. Virtually, all the insecticidal properties resided in HCH have meant its recent accreditation by the International Agency for Research on Cancer (IARC) as carcinogenic to humans: there is sufficient evidence in humans for lindane's carcinogenicity in non-Hodgkin lymphoma[83]. Others frequently reported effects are related to neurological disorders, endocrine disruption, reproductive disorders, cardiovascular effects and cancer[84-85-86]. However, despite its worldwide distribution, knowledge of β-HCH effects on human health is controversial and limited to studies in workers employed in the use and production of this pesticide[87]. By typing "β-hexachlorocyclohexane" into PubMed search engine, the results-by-year timeline shows 450 publications spanning from 1975 to 2019 (table 3); after adding the word "disease" to narrow the field and focus on β-HCH biological consequences, the number of available papers is reduced to 63. Conversely, literature outcomes for lindane provide 6594 scientific papers, of which 694 are found including the keyword "disease" in the search criteria. Such a difference between the two analogue

compounds could be explained by the fact that β-HCH is considered a waste by-product without insecticidal activity.

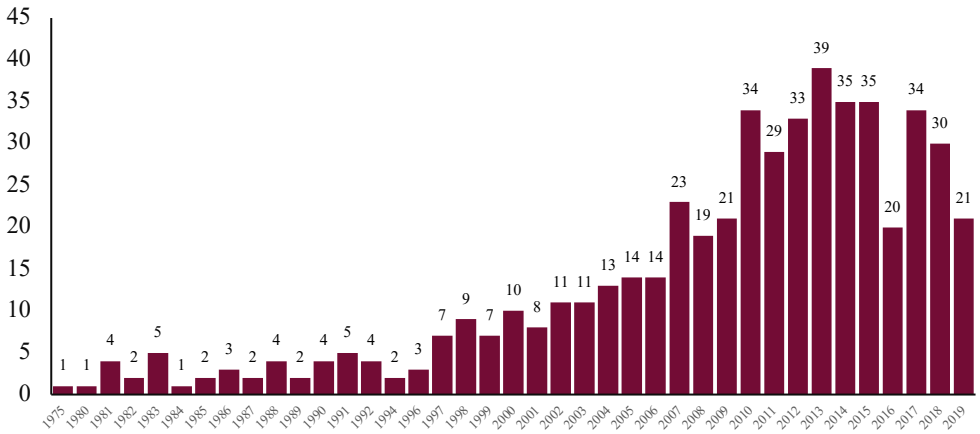

Table 3. Timeline by year (from 1975 to 2019) of results for "β-hexachlorocyclohexane" extrapolated from PubMed search engine.

Even so, β-HCH is potentially one of the main contributors to the so-called civilization diseases, which are pathological conditions (i.e. cancer, neurodegenerative diseases, metabolic disorders) mostly linked to exogenous factors rather than to an intrinsic impairment of human physiological processes. For this purpose, a panel of human continuous cell lines corresponding to different tissues (i.e. liver, lungs, prostate, breast), both normal and transformed, were tested with 10 μM β-HCH. The experimental concentration of the pesticide was chosen averaging across all the plasma concentration values detected in patients under the biomonitoring study carried out in the Valle del Sacco, in order to reproduce the real exposure conditions. After evaluating the effects of β-HCH on cellular viability, different types of analysis were performed to identify the biomolecules, together with the transduction cascades, involved in the molecular responses to β-HCH.

Furthermore, on the basis of the biological behavior reported in scientific literature for other organochlorine pesticides, the potential role of β-HCH as a contributor in tumor initiation and progression was inspected. On the other hand, the environmental persistence of β-HCH still represents an open question for the presence of massive illegal repositories all around the world. For this reason, β-HCH degradation through a copper-based Fenton-like method was explored by setting up a HPLC protocol under different experimental conditions. The process focused on the quantitative degradation of the parental β-HCH, since the detection of its breakdown products or transformed molecules would need a mass-spectrometry for their qualitative characterization.

6. Results: the multifaceted effects of β-HCH on human cells.

6.1. β-HCH molecular activation pathways.

β-HCH was tested on a panel of cell lines representing different human tumor types associated with the expression and activation of specific membrane and membrane associated tyrosine kinase receptors: human breast cancer MDA-MB468 ($EGFR^+$), human hepatoma HepG2 ($JAK2^+$), human prostate cancer LNCaP (AR^+), and human breast cancer MCF-7 ($Her2^+$). The experimental concentration of β-HCH (10 μM) was extrapolated from both the environmental-epidemiological investigation carried out on the exposed population living in the "Valle del Sacco"[46] and from previous *in vitro* studies[88]. First of all, the impact of β-HCH on cell proliferation and viability was verified on all the selected cell lines. No appreciable reduction in cell viability was observed upon cells exposure to 10 μM β-HCH, which, on the contrary, exhibited some proliferative effects.

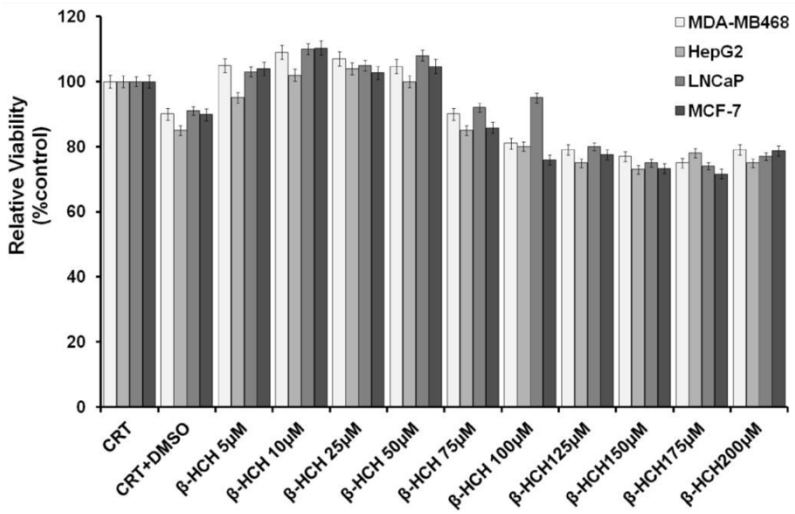

Figure 17. Viability assay performed on the selected cell lines at different β-HCH concentrations, ranging from 5 μM up to 200 μM

A reduction of cell viability can be observed only at higher β-HCH concentrations, as showed in figure 17.

Subsequently, experiments were performed on all four cell lines for identifying β-HCH activation pathways. Results from western blot and RT-qPCR analysis revealed the central role of STAT3 as a hub protein in the intracellular responses triggered by β-HCH by means of its canonical phosphorylation at Y705, also confirmed by using pharmacological inhibitors for each cell line-specific STAT3-mediated signaling. Then, the involvement of STAT3 in cellular energy metabolism was explored. In fact, STAT3 is a well-established master regulator in the metabolic shift toward aerobic glycolysis (Warburg Effect) by interplaying with protein partners such as PKM2 (Pyruvate Kinase M2) and HIF-1α (Hypoxia-inducible Factor 1α)[40]. Investigations carried out on all the selected cell lines show that, as a consequence of pY705-dependent canonical activation, STAT3 can also be phosphorylated at the serine residue 727, referred to as non-canonical pathway. The phosphorylation at S727 of STAT3 is a hallmark of oxidative stress conditions and is related to HIF-1α upregulation, together with an increased nuclear localization of PKM2. All these activated functions require an increased level of energy, and thus a burst in oxidative respiration, resulting in a ROS overproduction. Under the tested conditions, β-HCH induces a slight increase in ROS levels together with a decrease in GSH/GSSG ratio, testifying an alteration in cellular redox homeostasis. In conclusion, experimental outcomes suggest the involvement of STAT3 in β-HCH-induced toxicity through both its canonical and non-canonical pathways. Therefore, STAT3 may regulate the cellular responses to β-HCH, switching from an acute to chronic phase, and may be responsible for the progression of the tumor into an advanced clinical stage, as attested by the occurrence of a metabolic shift towards the aerobic glycolysis.

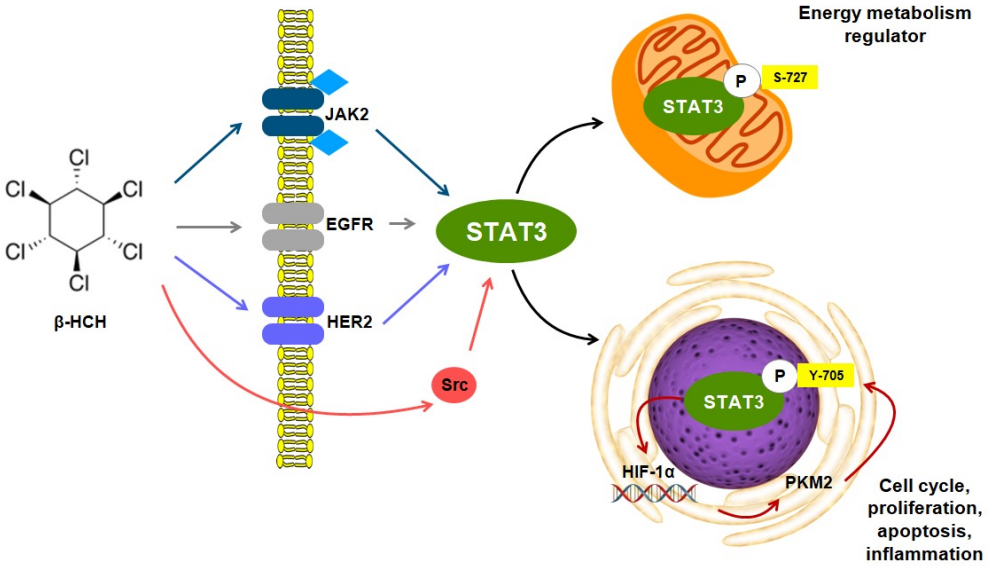

Figure 18. The hub role of STAT3 in the intracellular signaling network triggered by β-hexachlorocyclohexane. The canonical pY705-STAT3 activation occurs at different time points through a cell-line specific manner on the basis of the overexpression and activation status of the membrane and membrane associated tyrosine kinase receptors typical of each cell line. Activated STAT3 initiates and sustains a vicious cycle with the two protein partners HIF-1α and PKM2, responsible for a rewiring in cellular energy metabolism aimed to satisfy the growth requirements of a more aggressive tumor phenotype. Following phosphorylation at Y705, STAT3 is also phosphorylated at S727 which is involved in the cellular responses to β-HCH-induced oxidative stress conditions *(Rubini et al*. 2018).

All the reported results are discussed in detail in the scientific article entitled "*STAT3, a Hub Protein of Cellular Signaling Pathways, Is Triggered by β-Hexachlorocyclohexane*" and published on the International Journal of Molecular Sciences[89].

6.2. β-HCH: small molecule, big impact.

After identifying β-HCH activation pathways, the next step is to unravel the molecular mechanisms underlying β-HCH toxicity. Taking into account the tight correlation between structure and function of biomolecules, it is conceivable to hypothesize that β-HCH may:

1. act as an endocrine-disrupting chemical by interfering with hormone cascades;
2. interact with the Aryl Hydrocarbon Receptor (AhR), the xenobiotic sensor *par excellence*;
3. induce oxidative stress, consequently affecting energy homeostasis and metabolism;
4. cause DNA damage.

To clarify whether β-HCH at the exposure concentration value could be able to trigger the above-mentioned processes, experiments were performed on HepG2 (hepatocellular carcinoma) and LNCaP (prostate cancer) cell lines, which have already been employed as a model to demonstrate the hub role of STAT3 in β-HCH-induced molecular responses.

6.2.1. β-HCH as an endocrine disrupting chemical.

Many pesticides, classified as "endocrine disruptors", can mimic or block the transcriptional activation elicited by naturally circulating hormones because of their physicochemical characteristics and chemical structure.

Information regarding a possible role of β-HCH as an endocrine disrupting chemical are scarce and controversial, therefore shedding light on this mechanism could provide a further element to draw the toxicological profile of this substance. To understand whether β-HCH can interact with the Androgen Receptor (AR) signaling in the guise of agonist or antagonist, an

effective experimental approach consists in following AR nuclear translocation by immunoblot and immunofluorescence upon treatment of LNCaP (prostate cancer AR^+) cells with 10 μM β-HCH for 4 hours.

To confirm the impact of β-HCH on AR-signaling, samples were subjected to a pre-treatment step in the presence of the chemotherapeutic agent bicalutamide, an AR competitive inhibitor approved for prostate cancer therapy under the trade name Casodex[90].

Results from both western blot and immunofluorescence analysis highlighted the capability of bicalutamide to block AR nuclear translocation induced by testosterone and β-HCH, providing extra evidence of β-HCH endocrine-disrupting potential (figure 18).

To check if β-HCH could also activate AR from a transcriptional point of view and affect the expression of AR-target genes, the mRNA level of PSA (Prostate Specific Antigen) was evaluated through RT-qPCR (figure 19). Apart from being a biomarker of choice for prostate cancer, PSA is an AR-dependent gene and therefore constitutes a good candidate to verify AR activity as a transcription factor[91].

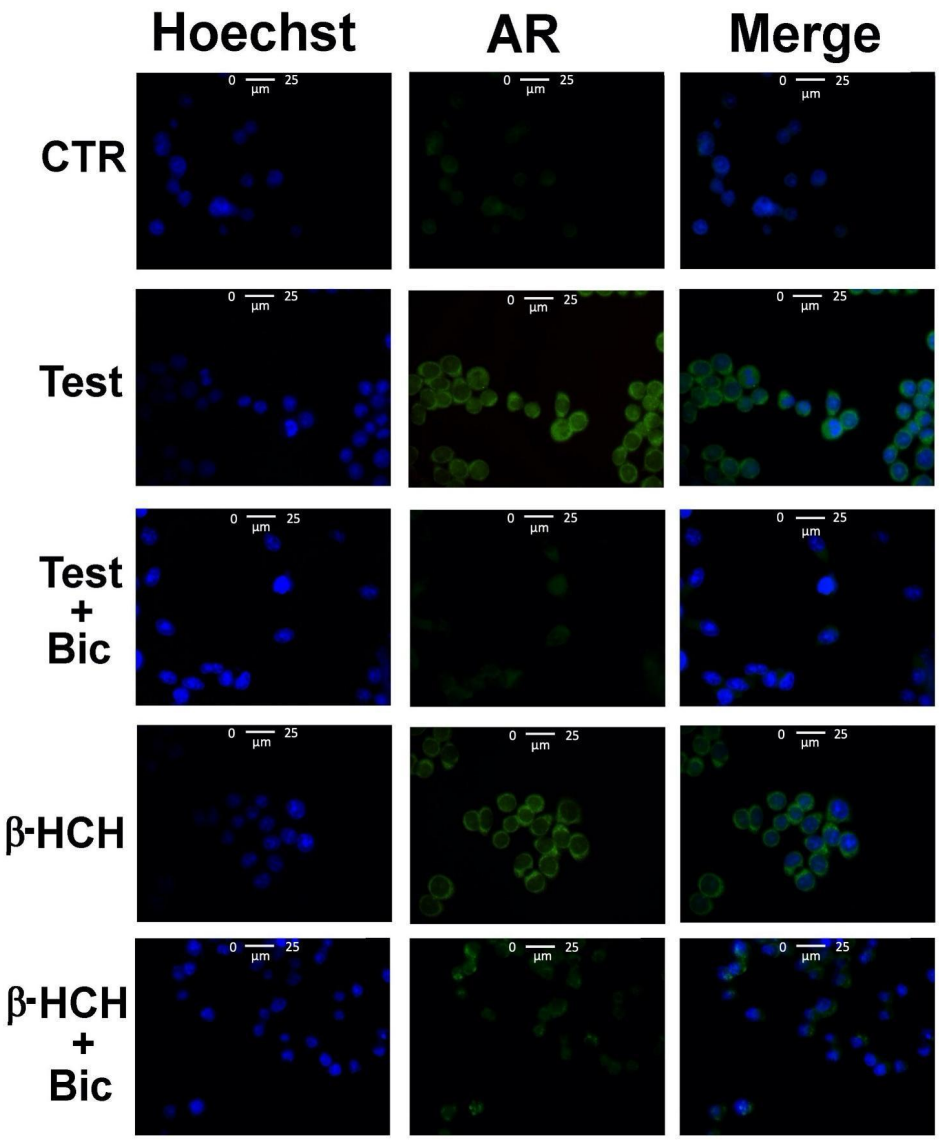

Figure 19. Cellular distribution of AR followed by immunofluorescence in LNCaP cells. CTR: control untreated cells; Test: cells subjected to a 4-hours stimulation with 30 nM testosterone; β-HCH: cells subjected to a 4-hours stimulation with 10 µM β-HCH; Bic: cells treated overnight with 120 nM bicalutamide. Samples referring to the images in the third and fifth rows of the panel ("Test + Bic" and "β-HCH + Bic") were pretreated overnight with 120 nM bicalutamide and then subjected to a 4-hours stimulation with β-HCH or testosterone. AR nuclear localization induced by both β-HCH and testosterone, as evidenced by the images in the second and fourth rows, results inhibited by bicalutamide pretreatment.

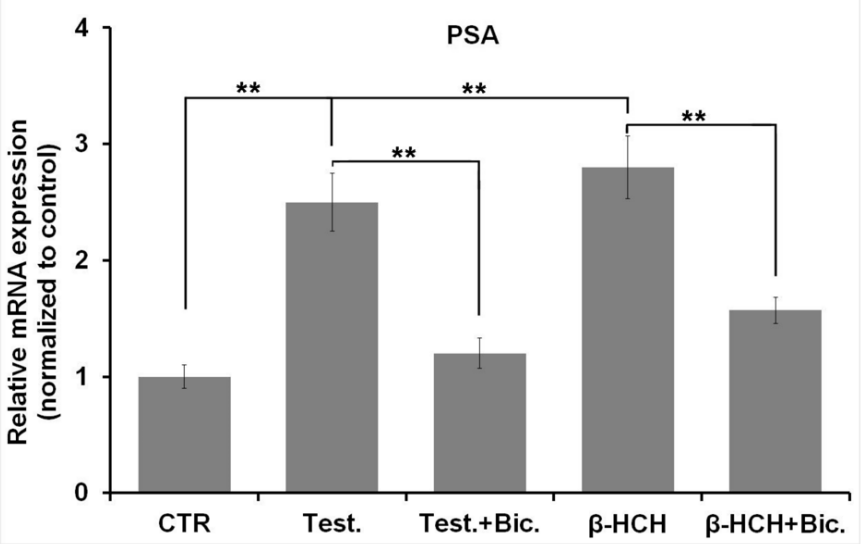

Figure 20. mRNA expression levels for PSA were analyzed by RT-qPCR. The exposure of LNCaP cells for 4 h to 10 μM β-HCH or 30 nM testosterone results in a two-fold PSA overexpression compared to the control untreated cells. Overnight pretreatment with 120 nM bicalutamide largely prevents the increase in PSA mRNA level. PSA expression values were normalized to β-actin as a housekeeping gene and expression levels of untreated cells were set to 1. CTR: control untreated cells; Test: cells subjected to a 4-hours stimulation with 30 nM testosterone; β-HCH: cells subjected to a 4-hours stimulation with 10 μM β-HCH; Bic: cells treated overnight with 120 nM bicalutamide. Statistically significant differences (**$p<0.01$) are marked with asterisks.

6.2.2. β-HCH activates AhR pathway.

To demonstrate the capability of β-HCH to activate AhR genomic pathway, AhR nuclear localization was verified through both immunoblotting and immunofluorescence performed on nuclear extracts obtained from LNCaP and HepG2 cells exposed to β-HCH and pre-treated or not with the AhR antagonist CH223191[92]. Obtained results highlight the nuclear localization of AhR upon β-HCH, supporting its function as an activator of AhR-signaling.

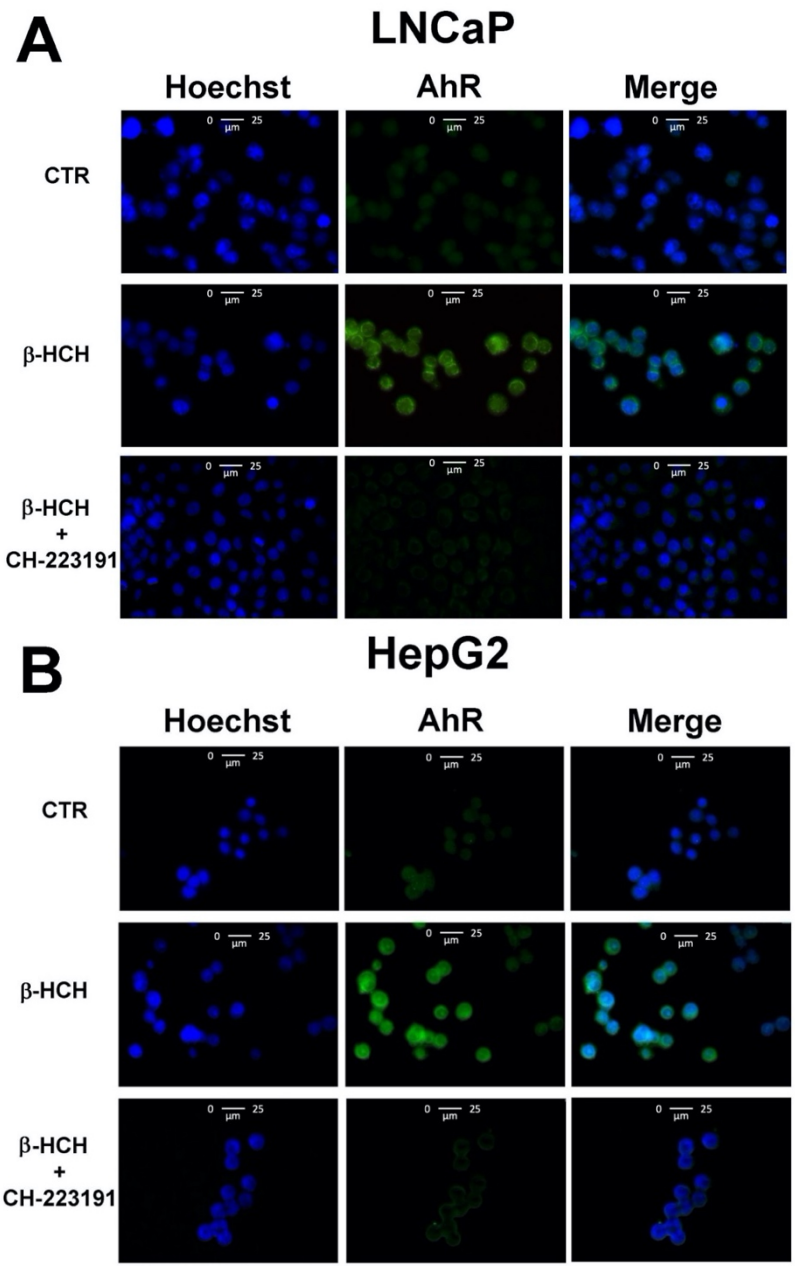

Figure 21. Cellular distribution of AhR followed by immunofluorescence in LNCaP (A) and HepG2 (B) cells. CTR: control untreated cells; β-HCH: cells after 4h of 10 μM β-HCH stimulation; β-HCH + CH223191: cells after 2h pre-incubation with 150 nM CH223191 followed by 4h of 10 μM β-HCH stimulation.

6.2.3. Impact of β-HCH on oxidative stress and energy metabolism.

The capability of OCPs of inducing the formation of reactive oxygen species (ROS), responsible for the establishment of an overall oxidative stress condition, has been well-established. A recently published article provided evidence that 20 μM β-HCH can induce a substantial ROS increase in HOSE ovary cells[93]. To confirm this outcome, ROS production was quantified by performing CellRox assay on both LNCaP and HepG2 cells treated with 10 μM β-HCH for 6 hours. A significant intensification of the fluorescence after β-HCH stimulation occurs, thus indicating an enhanced ROS production.

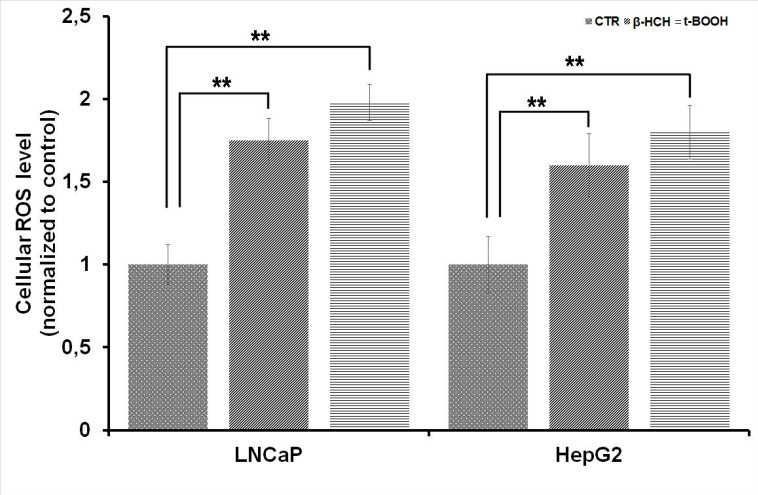

Figure 22. ROS production detected by CellROX assay. The histogram shows an approximately two-fold increase in fluorescence intensity in samples treated with 10 μM β-HCH for 6 hours compared to untreated cells. 75 μM Tert-Butyl Hydroperoxide (t-BuOOH) was used as a positive control for ROS induction. Statistically significative differences (**p<0.01) are marked with asterisks.

Taking into account that glutathione redox status constitutes another reliable biomarker of oxidative stress[94], the same samples were subjected to measurement of the GSH/GSSG ratio. Results reported in figure 23 show a marked increase in the glutathione oxidized form (GSSG), with a consequent decrease in GSH/GSSG ratio, demonstrating the induction of oxidative stress

in response to β-HCH. The establishment of an overall oxidative stress condition is often associated with a reprogramming of cellular bioenergetics; for this reason, additional studies are needed to evaluate the extent to which an imbalance in redox homeostasis is reflected in energy metabolism. Highly aggressive tumors are likely to display a particular metabolic condition known as aerobic glycolysis or Warburg Effect, characterized by the preferential conversion of pyruvate to lactate, rather than to acetyl-CoA, even in normoxia[95]. In this context, the potential impact of β-HCH on cell metabolism was inspected by determining the lactate/pyruvate ratio in the culture media of cells treated or not with β-HCH. As is clear from figure 23, lactate is predominant in stimulated samples, attesting the influence of β-HCH molecular action on cellular metabolic rewiring.

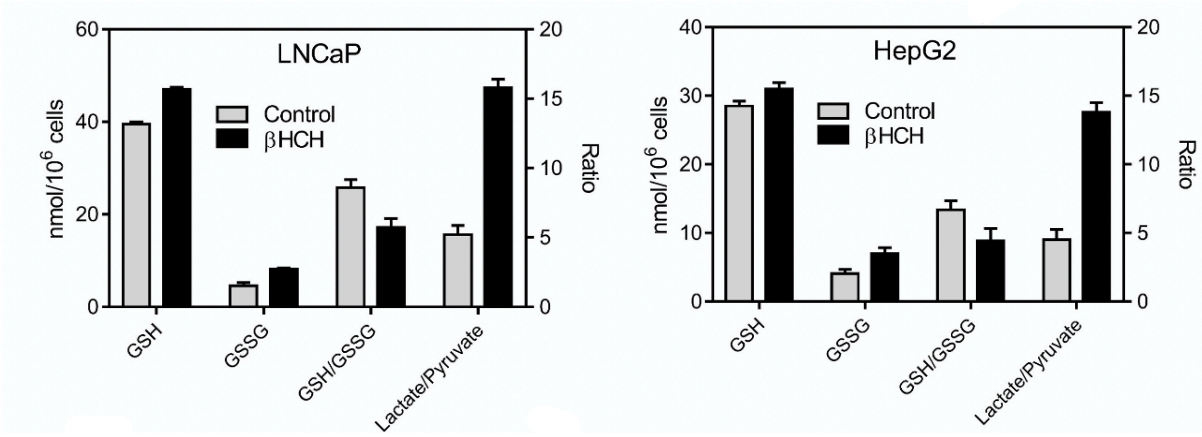

Figure 23. Impact of β-HCH on glutathione redox state and cell metabolism. The increase in glutathione oxidized form (GSSG), with a consequent decrease in GSH (reduced glutathione)/GSSG ratio, proves that 10 μM β-HCH can induce oxidative stress after 6 h treatment in both LNCaP and HepG2 cells. Analysis were carried out on 10^6cells. In addition, a sharp increase in Lactate/Pyruvate ratio is detectable in the culture media of both LNCaP and HepG2 cells stimulated with 10 μM β-HCH for 6 h, demonstrating an enhancement in lactate production induced by β-HCH. All the differences between control and β-HCH treated samples are statistically significant.

6.2.4. β-HCH induces DNA damage.

The relationship between DNA damage and sustained exposure to environmental pollutants is widely described in the scientific literature and is probably linked to the redox signaling triggered by OCPs[96]. For some pesticides, the processes leading to alterations in the cellular homeostasis are partially understood, but commonly recognized mechanisms include their enzymatic conversion to secondary reactive products, depletion of cellular antioxidant defenses and/or impairment of antioxidant enzyme functions[97].The phosphorylation of histone H2AX at serine 139 is a post-translational modification that constitutes a solid and versatile endpoint to investigate the genotoxic potential of a chemical[98]. LNCaP and HepG2 cells were stimulated with β-HCH or tert-butyl Hydroperoxide (t-BuOOH) as positive control[99] and nuclear fractions subjected to immunoblotting. With respect to the untreated control, H2AX results phosphorylated following β-HCH exposition in both the considered cell lines.

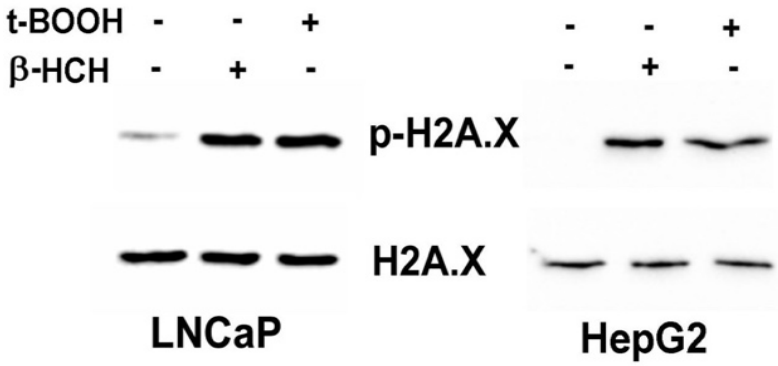

Figure 24. β-HCH induces the phosphorylation of H2AX at Serine 139. Nuclear protein extracts were obtained from both LNCaP and HepG2 exposed to 10 μM β-HCH for 4 hours or 75 μM t-BuOOH for 1 hour used as a positive control for DNA damage.

Reported results are further discussed in the paper entitled "*β-Hexachlorocyclohexane: A Small Molecule with a Big Impact on Human Cellular Biochemistry*" published in Biomedicines[100].

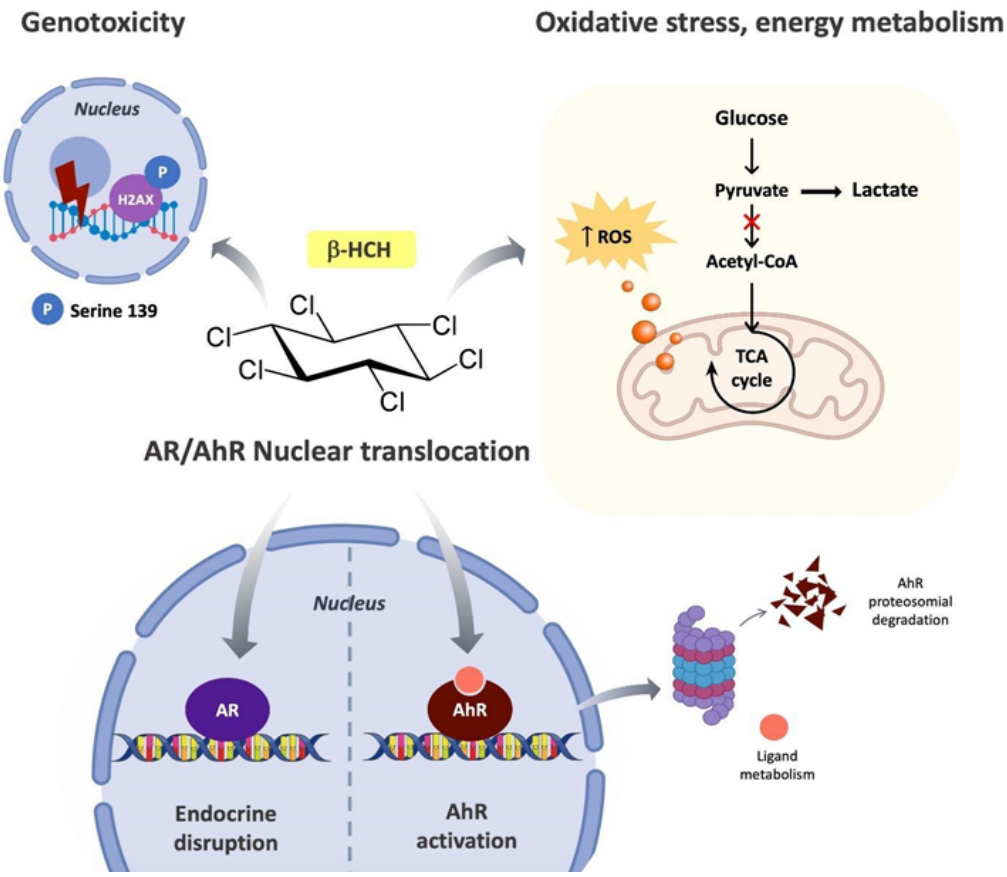

Figure 25. Schematic overview of β-HCH multifaceted intracellular functions.

6.3. β-HCH induces malignant transformation in BEAS-2B cells.

The correlation between synthetic chemicals and carcinogenesis was originally identified in the middle 1700s[101], but it was only in 1915 that Yamagiwa published the first experimental study on cancer pathogenesis in association with environmental contaminants exposure[102]. Although the carcinogenicity of the most popular OCPs has currently been established[103], significant gaps still remain in the knowledge of less renowned compounds such as β-HCH. To investigate whether also β-HCH could trigger cellular malignant transformation toward cancer development, experiments were performed on human continuous cell line BEAS-2B (normal bronchial epithelium) in order to evaluate both the possibleeffects of this pollutant on tumour initiation.

6.3.1. Effects of β-HCH on cells viability.

First of all, cell viability was assessed by performing MTT assay on BEAS-2B cells after 24 hours of exposure to increasing concentration of β-HCH. Cells exposure up to 25 μM concentration revealed >100% cell viability; in addition, 10 μM β-HCH (selected working concentration) exhibits some proliferative effects in accordance with what has been previously demonstrated for other cell lines. However, exposure to β-HCH at high concentration (>25 μM) results toxic. Results are reported in figure 26.

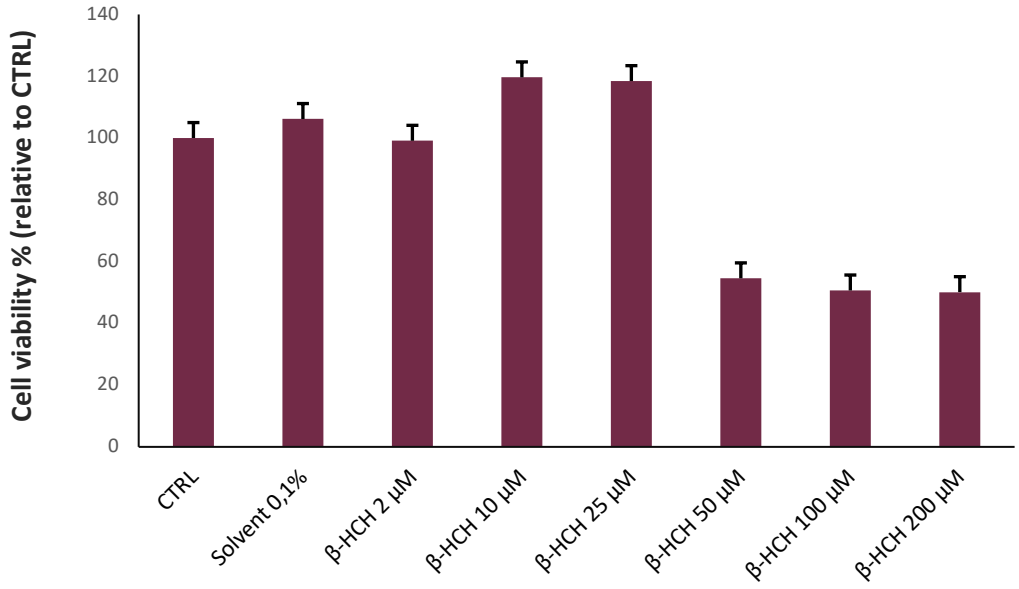

Figure 26. MTT assay on BEAS-2B cells at β-HCH concentrations ranging from 2 µM up to 200 µM.

6.3.2. β-HCH activation pathway in BEAS-2B cells.

In our previous work[89], it has been demonstrated that β-HCH can activate different signaling pathways in a cell-line specific manner. To identify the intracellular cascade triggered by β-HCH in BEAS-2B cells, a time course assay was performed. Samples were treated with 10 µM β-HCH at different time points ranging from 5 minutes to 6 hours and various hypothesis were tested. Immunoblotting carried out on total protein extracts revealed that β-HCH can induce ERK-1/2 phosphorylation already after 5 minutes of treatment (figure 27).

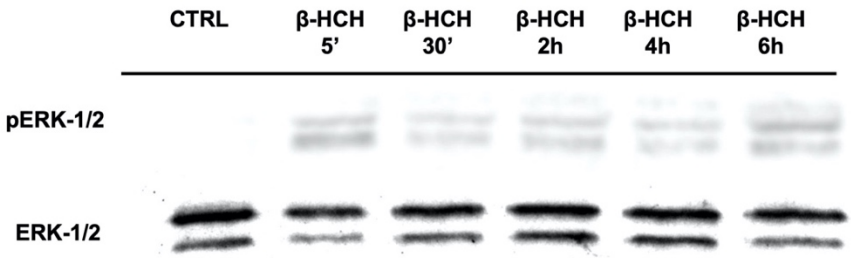

Figure 27. Time course assay on BEAS-2B cells. Cells were treated with 10 μM β-HCH from 5 minutes up to 6 hours. The phosphorylation of ERK-1/2 occurs after 5 minutes of incubation, as clearly demonstrated by western blot. ERK-1/2 phosphorylation levels were measured on the total amount of ERK-1/2 present in each sample and normalized to the control.

6.3.3. Impact of β-HCH on cell morphology.

The impact of β-HCH on BEAS-2B cell morphology was assessed by following for 48 hours the growth of cells exposed to 10 μM β-HCH. As showed in figure 28, treated BEAS-2B cells appear to assume a different growth path on the well surface compared to the control, suggesting a β-HCH-induced morphological change.

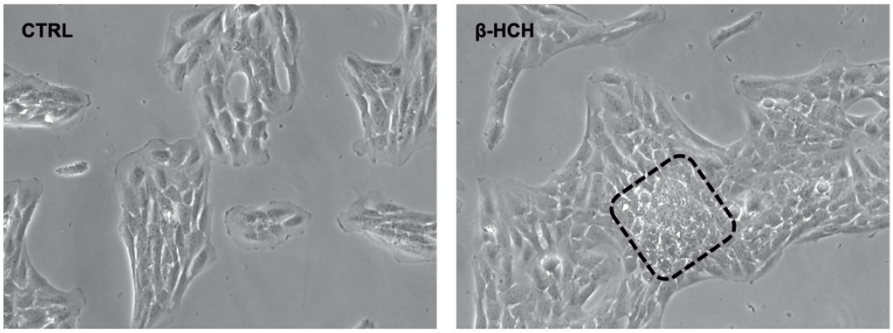

Figure 28. β-HCH-induced morphological changes in BEAS-2B cells. Cells were seeded at 300'000 cells/well and, after 24 hours, were exposed to 10 μM β-HCH for 48 hours. The different arrangement of cells induced by β-HCH is evidenced in a black dotted box. Selected images are representative of three independent experiments.

To confirm this observation, cells were immunoassayed with the mesenchymal marker vimentin. Vimentin is a structural protein that plays an important role in the dynamic organization of cytoskeleton, maintaining cellular integrity and providing resistance against stress[104]. In recent years, vimentin has been considered a predominant intermediate filaments protein in the cytoplasm of mesenchymal cells and, for this reason, has been identified as a mesenchymal marker of epithelial-mesenchymal transition[105]. Cells were treated with 10 µM β-HCH for 48 hours and analyzed by immunofluorescence. Compared to the control, cells exposed to β-HCH exhibit a punctuated pattern for vimentin, testifying a rearrangement of the protein typical of morphological changes in spreading cells[106-107].

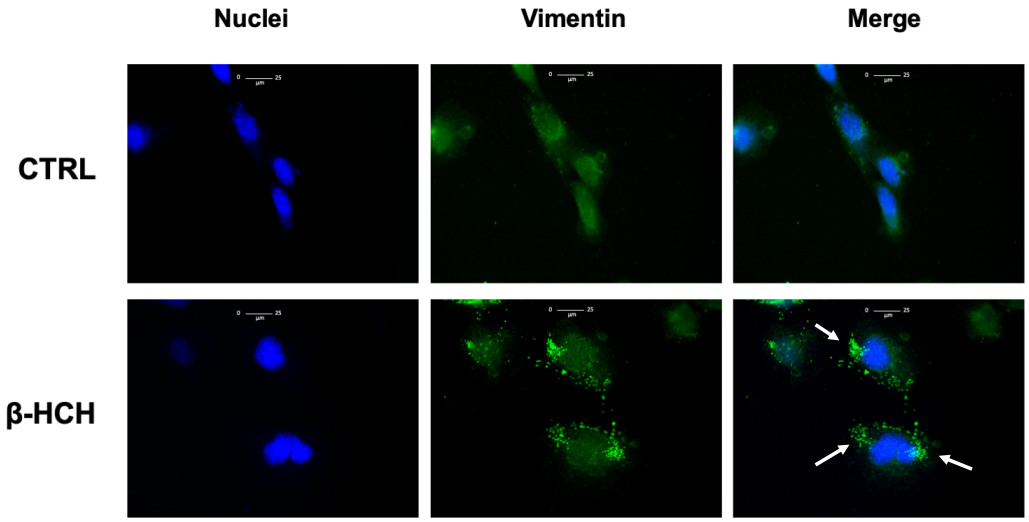

Figure 29. β-HCH induces a rearrangement in vimentin organization. Cells were exposed to 10 µM β-HCH for 48 hours and subjected to immunofluorescence analysis using a specific antibody against vimentin. White arrows indicate the punctuated pattern assumed by vimentin in treated cells, testifying a morphological change. Selected images are representative of three independent experiments and were captured under the same acquisition parameters.

6.3.4. β-HCH induces EGF secretion.

The Epidermal Growth Factor (EGF) plays an important role in the regulation of *in vitro* cells growth. In particular, due to its capability to enhance cell proliferation, EGF levels correlate with tumor initiation and progression[108]. Considering that a slight increase in cells viability was observed through the MTT assay upon stimulation with 10 µM β-HCH, the possible β-HCH-induced release of EGF was investigated. After treating cells for 48 hours with 5 and 10 µM β-HCH, conditioned medium was collected and an aliquot of 500 µL was subjected to dot blot using a specific antibody against EGF (figure 30). A calibration curve was constructed by loading a known amount of standard EGF on the membrane. Were loaded, respectively: 0.1 µg, 0.2 µg, 0.5 µg, 1 µg and 2 µg of EGF.

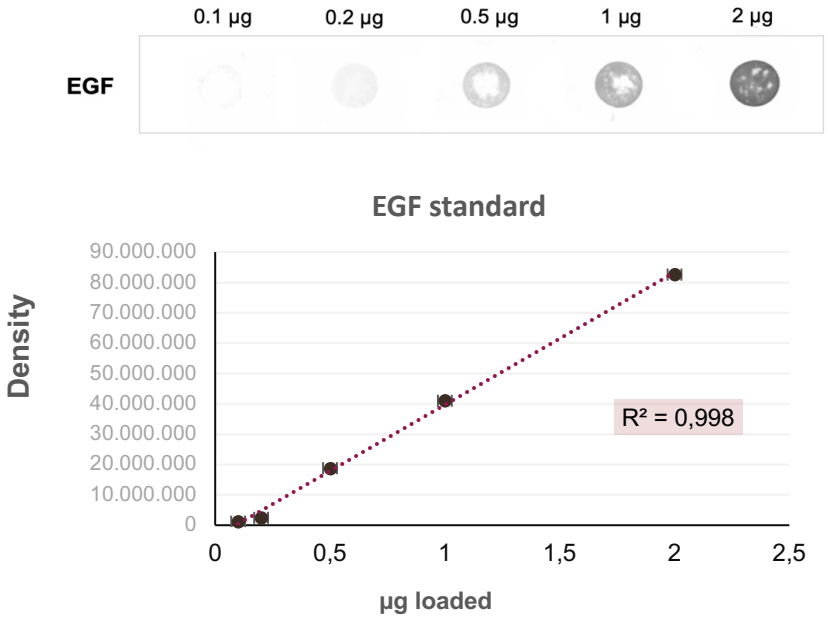

Figure 30. Calibration curve of the dot-blot assay obtained with pure EGF. The average of densitometric analysis was plotted against the loaded amount of EGF: 0.1 µg, 0.2 µg, 0.5 µg, 1 µg and 2 µg.

As showed in figure 31 and supported by densitometric analysis, an increase in EGF secretion occurs in the culture medium of cells stimulated with 48 hours with both 5 and 10 µM β-HCH compared to the control.

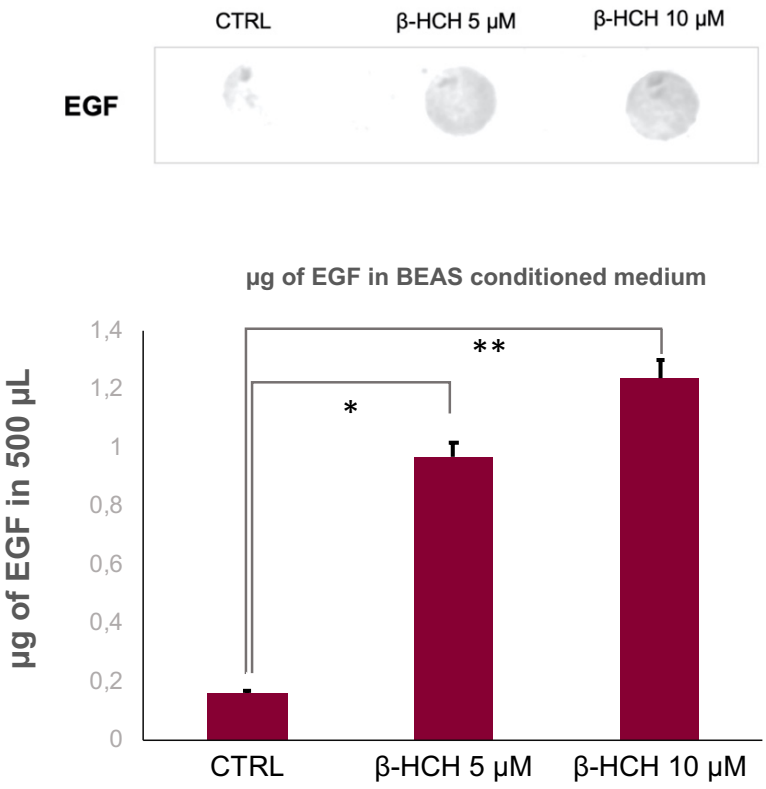

Figure 31. Dot blot analysis for EGF secretion in BEAS-2B conditioned medium after a 48 hours treatment with 5 and 10 µM β-HCH. An aliquot of 500 µL of medium from stimulated BEAS-2B cells was loaded on a nitrocellulose membrane and EGF was detected using a specific primary antibody through immunoblotting. The obtained signal was compared by densitometric analysis to the standard and EGF amount was estimated. Statistically significative differences (*$p<0.05$; **$p<0.01$) are marked with asterisks.

6.3.5. β-HCH effects on apoptosis and cell cycle.

In order to confirm the abovementioned results, the antiapoptotic activity of β-HCH on BEAS-2B cells was investigated by performing the Annexin V-FITC assay by flow cytometry. Cells were subjected to a 24 hours stimulation with 10 µM β-HCH and the chemotherapeutic agent camptothecin was used as a positive control for the apoptosis at a final concentration of 10 µM[109]. The graphics and the histogram reported in figure 32 clearly show that there are no significant differences between β-HCH and the control sample, confirming that β-HCH is not an apoptosis inducer.

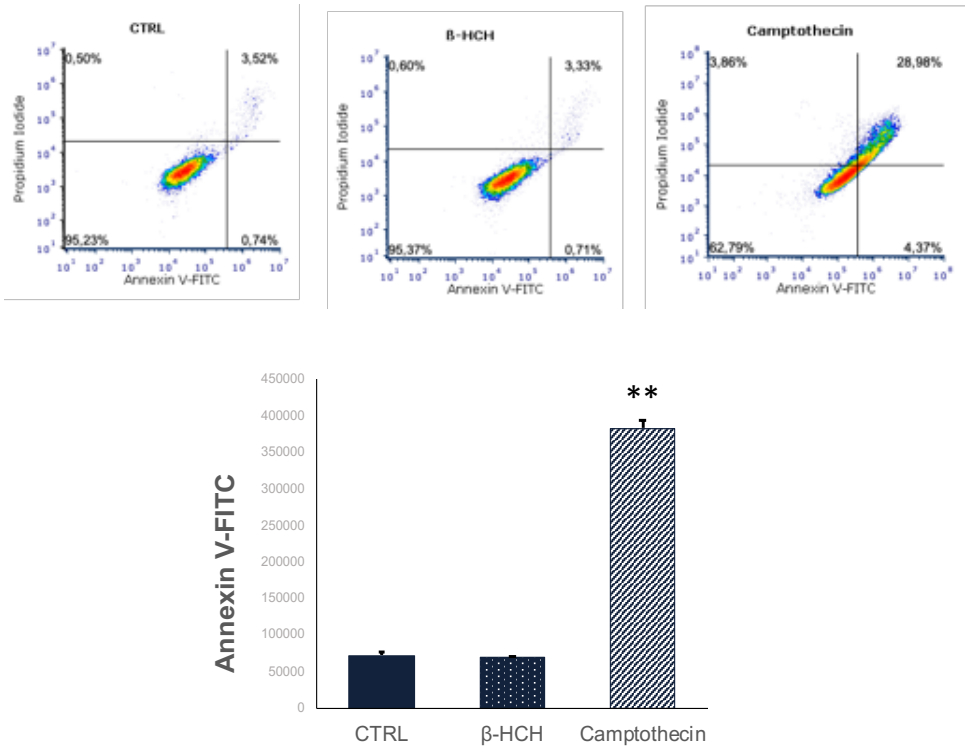

Figure 32. Annexin V-FITC assay performed on BEAS-2B cells treated with β-HCH. Cells were exposed for 24 hours to 10 µM β-HCH and 10 µM camptothecin was used as a positive control for apoptosis induction. Results show that β-HCH did non induce apoptosis. Statistically significative differences (**p<0.01) are marked with asterisks.

On the light of these outcomes, the impact of β-HCH on cell cycle was evaluated. The cell cycle is a 4-stage process consisting of Gap1 (G1), synthesis (S-phase), Gap2 (G2) and mitosis (M). Cell cycle progression plays an important role in cell proliferation and its alteration has been acknowledged as one of the hallmarks of cancer[110]. Cells were exposed for 48 hours to 10 µM β-HCH and then were analyzed by flow cytometry following staining with propidium iodide. The histogram and the relative graphics reported in figure 33 demonstrate that β-HCH induces a slight increase in the percentage of cells in G2M phase. Since a checkpoint is operational in the late G2 phase to allow the repair of damaged DNA[111], the increase in G2M peak is not necessarily reflected in a cell cycle arrest, but it could mean a delay in the cell cycle duration due to the establishment of repair processes that prevent cells from entering mitosis.

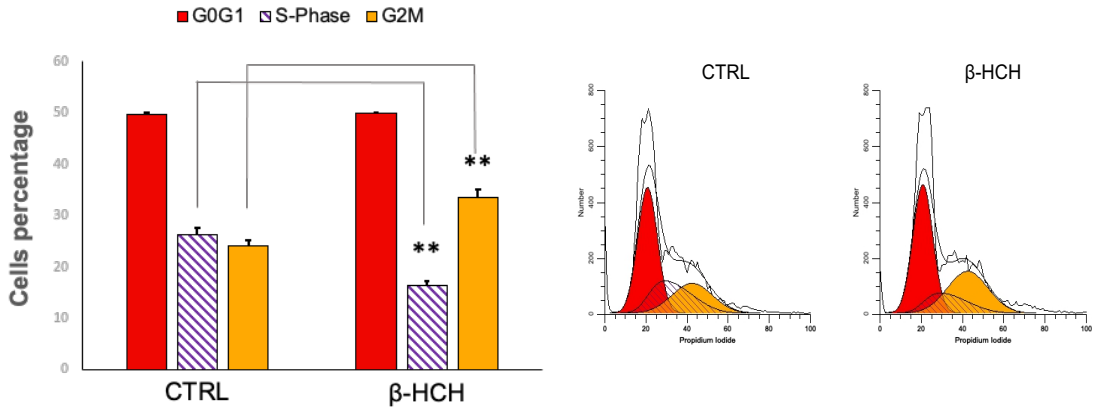

Figure 33. Effects of β-HCH on cell cycle profile in BEAS-2B cells. Exposition to 10 µM β-HCH for 48 hours induces an increase in the percentage of propidium iodide-stained cells in G2M phase. This result could relate with the establishment of repair mechanisms that prevent cells from entering mitosis. Statistically significative differences (**p<0.01) are marked with asterisks.

6.3.6. β-HCH induces H2A.X phosphorylation in BEAS-2B cells.

Some studies already established the susceptibility of BEAS-2B to DNA damage induced by environmental pollutants[112]. In addition, there is strong evidence of a correlation between H2A.X phosphorylation and the activation of the G2M checkpoint[113]. To verify whether also β-HCH can induce DNA damage on BEAS-2B through phosphorylation of histone H2AX at serine 139, cells were treated with 10 µM β-HCH at different time points and protein extracts were analyzed by western blot. Cells treated with 75 µM t-BuOOH for 1 hour were used as a positive control. As is clear from the blot reported in figure 34, phosphorylated H2A.X is detectable in samples treated with β-HCH after 12, 24, 48 and 72 hours.

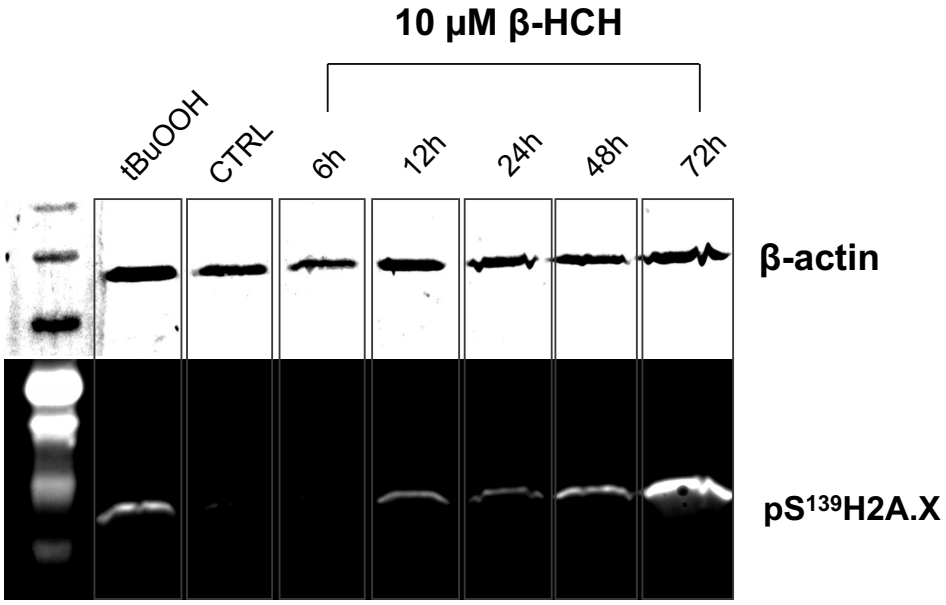

Figure 34. β-HCH induces the phosphorylation of H2A.X at Serine 139 in BEAS-2B cells. Total protein extracts were obtained from cells exposed to 10 µM β-HCH at different time points or 75 µM t-BuOOH for 1 hour used as a positive control for DNA damage**.** An Alexa647-conjugated primary antibody was used to detect pS[139]H2A.X.

6.3.7. β-HCH induces oxidative stress in BEAS-2B cells.

As previously discussed, β-HCH has been shown to induce oxidative stress in different cell lines. For this reason, CellRox was performed on BEAS-2B cells treated for 48 hours with 10 µM β-HCH and t-BuOOH was used as a positive control for ROS induction. An intensification in the fluorescence is observable upon β-HCH treatment (figure 35), attesting the increase in ROS levels.

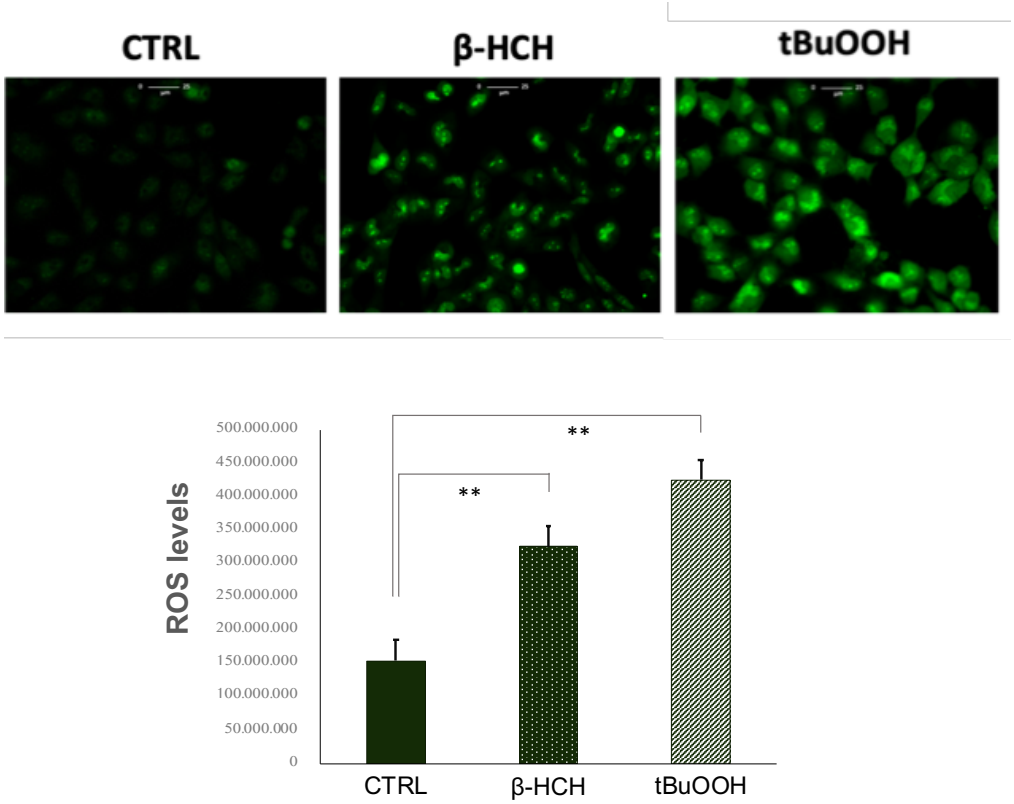

Figure 35. β-HCH induces ROS production. The images and the relative fluorescence quantification reported in the histogram clearly show an increase in ROS levels upon treatment with 10 µM β-HCH for 48 hours compared to the control; 75 µM t-BuOOH for 1 hour was used as a positive control. Fluorescence intensity was then quantified averaging across the CTCF (Corrected Total Cell Fluorescence) calculated with ImageJ. Images were captured under the same acquisition parameters and are representative of three independent experiments. Statistically significative differences (**p<0.01) are marked with asterisks.

6.3.8. β-HCH induces an increase in Ki67-positive cells.

Ki67 staining is widely used as a proliferation indicator in the clinic as its expression is strongly associated with cell proliferation and tumor progression[114]. For this reason, the impact of β-HCH on Ki67 was evaluated by immunofluorescence analysis. Figure 36 demonstrates a marked increase in Ki67-positive cells in sample treated for 24 hours with 10 μM β-HCH. Fluorescence intensity was quantified for the same number of cells from different images for both control and treated samples; the variation in fluorescence intensity is displayed in the histogram.

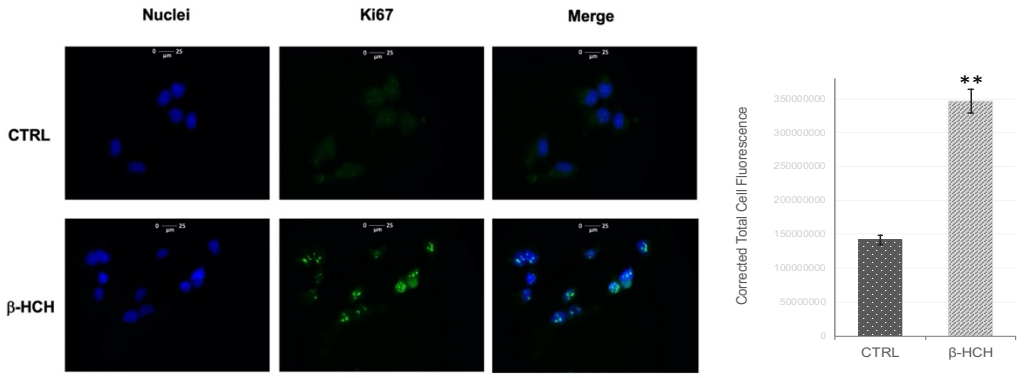

Figure 36. Impact of β-HCH on Ki67 in BEAS-2B cells. After a 24 hours treatment with 10 μM, cells were fixed, permeabilized and subjected to immunofluorescence analysis using a specific antibody against Ki67. Images clearly show an increase in Ki67-positive cells upon β-HCH stimulation. Fluorescence intensity was then quantified averaging across the CTCF (Corrected Total Cell Fluorescence) calculated with ImageJ on the same number of cells for both control and treated sample from different images. The increase in fluorescence intensity after 24 hours of treatment with β-HCH is visualized in the histogram. Images for both CTRL and β-HCH samples were captured under the same acquisition parameters and were background subtracted before analysis; selected images are representative of three independent experiments. Statistically significative differences (**$p<0.01$) are marked with asterisks.

6.4. β-HCH promotes chemoresistance in H358 cells.

It is fair to state that β-HCH can deeply impact on cellular homeostasis, contributing to the establishment of stressful conditions by means of different molecular mechanisms. In addition, β-HCH has been shown to cause the release of EGF in the medium of the normal bronchial epithelium cell line BEAS-2B, inducing a proliferative response. For this reason, the next question to answer is whether the exposure to β-HCH may lead to a loss of response to chemotherapeutic agents (i.e. tyrosine kinases inhibitors) as a result of its capability to induce cancer progression toward a more aggressive phenotype, on par with other pollutants[115]. To explore this possibility, experiments were initially carried out on H358 (human bronchioalveolar carcinoma) cells. This cellular model was chosen because H358 cells derive from non-small cell lung cancer (NSCLC): beside representing a HER2-positive tumor among the most studied from the clinical point of view, lung cancer exhibits a greater tendency to develop chemoresistance to HER2-targeted therapies especially in case of relapse[116]. As for all the tested cell lines, an MTT assay was preliminarily performed at different β-HCH concentrations and the non-lethal effect of 10 μM β-HCH was also confirmed on H358 (figure 37).

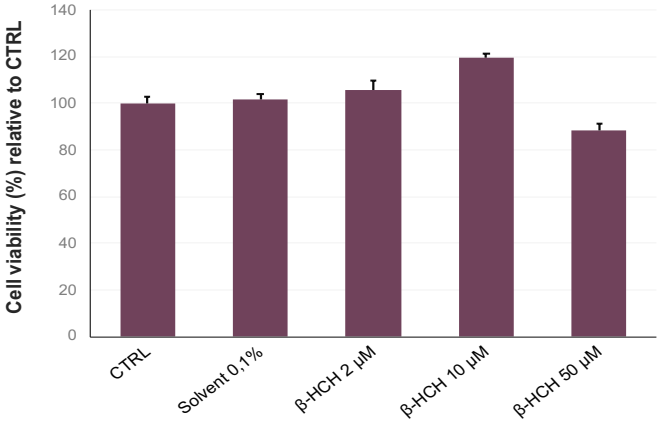

Figure 37. MTT assay on H358 cells at three different β-HCH concentrations (from 2 μM up to 50 μM).

After ensuring that β-HCH did not exhibit toxicity at the used concentration, HER2 activation upon treatment with 10 μM β-HCH was verified through a time course assay. As showed in figure 38, HER2 phosphorylation occurs already after 5 minutes.

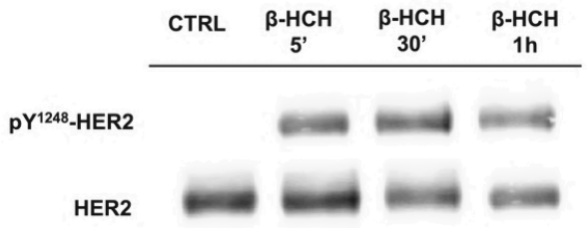

Figure 38. β-HCH induces HER2 phosphorylation in H358 cells. Time course assay at different time points on H358 cells reveals that HER2 activation via phosphorylation at the tyrosine residue 1248 in response to 10 μM β-HCH occurs already after 5 minutes. Each sample was normalized against the unmodified HER2 levels present in the same protein extract.

To further confirm the β-HCH-dependent HER2 activation in H358 cells, the specific HER2 inhibitor lapatinib[117] was tested. Cells were incubated with 10 μM β-HCH for 30 minutes following or not an overnight inhibition step with 500 nM lapatinib. Western blot reported in figure 39 evidenced the capability of lapatinib to inhibit β-HCH-induced HER2 phosphorylation.

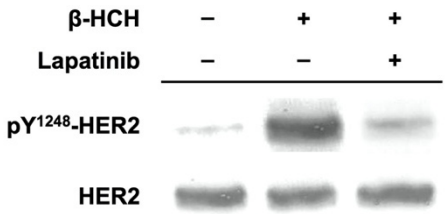

Figure 39. Lapatinib inhibits β-HCH-induced HER2 phosphorylation in H358 cells. Cells were stimulated for 30 minutes with 10 μM β-HCH following or not an overnight pre-treatment with 500 nM lapatinib. Total protein extracts were subjected to immunoblotting and obtained results show a decrease in HER2 phosphorylation upon treatment with lapatinib together with β-HCH. Each sample was normalized against the unmodified HER2 levels present in the same protein extract.

To clarify whether the concomitant presence of β-HCH could alter the proper cellular responses to the tyrosine kinase inhibitor lapatinib, an MTT assay was performed to follow the viability of H358.

Samples were inhibited overnight with 500 nM and then 10 μM β-HCH was added for 24 hours. As presented in the histogram (figure 40), β-HCH induces a slight increase in cell growth, whereas the inhibitory effect of lapatinib seems to be reversed by the co-treatment suggesting that β-HCH could somehow interfere with lapatinib activity.

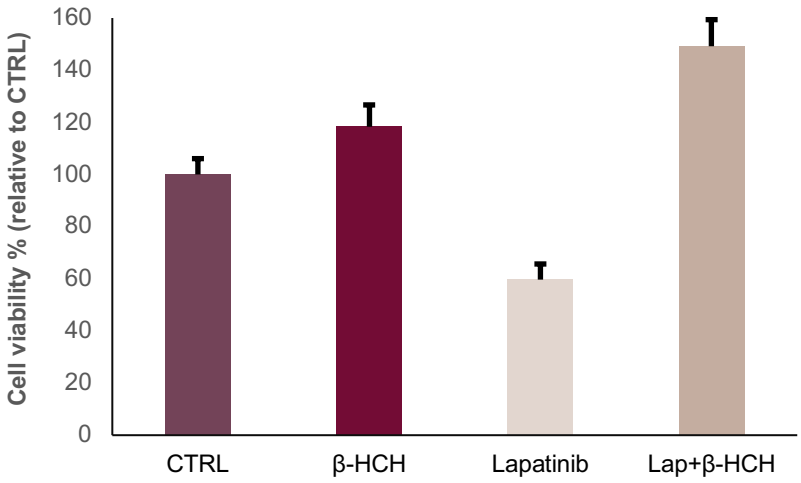

Figure 40. MTT assay performed on H385 cells subjected to β-HCH and lapatinib treatment. Cells were seeded at 12'000 cells/well and, after attaching, were inhibited overnight with 500 nM lapatinib. Then, 10 μM β-HCH was added and cells were incubated for 24 hours before reading. As showed in the graphic, the inhibitory effect of lapatinib is reversed by the concurrent presence of β-HCH, responsible for an even higher growth rate compared to samples stimulated with β-HCH alone. All the differences between control and treated samples are statistically significant.

To further confirm this outcome, a wound healing assay was performed under the same experimental condition. Cells were inhibited overnight with 500 nM lapatinib and then exposed to 10 µM β-HCH for 24 hours. The panel displayed in figure 41 shows that cells subjected to 10 µM β-HCH treatment cover the scratch to a larger extent than the untreated sample, whereas cells detachment occurs upon 500 nM lapatinib administered alone. Surprisingly, no cellular death was observed in the presence of both lapatinib and β-HCH, suggesting that β-HCH could somehow counteract the inhibitory action of lapatinib, leading to a higher proliferation rate compared to the control contrary to expectations.

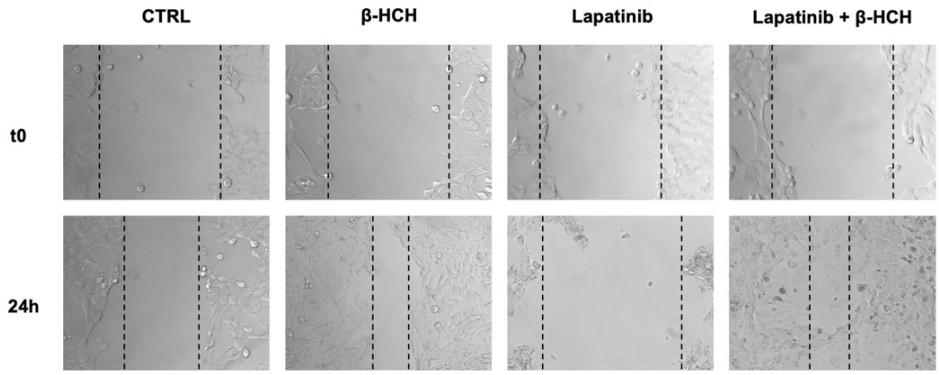

Figure 41. Wound healing assay on H358 cells. Cells were seeded on a 6-wells plate at 150'000 cells/well and a scratch was made after they reached a confluence of 70%. Images corresponding to t_0 were collected immediately after scratching the cell monolayer. Samples were inhibited overnight with 500 nM and then 10 µM β-HCH was added for 24 hours (cumulative incubation time of approximately 36 hours). Results show that β-HCH can reverse lapatinib effects on the HER2-positive H358 cells.

These outcomes led to the hypothesis that, in the presence of lapatinib, β-HCH may activate a compensatory pathway that enables tumour cells to escape inhibition, leading to a more aggressive phenotype. Our previous work attested that HER2-positive cell lines exhibit a delayed activation of the protein STAT3[89]. To verify whether the survival signal triggered by β-HCH could involve a switch from the HER2 to the STAT3 pathway, cells were treated with 500 nM lapatinib and 10 μM β-HCH under the same experimental conditions used for the wound healing assay but, in this case, samples were also incubated together with the STAT3 inhibitor S3I-201[118] approximately 12 hours after β-HCH was administered to cells. Specimens were analysed by immunoblotting, confirming that STAT3 phosphorylation occurs in the presence of both β-HCH and lapatinib and is suppressed by S3I-201 (figure 42). The high concentration value of 100 μM used for S3I-201 ensured the total inhibition of STAT3.

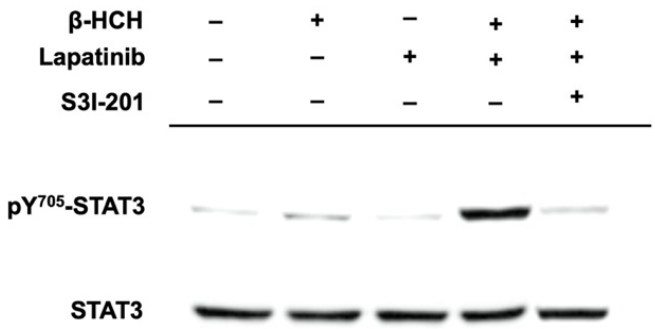

Figure 42. S3I-201 inhibits STAT3 phosphorylation induced by β-HCH and lapatinib. Samples were inhibited overnight with 500 nM lapatinib and then 10 μM β-HCH was added for 24 hours (cumulative incubation time of approximately 36 hours). Cells were then incubated overnight with 100 μM STAT3 inhibitor S3I-201 roughly 12 hours after β-HCH treatment initiation. A sharp band for pY^{705}-STAT3 is detectable in the presence of β-HCH and lapatinib, but it disappears upon S3I-201 treatment. Each sample was normalized against the unmodified STAT3 levels present in the same protein extract.

Obtained results indicate STAT3 as a possible target to reverse the signaling switch induced by the contemporary presence of lapatinib and β-HCH, which is responsible for a loss of cells sensibility to lapatinib. To have an additional proof of this hypothesis, a wound healing assay was performed under the same experimental conditions as the western blot. As shown in the panel below (figure 43), it is possible to observe that 100 μM S3I-201 counteracts the synergistic effects of β-HCH and lapatinib together, inducing the cell growth inhibition.

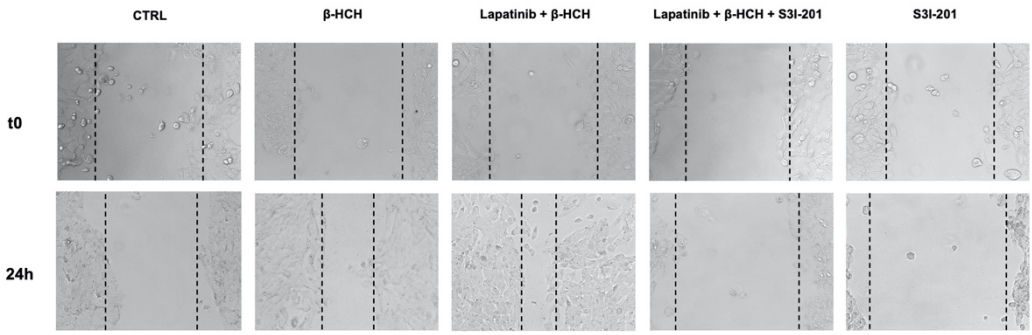

Figure 43. Wound healing assay on H358 cells in the presence of 500 nM lapatinib, 10 μM β-HCH and 100 μM S3I-201. Cells were seeded on a 6-wells plate at 150'000 cells/well and a scratch was made after they reached a confluence of 70%. Images corresponding to t_0 were collected immediately after scratching the cell monolayer. Samples were inhibited overnight with 500 nM and then were exposed to 10 μM β-HCH 24 hours. Approximately 12 hours after β-HCH was added, cells were incubated overnight with 100 μM S3I-201 (cumulative treatment time of approximately 36 hours).

On the light of these considerations, it is legit to wonder whether β-HCH could also interfere with the inhibitory activity of other commonly used chemotherapeutic agents. For this purpose, an MTT assay was performed by treating H358 cells with compounds selected on the basis of their diversified mechanisms of action: beside lapatinib, camptothecin[119], paclitaxel[120] and cisplatin[121] were tested. Drugs concentration was obtained from data present in literature.

Cells were seeded on a 96-wells plate at 12'000 cells/well and were pre-inhibited overnight before adding 10 µM β-HCH for 24 hours. Preliminary experimental outcomes evidenced that β-HCH seems to bring a loss in cell growth inhibition even concurrently with other chemotherapeutic agents, suggesting its potential role in the development of chemoresistance phenomena (figure 44). This aspect is still under investigation and needs to be explored in-depth.

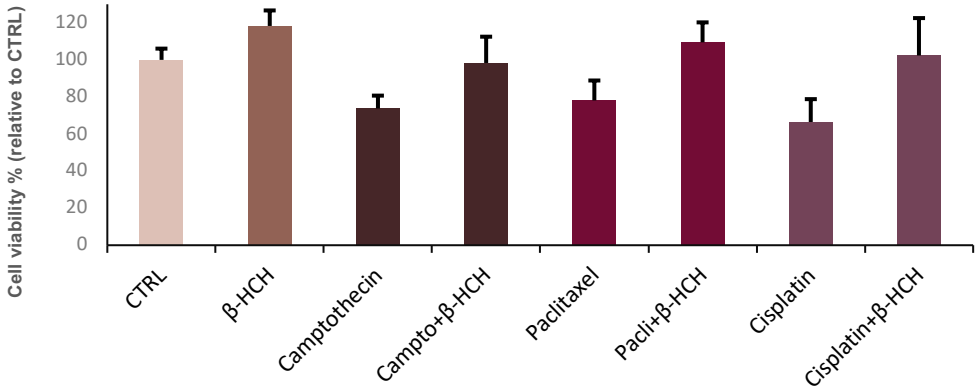

Figure 44. MTT assay on H358 cells stimulated with 250 nM camptothecin, 5 nM paclitaxel and 20 µM cisplatin. Cells were treated overnight with the inhibitors and then β-HCH was added for 24 hours. All the differences between control and treated samples are statistically significant.

6.4.1. Ongoing experiments.

Cellular processes responsible for the acquisition of chemoresistance associated with β-HCH exposure need to be further inspected. To confirm the critical involvement of STAT3 in a possible β-HCH-dependent tumour progression, experiments are currently ongoing on a STAT3-null cell line (PC3, prostate cancer) transfected with the full-length protein. Beside the use of a pharmacological inhibitor, this cellular model could unequivocally confirm STAT3 role in the mechanisms underlying chemoresistance development.

6.5. Material and Methods.

6.5.1. Cell cultures.

Human prostate cancer cell line LNCaP, human breast cancer cell lines MCF-7 and MDA-MB468, human hepatoma cell line HepG2, human normal bronchial epithelium cell line BEAS-2B and human bronchioalveolar carcinoma cell line H358 were obtained from American Type Culture Collection (ATCC). Cells were grown to 80% confluence at 37 °C in 5% CO_2 in the appropriate culture medium, RPMI 1640 (Sigma-Aldrich, Milano, Italy) or DMEM-LG (Sigma-Aldrich), supplemented with 1% sodium pyruvate, 10% fetal bovine serum, 2 mM glutamine, 100 µg/mL streptomycin, and 100 U/mL penicillin. Beta-hexachlorocyclohexane (β-HCH) (Sigma-Aldrich, 33376) was tested on each cell line at a final concentration of 10 µM. The impact of β-HCH on cell viability was evaluated by seeding 12'000 cells/well in 96-well plates and determining cell viability after 24 or 48 hours of incubation upon different concentrations of β-HCH (2, 5, 10, 25, 50, 75, 100, 125, 150, 175, and 200 µM). Cell viability was measured using MTT (3-(4,5-dimethylthiazol-2-yl)-2,5-diphenyl-2H-tetrazolium bromide) (Sigma-Aldrich, M2128). Briefly, the culture medium was removed and 125 µL of MTT solution (0.5 mg/mL MTT in culture medium) was added to each well. After 3 h incubation, the solution was removed and the insoluble formazan dye, resulting from the conversion of tetrazolium salt by metabolically active cells, was dissolved by adding 125 µL/well of DMSO and measured at 570 nm using the Appliskan plate reader (Thermo Scientific).

To demonstrate that STAT3 activation occurs following cell-line specific pathways related to the expression and activation of characteristic membrane and membrane associated tyrosine kinase receptors, LNCaP, MCF-7, MDA-MB468 and HepG2 cells were pre-incubated with selected inhibitors before β-

HCH treatment: 6 μM AZD1480 (Sigma-Aldrich, SML1505), 100 μM S3I-201 (Sigma-Aldrich, SML0330), 70 nM Dasatinib (Selleckchem, Roma, Italy, Cat. No. S1021), 0.8 μM Lapatinib (Sigma-Aldrich, CDS022971), and 15 μM Gefitinib (Sigma-Aldrich, SLM1657). To investigate the capability of β-HCH to act as an endocrine disrupting chemical, LNCaP were treated with 10 μM β-HCH and 30 nM Testosterone (Sigma-Aldrich, cat. 86500) at variable time-points depending on the experiment type. To follow the receptors nuclear translocation, cells were treated for 4 hours with 10 μM β-HCH or 30 nM testosterone. In order to assess the AR agonism of β-HCH, cells were subjected to an overnight pre-treatment with 120 nM bicalutamide (Sigma Aldrich, cat. B9061) before 4 hours of incubation with 10 μM β-HCH or 30 nM testosterone. Instead, to demonstrate the activation of AhR, LNCaP and HepG2 cells were incubated for 4 hours with 10 μM β-HCH following a 2 hours pre-treatment with 150 nM CH223191 (Sigma Aldrich, cat. C8124) or 2 μM MG-132 (Sigma Aldrich, cat. M8699). For oxidative stress and DNA damage induction, cells were stimulated with 75 μM tert-butyl hydro peroxide for 1 hour (Sigma Aldrich, 458139). DNA damage was observed after a treatment of 4 hours. ROS production, GSH/GSSG ratio and lactate/pyruvate ratio were determined on all the cell lines following treatment with 10 μM β-HCH after different incubation time-points depending on the experiment type. For experiments on the carcinogenesis topic, BEAS-2B were treated with 10 μM β-HCH at different incubation times depending on the analysis.

For experiments regarding β-HCH-induced chemoresistance in H358 cells, samples were stimulated, as previously described, with the following inhibitors: 100 μM S3I-201 (Sigma Aldrich, cat. SML0330), 20 μM cisplatin (Sigma Aldrich, cat. 232120), 250 nM camptothecin (Sigma Aldrich, cat. C9911) and 5 nM paclitaxel (Sigma Aldrich, cat. T7191).

6.5.2. Protein extraction and immunoblotting.

Protein extraction and immunoblotting analysis were performed essentially according to Rubini et al[89]. Cells cultured on 6-well plates were scraped, harvested by centrifugation, and washed in PBS. Total protein extracts were obtained using a lysis buffer containing 2% SDS, 20 mM Tris-hydrochloride pH 7.4, 2 M urea, 10% glycerol added with 2 mM sodium orthovanadate, 10 mM DTT, and a protease inhibitors cocktail diluted 1:100 (Sigma-Aldrich). Nuclei were obtained from cell pellets using a hypotonic buffer (10 mM HEPES, pH 7.5), 10 mM KCl, 1.5 mM $MgCl_2$, 0.5 mM DTT) added with 0.05% Triton-X, 2 mM sodium orthovanadate, and a protease inhibitors cocktail diluted 1:100 (Sigma-Aldrich). Thus, nuclei were harvested by centrifugation and washed in a hypotonic buffer, and nuclear protein extracts were obtained as described above for total protein extracts. Proteins were resolved by SDS-PAGE 10% TGX FastCastTM Acrylamide gel (BioRad, cat. 161-0183) and transferred on PVDF membranes using Trans-Blot® TurboTM Transfer System (BioRad, cat. 170-4247). The membranes were blocked with 3% w/v non-fat dried milk or 0.2% w/v I-block (Thermo Fisher Scientific, T2015) in Tris-buffered saline containing 0.05% Tween-20 (TBS-T) and incubated with a specific primary antibody for 1 h. Subsequently, membranes were washed three times in TBS-T, and then incubated for an additional hour with appropriate alkaline horseradish peroxidase- (Jackson ImmunoResearch, dilution 1:5000) or phosphatase-conjugated secondary antibody (Sigma-Aldrich, cat. A3687-A3688, dilution 1:5000). The alkaline phosphatase signal was detected with BCIP/NBT reagents (Carl Roth, cat. 298-83-9 and 6578-06-9). The peroxidase signal was detected with ECL Fast Femto reagent (Immunological Science, Roma, Italy), acquired by Molecular Imager® ChemiDoc™ MP System (Bio-Rad), and the intensity of protein bands was

quantified using the ImageLab Software. The immunoblotting detection was carried out using specific primary antibodies diluted according to manufacturer's instruction depending on the experiment. Each experiment was replicated at least three times.

6.5.3. Dot Blot.

Dot blot is a technique for detecting, analyzing, and identifying proteins, similar to the western blot with the difference that protein samples are not separated electrophoretically but are spotted through circular templates directly onto the membrane or paper substrate. Concentration of proteins in crude preparations (such as culture supernatant) can be estimated semi-quantitatively by using purified protein and specific antibody against it. After preparing nitrocellulose membrane and mounting the support, 500 µL of conditioned medium from BEAS-2B cells were spotted at the center of the grid. The EGF standard curve was prepared used known amount of purified protein (Sigma Aldrich, cat. E9644): 0.1 µg, 0.2 µg, 0.5 µg, 1 µg and 2 µg. Then membrane was blocked overnight and EGF was detected using a specific antibody following the traditional colorimetric protocol.

6.5.4. Immunofluorescence.

Immunofluorescence analysis was performed essentially according to Cocchiola et al[122]. Cultured cells were grown on coverslips and treated with β-HCH or testosterone following or not bicalutamide pretreatment upon the same aforementioned experimental conditions. Cells grown on coverslips were washed with PBS, fixed with 4% formaldehyde for 15 min, and then rinsed with PBS. Cells were permeabilized with cold methanol (−20◦C) for 5 min. After washing three times with PBS, the cells were blocked overnight with 3%

w/*v* BSA (Sigma-Aldrich) in PBS. Fixed cells were processed for immunofluorescence staining using specific primary antibodies diluted in PBS containing 2% *w*/*v* BSA for 1 h. Following three washes with PBS added to with 0.05% Triton and 2% *w*/*v* BSA (PBS-T), cells were incubated for 1 h in the darkness with an FITC-conjugated secondary antibody (Jackson Immunoresearch, AlexaFluor 488-conjugated, cat. 211-545-109, dilution 1:800). Cell nuclei were counterstained with 100 ng/mL Hoechst (Sigma Aldrich, cat. 94403) for 15 min. After washing with PBS-T, coverslips were mounted on glass microscope slides with Duolink™ Mounting Medium and examined using a fluorescence microscope (Leica AF6000 Modular System) with 63× oil immersion objective.

6.5.5. RNA extraction and RT-qPCR.

Total RNA was extracted from treated cells using TRIzol reagent (Invitrogen, cat. 15596026) in accordance with the manufacturer's instructions as already described by Rubini et al[89]. RNA was quantified spectrophotometrically, and its quality was assessed by 1.5% agarose gel electrophoresis and staining with ethidium bromide. The reverse transcription was carried out by Thermo Scientific RevertAid First Strand cDNA Synthesis Kit (Thermo Fisher Scientific, Life Technologies, Monza, Italy, cat. K1622) in accordance with the manufacturer's instructions. Gene expression was evaluated with specific primers using CFX ConnectTM Real-Time PCR Detection System (BioRad Laboratories) with a SYBR-Green fluorophore based real-time reaction (Brilliant SYBR Green QPCR Master Mix, Thermo Fisher Scientific). Gene expression analysis was performed using CFX ManagerTM Real Time PCR Detection System Software, Version 3.1 (BioRad).

6.5.6. Reactive Oxygen Species (ROS) detection.

Reactive oxygen species (ROS) generated by stressing cells with 75 μM tBuOOH were quantified using the CellROX Green Flow Cytometry Assay Kit (Thermo Fisher Scientific, cat. C10492) following the manufacturer's instructions. Samples were analyzed by a BD Accuri C6 flow cytometer (BD Biosciences) or by fluorescent microscope.

6.5.7. Determination of apoptosis.

Cells were treated for 24 hours with 10 μM β-HCH and 10 μM camptothecin (Sigma Aldrich, cat. 208925) as a positive control. Apoptosis was determined by flow cytometry using Annexin V-FITC (Immunological Sciences, cat. IK-11120) according to the manufacturer's instructions. Samples were analyzed using a BD Accuri C6 flow cytometer (BD Biosciences).

6.5.8. Cell cycle analysis.

In order to analyze cell cycle by flow cytometry, cells were treated with 10 μM β-HCH for 48 hours. Then, after detaching them with trypsin, cells were washed with HBSS (Sigma Aldrich, cat. 55021C) and fixed with 70% cold ethanol. Ethanol was added drop wise to the pellet while mixing by inversion. Samples were fixed to 30 minutes at 4°C and then washed twice in HBSS. RNAse was then added at a final concentration of 0.2 mg/mL and incubated for 5 minutes at 37°C. Then, 60 μg/mL final concentrated propidium iodide was added and samples were incubated for 45 minutes at 37°C in the dark. Before flow cytometry analysis, samples were centrifuged and resuspended in the proper volume of HBSS. Samples were analyzed using a BD Accuri C6 flow cytometer (BD Biosciences).

6.5.9. Statistical analysis.

The repeatability of results was confirmed by performing all experiments at least three times. The obtained values are presented as mean and standard deviation. Statistical analysis was performed with GraphPad Prism software using a Student's *t*-test.

6.5.10. Determination of GSH/GSSG ratio.

Reduced (GSH) and oxidized (GSSG) glutathione were measured by HPLC-UV according to Marrocco et al[123].Briefly, cell pellets (1x10^6 cells) were suspended in 10% ice-cold TCA and centrifuged for 15 min at 9000× *g*. The supernatant was collected and GSH and GSSG were measured by HPLC using a poroshell 120 EC-C18 column (3 × 150 mm, 2.7 μm) with UV detection at 215 nm. The mobile phase consisted of two solvent systems (A: 0.1% trifluoroacetic acid in water, and B: 100% 0.1% trifluoroacetic acid in water/acetonitrile 93:7) and the separation was achieved at a flow rate of 0.8 mL/min with the following elution gradient: 0–3 min 100% A + 0% B, 3–10 min from 100% A to 100% B .

6.5.11. Determination of lactate/pyruvate ratio.

Determination of the lactate/pyruvate ratio was performed essentially according to Marrocco et al[123]. Lactic acid and pyruvic acid were analyzed by GC–MS as methoxime/tertbutyldimethylsilyl derivatives as previously described by Paik et al[124]. GC-MS analyses were performed with an Agilent 6850A gas chromatograph coupled to a 5973N quadrupole mass selective detector (Agilent Technologies, Palo Alto, CA, USA). Chromatographic separations were carried out with an Agilent HP5ms fused-silica capillary column (30 m × 0.25 mm i.d.) coated with 5%-phenyl/95%-dimethylpolysiloxane (film thickness 0.25 μm) as stationary phase, using

helium as the carrier gas at a constant flow rate of 1.0 mL/min, splitless injection mode at a temperature of 280 °C, and the following column temperature program: 70 °C (1 min) then to 300 °C at a rate of 20 °C/min and held for 10 min. The spectra were obtained in the electron impact mode at 70 eV ionization energy (ion source 280 °C and ion source vacuum 10−5 Torr). MS analysis was performed simultaneously in TIC (mass range scan from *m*/*z* 50 to 600 at a rate of 0.42 scans s−1) and SIM mode. GC-SIM-MS analysis was performed selecting the following ions: *m*/*z* 174 for pyruvate, *m*/*z* 261 for lactate, and *m*/*z* 239 for 3,4-dimethoxybenzoic acid (internal standard). Results were normalized on cell number and expressed as fold change relative to control samples.

6.5.12. Primary antibodies.

Anti-AR (Cell Signaling, cat. D6F11), anti-AhR (Invitrogen, cat. MA1-514), anti-STAT3 (Cell signaling, cat. 124H6), anti-pY^{705}STAT3 (Cell Signaling, cat. D3A7), anti-pS^{139}H2AX (Santa Cruz Biotechnology, cat. 101696), anti-H2A.X (Santa Cruz Biotechnology, cat. sc-54606; Abcam, cat. ab195189), anti-β-actin (Sigma-Aldrich, cat. A1978 clone AC-15), anti-lamin A (Abcam, cat. AB26300), anti-PKM2 (Cell Signaling, cat. D78A4), anti- HIF-1α (Invitrogen, MA1-516), anti-pS^{727}STAT3 (Sigma-Aldrich, cat. SAB4300034), anti-JAK2 (Cell Signaling, cat. D2E12), anti-PY$^{1007/1008}$JAK2 (Cell Signaling, cat. C80C3), anti-EGFR (Cell Signaling, cat. D38B1), anti-pY^{1173}EGFR (Cell Signaling, cat. 53A5), anti-Src (Cell Signaling, cat. 32G6) and anti-pY^{416}Src (Cell Signaling, cat. 6943S), anti-Vimentin (Cell Signaling, 5741S), anti-Ki-67 (Cell Signaling, cat. 9027S), anti-EGF (Invitrogen, cat. M805), anti-p44/42 MAPK (ERK1/2, Cell Signaling, cat. 9101S), anti-pT$^{202-204}$p44/42 MAPK

(pT$^{202-204}$ERK1/2, Cell Signaling, cat. 9102S), anti-HER2 (Invitrogen, #280004), pY^{1248}HER (Cell Signaling, cat. 2247S).

6.5.13. Primers.

CDC25A (Qiagen, cat. NM_001789) BIRC-5 (Qiagen, cat. NM_001168), c-MYC (Qiagen, cat. NM_002467), CRP (Qiagen, cat. NM_000567), p21 (Qiagen, cat. NM_000389), HIF-1α (Qiagen, cat. NM_001530), PKM2 (Qiagen, cat. NM_002654), S18 (Qiagen, cat. NM_02255), PSA (Qiagen, cat. NM_001101), β-actin (Qiagen, cat. NM_001648).

7. Results: β-HCH degradation.

7.1. Experimental background.

The physicochemical stability of hexachlorocyclohexane (HCH) isomers, reflected in their environmental persistence and accumulation potential, pose a difficult challenge for degradation strategies. Several efficient methods and metabolic routes are proposed in literature for γ-HCH[65], better known as Lindane, which is the most famous among all HCH isomers and is the only one with insecticidal properties. Unfortunately, these approaches are sometimes not applicable to the other members of the HCHs family.

In fact, even though they share an almost equal chemical structure, the different spatial arrangement of the chlorine atoms confers distinctive properties to each isomer[125]. Substituents in equatorial position with respect to the chair conformation increase the energetic stability of cyclohexane-based molecules; in fact, when substituents are located in axial position, they tend to be subjected to unfavorable interactions with other axial atoms on the same side because of a greater steric crowding. In the light of these considerations, the equatorial orientation assumed by all the six chlorines in β-HCH deeply influences its chemical properties, one above all: solubility.

Several efforts were made to identify the best experimental conditions and a wide range of methodologies were explored. The first attempt at β-HCH degradation detection included spectrophotometric analysis using an UV-Vis system (lambda = 254 nm) following Fenton, Fenton-like, Photo-Fenton and enzymatic reactions. Among the issues needed to be overcome, there was the difficult to find a good compromise between the suitability of the analysis, the experimental set-up based on literature data, and the sensitivity of the method. Even if no significant results were obtained, in return, the numerous tests

performed provided an indication of which could be the best experimental conditions. Therefore, the focus was shifted toward the development of a valid HPLC-UV-Vis process to reveal the possible breakdown of β-HCH upon both chemical and enzymatic reactions. HPLC-UV-Vis techniques, in fact, have already been employed for this kind of studies on lindane[126-127].

7.2. β-HCH degradation: method fine-tuning.

In order to assess β-HCH breakdown, different reaction conditions were examined. In the first place, a calibration curve was constructed plotting the peak areas from chromatograms against the corresponding solutions containing a known concentration of β-HCH (expressed in mg/mL) diluted in MeCN (figures 45-46). The choice of the solvent and the set-up of HPLC run parameters were based on information available in literature.

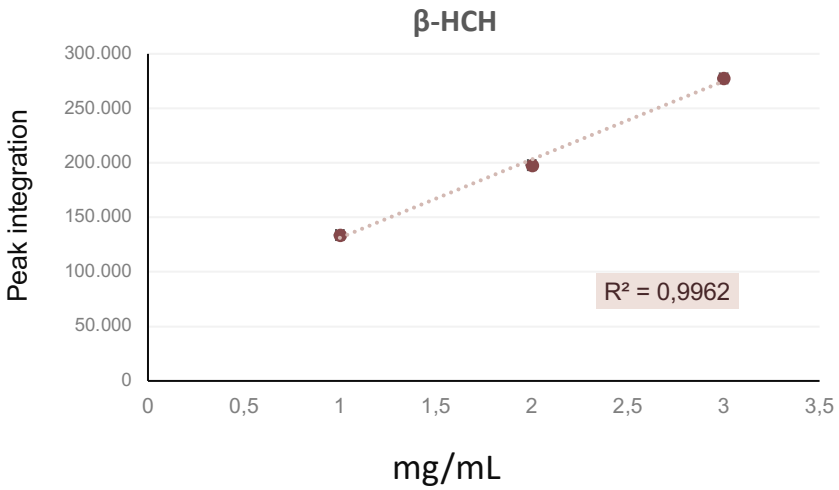

Figure 45. Calibration curve for β-HCH obtained plotting peak areas against standard solutions containing, respectively: 0.175 mg/mL, 0.230 mg/mL and 0.35 mg/mL of β-HCH dissolved in MeCN. Analyses carried out on values derived from two different HPLC runs.

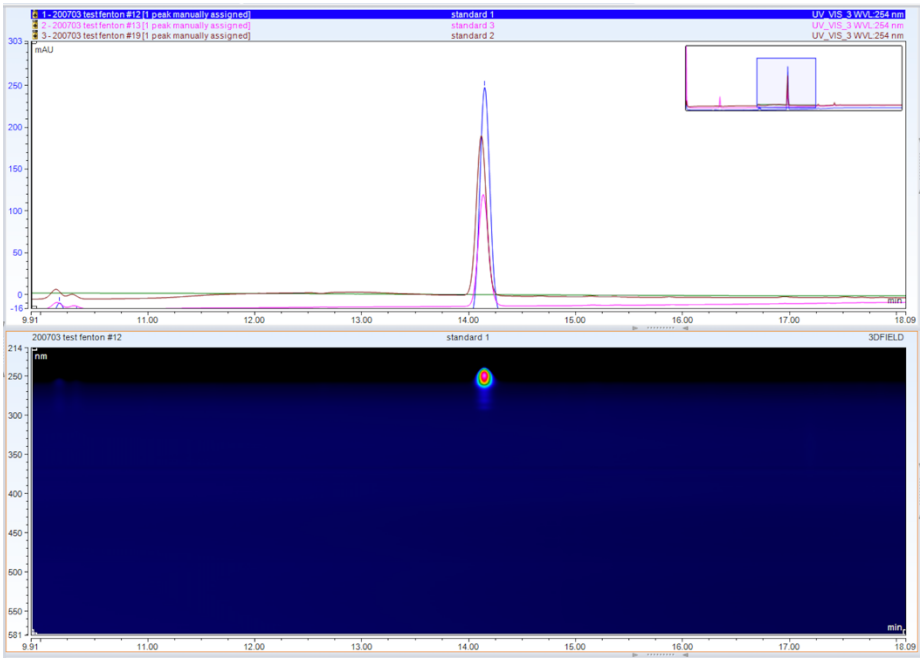

Figure 46. Chromatogram for β-HCH standard solutions. The chromatographic peak for β-HCH was observed at a retention time of approximately 14 minutes. The analyte was eluted using a 30 minutes linear gradient from 50% to 100% MeCN. The peak was detected at 254 nm wavelength; the 3D field spectrum confirmed the purity of β-HCH.

The copper-based Fenton-like reaction has been preferred right away compared to the classic iron-catalyzed oxidation. In fact, the binomen Cu^{2+}/H_2O_2 requires mild pH conditions (NaH_2PO_4/Na_2HPO_4 buffer at pH=7) compatible with enzymatic and biological systems, presenting a better fit to the purposes of the study. After several tries for optimizing the process, 80% degradation for 1 mM β-HCH was observed after 30 minutes under copper-catalyzed H_2O_2-mediated oxidation; the compound resulted almost completely degraded after 3 hours (figure 42). No substantial differences were observed between dark Fenton and photo-Fenton reactions.

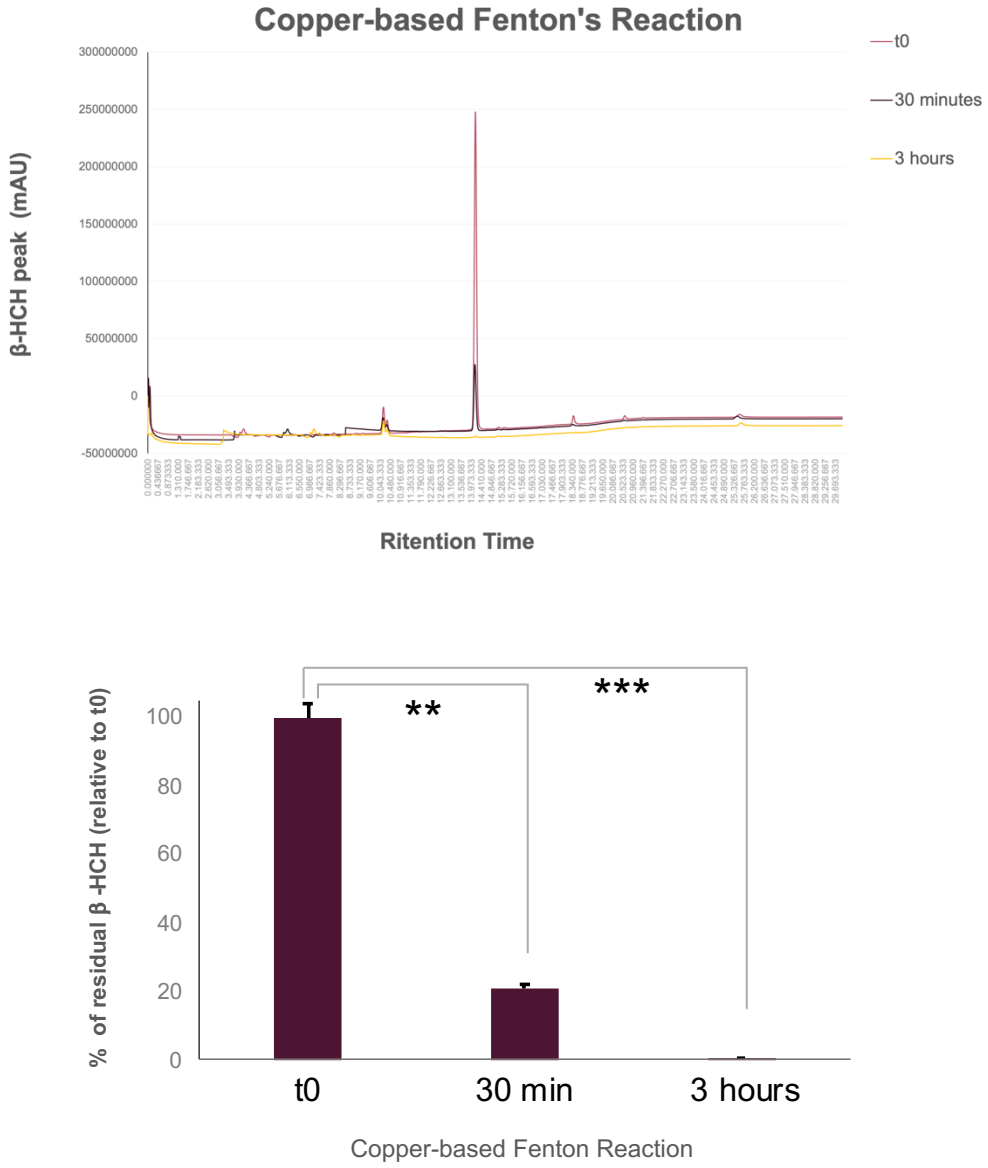

Figure 47. Chromatograms for β-HCH degradation upon Copper-based Fenton's Reaction after 30 minutes and 3 hours. The analyte β-HCH was dissolved in MeCN at the concentration of 1 mM and was incubated with 40 mM H2O2 and 1.6 mM CuSO4 in 50 mM NaH2PO4/Na2HPO4 buffer at pH =7. The histogram relative to the residual β-HCH was constructed by integrating the peak areas and the percentage was calculated at t0 (just immediately before the reaction started). Statistically significative differences (**p<0.01; ***p<0.001) are marked with asterisks.

Further experiments were carried out varying the pH conditions (pH=5) and adding some enhancers (i.e. chlorophyllin[128]) to try to increase the efficiency of light-driven oxidation reaction; however, the Cu^{2+}/H_2O_2 system at pH=7 seems the one that better works in terms of costs and β-HCH removal rate. This chemical approach may be particularly advantageous considering that β-HCH is mostly present as a contaminant in the form of massive physical stockpiles.

7.2.2. Remarks and future perspectives.

The mild experimental conditions (aqueous environment at a neutral pH range) employed for these studies may open up the possibility to inspect the capability of enzymatic systems, such as laccases, for β-HCH removal. Preliminary analyses were performed using a commercially available laccase (Novozyme, cat. 51003) in combination with different well-established mediators[129-130]. Unfortunately, COVID-19 pandemic outbreak imposed a forced stop and was not possible to conduct further experiments. However, the bioremediation of β-HCH by combining enzymatic and chemical approaches is very promising and, in the future, need to be explored in detail.

In addition, possible β-HCH breakdown products should be identified and subjected to molecular and cellular studies in order to clarify whether the removal-derived compounds are less toxic than β-HCH.

7.3. Materials and methods.

β-HCH powder was purchased from Sigma Aldrich (cat. 33376) and was dissolved in pure acetonitrile for the analyses. β-HCH removal studies were carried out in Eppendorf tubes. Reaction solutions (1 mL) contained 1 mM β-HCH, 40 mM H_2O_2 and 1.6 mM $CuSO_4$ in 50 mM NaH_2PO_4/Na_2HPO_4 buffer

at pH =7. The process was conducted at 37°C under constant agitation and the incubation time points ranged from 60 up to 180 minutes. After the oxidation reaction, the protocol employed by *Kruid et al.*[79] for BPA detection has been optimized for β-HCH analyses. A 150 µL aliquot from the reaction solution was quenched with 12 µL of 1M NaOH and subsequently diluted with 600 µL. After centrifuging, 175 µL of supernatant were analyzed by HPLC.

Measurements were made with an Ultimate3000 HPLC equipped with a UV-Vis detector and each sample was analyzed on a Luna Omega C18 polar column Phenomenex. The analyte was eluted using a 30 minutes linear gradient from 50% to 100% MeCN at a flow rate of 0.5 mL/min. β-HCH was detected at 254 nm wavelength. Glass pipettes and vials were used during the entire process.

8. Results: STAT3 in prostate cancer progression.

8.1. STAT3 in prostate cancer.

Prostate cancer (PCa) represents one of the leading causes of morbidity and mortality among adult males in Western countries. It is a multifactorial and biologically heterogeneous disease that could progress to an advanced hormone-refractory stage, which is still considered incurable. The molecular basis of PCa pathogenesis and evolution are marked by the aberrant activity of alternative regulatory pathways other than the androgen receptors (ARs)[131]. Several *in vitro* and *in vivo* studies identify STAT3 (Signal Transducer and Activator of Transcription 3) as a main player in cellular events responsible for the insurgence, progression and development of metastatic PCa[132].

8.2. Study of STAT3 PTMs pattern in prostate cancer.

STAT3 represents a hub protein in the intricate network of intracellular pathways and its different PTMs (p-Y705, p-S727, Ac-K685 and Glut-C328/C542) orchestrate its pleiotropic activity, reflecting specific cellular states as inflammation or oxidative stress[133]. In a previous paper from our research group entitled *Analysis of STAT3 post-translational modifications (PTMs) in human prostate cancer with different Gleason Score* [134] the pattern of STAT3 PTMs was investigated on human prostate FFPE tissue samples at different Gleason Score, collected from 63 patients who underwent total prostatectomy. The Gleason score is a grading system that identifies the aggressiveness of prostate cancer based on its morphological characteristics. In particular, prostate cancer with higher Gleason scores is more aggressive and is associated with a worse prognosis compared with those at lower Gleason scores[135]. This study found out that the distribution of specific STAT3 PTMs in prostate tissues at different Gleason scores follows a specific expression

program. Indeed, while STAT3 acetylation at K685 was observed in tissues with a value of Gleason score 6, characterized by an overall inflammatory condition, STAT3 glutathionylation and phosphorylation at S727 were present in Gleason Score 9, where the oxidative stress is predominant.

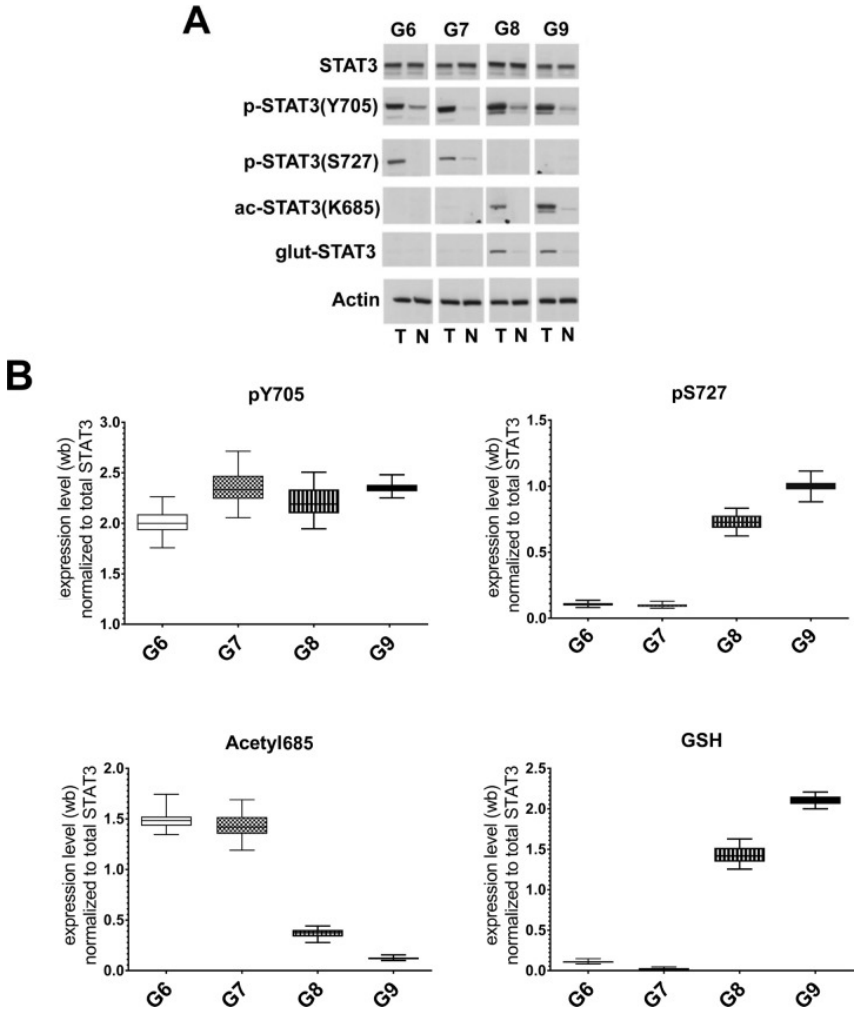

Figure 48. (A) Representative western blot analysis of protein extracted from FFPE corresponding to Gleason Scores (G) 6, 7, 8 and 9. T: prostate carcinomas; N: normal tissue, adjacent to tumor. (B) Cumulative results of STAT3 PTMs levels in tumor prostate tissues from 65 matched prostate tumors. *Cocchiola et al. 2017.*

A follow-up study in cellular models entitled *STAT3 Post-Translational Modifications Drive Cellular Signaling Pathways in Prostate Cancer Cells*[122] corroborated the existence of a link between PTMs and specific STAT3-mediated pathways in dependence on cellular environmental conditions. Experiments were performed on less aggressive LNCaP and more aggressive DU-145 prostate cancer cell lines simulating inflammation and oxidative stress. The more aggressive DU-145 cell line, characterized by constitutive oxidative-stress conditions, typical of tumors at advanced clinical phases, was used to compare the results obtained on LNCaP cells. The phosphorylation at Y705 was confirmed to be the common denominator of STAT3 signaling cascades; in addition, STAT3 was acetylated in response to cytokines, whereas its glutathionylation and phosphorylation at S727 occurred upon treatment with tert-butyl hydroperoxide (t-BHP). Furthermore, this research identified some modulators of STAT3 PTMs. In fact, all STAT3 PTMs reflect the dynamic balance between epigenetic "writers" and "erasers" that interplay with each other to adapt to intracellular state variations. In particular, the acetyltransferase P300 has been identified as a STAT3 co-interactor in samples treated with IL-6, while APE1/Ref-1, a multifunctional protein responsible for controlling the intracellular response to oxidative stress, was detected in conjunction with STAT3 glutathionylation induced by t-BHP.

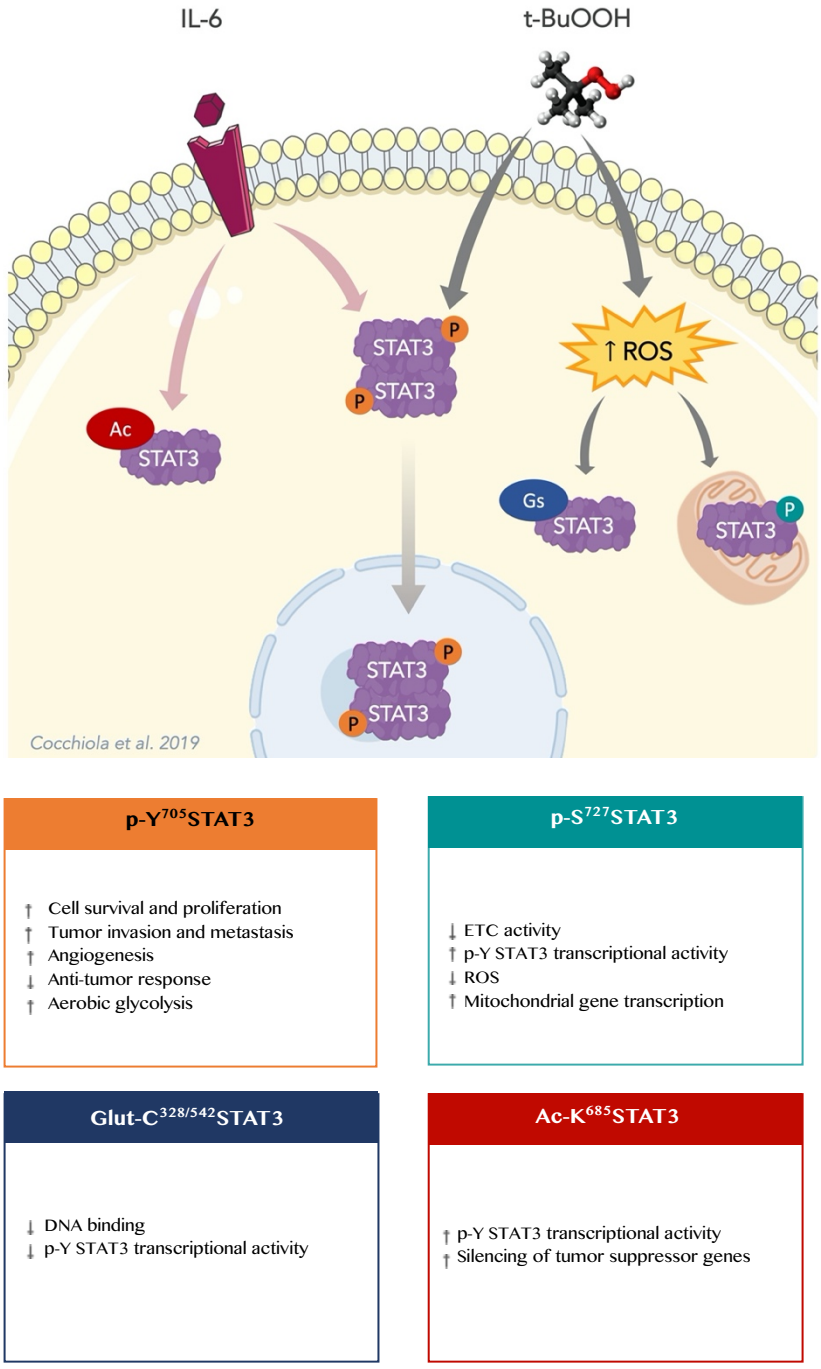

Figure 49. STAT3 PTMs drive the transcriptional program of STAT3 in prostate cancer in a stimulus-specific manner. Adapted from *Cocchiola et al.* 2019.

8.3. STAT3 in prostate cancer energy metabolism.

Prostate cancer (PCa) is a multifactorial disease characterized by the aberrant activity of different regulatory pathways, including those mediated by the protein STAT3. In particular, these pathways are able to interfere with cellular energy metabolism by redirecting glycolysis to lactate production, triggering the Warburg effect under normoxic conditions[136]. The establishment of the Warburg effect drives tumor cells to high glucose consumption, a reduction in cellular respiration, and an increased synthesis of one-carbon units for the biosynthesis of nucleotides, proteins, and lipids, together with glutathione. As result of this metabolic shift, PCa cells survive, even in the presence of a significantly increased demand of precursors that occurs during uncontrolled proliferation. The requirement of higher energy levels is supplied by a rise in oxidative phosphorylation that, in turn, could result in an increased and harmful ROS production [137]. Recently, a STAT3-dependent maintenance of the Warburg effect has been described under hypoxia or oxidative stress conditions via activation of a STAT3/HIF-1α/PKM2 loop[40]. HIF-1α (Hypoxia Inducible Factor 1-α) is a transcription factor that acts as a protein sensor of hypoxia and/or oxidative stress conditions[138]; PKM2 is a pyruvate kinase isoform expressed during embryonic development, regeneration, and tumorigenesis that catalyses the conversion of phosphoenolpyruvate to pyruvate with different efficacy depending on its quaternary state (tetrameric or dimeric)[139]. The Warburg effect is also related to an active one-carbon unit metabolism, primarily involving the amino acid serine, which is an allosteric modulator of PKM2[140]. Serine is also a substrate for the mitochondrial enzyme SHMT2 (Serine Hydroxymethyl-Transferase 2)[141]. A bioinformatic analysis indicated a STAT3 binding site in the upstream region of SHMT2 gene. We

demonstrated that in LNCaP cells (human prostate cancer) SHMT2 expression is upregulated by the JAK2/STAT3 canonical pathway upon IL-6 stimulation. Activation of SHTM2 leads to a decrease in serine levels, pushing PKM2 towards the nuclear compartment where it can activate STAT3 in a non-canonical fashion that, in turn, promotes a transient shift toward anaerobic metabolism. These results were also confirmed on FFPE prostate tissue sections at different Gleason scores. STAT3/SHMT2/PKM2 loop in LNCaP cells can modulate a metabolic shift in response to inflammation at early stages of cancer progression, whereas a non-canonical STAT3 activation involving the STAT3/HIF-1α/PKM2 loop is responsible for the maintenance of Warburg effect distinctive of more aggressive PCa cells. SHMT2 could represent a missing factor to further understand the molecular mechanisms responsible for the transition of prostate cancer towards a more aggressive phenotype[123].

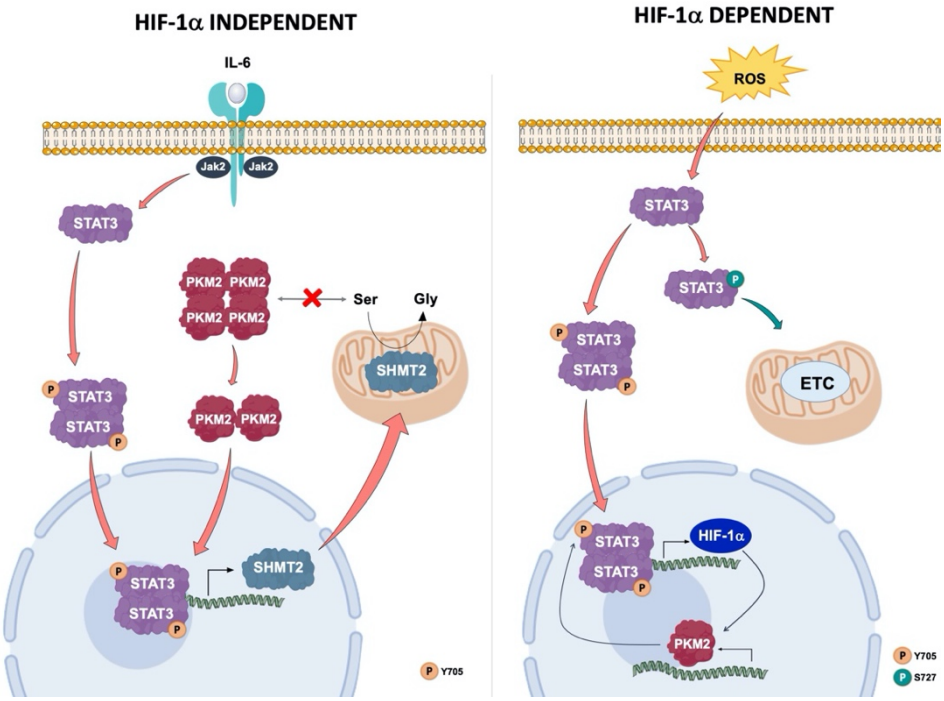

Figure 50. Model loops involving STAT3 and PKM2

9. Conclusions.

Over the past few years ecological awareness has progressively permeated the public opinion, impacting especially on young people.

The need to turn the tide toward a sustainable world is becoming increasingly urgent and is addressing the efforts of the scientific community to the problem of environmental pollution. In order to achieve this challenging goal, nothing can be left out or underestimated, not even apparently marginal situations. The β-isomer of hexachlorocyclohexane is a small molecule unknown to most and, for this reason, is poorly studied. Nevertheless, in contrast to its little fame, β-HCH is widely diffused all around the world, accounting for millions of tons illegally buried in many different countries.

The lack of knowledge about β-HCH, compared to the best-known lindane, means that any new information could provide an important element to achieve a more comprehensive overview on this compound, opening the way to further research insights. In this context, results from our studies are particularly significant and represent a starting point for delving into the still little-known world of β-HCH.

Appendix

International Journal of *Molecular Sciences*

MDPI

Article

STAT3 is a hub protein of cellular signaling pathways triggered by β-hexachlorocyclohexane

Elisabetta Rubini [1], Fabio Altieri [1,2], Silvia Chichiarelli [1], Flavia Giamogante [1], Stefania Carissimi [1], Giuliano Paglia [1], Alberto Macone [1] and Margherita Eufemi [1,2,*]

[1] Department of Biochemical Sciences, A. Rossi Fanelli, Sapienza University, P.le A. Moro 5, 00185 Rome, Italy; elisabetta.rubini@uniroma1.it (E.R.); fabio.altieri@uniroma1.it (F.A.); silvia.chichiarelli@uniroma1.it (S.C.); flavia.giamogante@uniroma1.it (F.G.); stefania.carissimi@uniroma1.it (S.C.); giuliano.pag@gmail.com (G.P.); alberto.macone@uniroma1.it (A.M.)

[2] Istituto Pasteur-Fondazione Cenci Bolognetti, Sapienza University, P.le A. Moro 5, 00185 Rome, Italy

* Correspondence: margherita.eufemi@uniroma1.it; Tel.: +39-06-49910598

Received: 26 June 2018; Accepted: 17 July 2018; Published: 20 July 2018

check for updates

Abstract: Background: Organochlorine pesticides (OCPs) are widely distributed in the environment and their toxicity is mostly associated with the molecular mechanisms of endocrine disruption. Among OCPs, particular attention was focused on the effects of β-hexaclorocyclohexane (β-HCH), a widely common pollutant. A detailed epidemiological study carried out on exposed population in the "Valle del Sacco" found correlations between the incidence of a wide range of diseases and the occurrence of β-HCH contamination. Taking into account the pleiotropic role of the protein signal transducer and activator of transcription 3 (STAT3), its function as a hub protein in cellular signaling pathways triggered by β-HCH was investigated in different cell lines corresponding to tissues that are especially vulnerable to damage by environmental pollutants. Materials and Methods: Human prostate cancer (LNCaP), human breast cancer (MCF-7 and MDA-MB 468), and human hepatoma (HepG2) cell lines were treated with 10 μM β-HCH in the presence or absence of specific inhibitors for different receptors. All samples were subjected to analysis by immunoblotting and RT-qPCR. Results and Conclusions: The preliminary results allow us to hypothesize the involvement of STAT3, through both its canonical and non-canonical pathways, in response to β-HCH. Moreover, we ascertained the role of STAT3 as a master regulator of energy metabolism via the altered expression and localization of HIF-1α and PKM2, respectively, resulting in a Warburg-like effect.

Keywords: STAT3; β-hexaclorocyclohexane (β-HCH); signal transduction; energy metabolism

1. Introduction

Organochlorine compounds are widely distributed in the environment and several studies link their basic molecular mechanism of endocrine disruption [1,2] with the onset of many pathological conditions such as chronic inflammatory processes, cardiovascular diseases, neurological and metabolic disorders, and oncogenesis [3–5]. The toxicity of organochlorine compounds is related to their physicochemical properties, because these pollutants belong to a group of organic compounds, known as "persistent organic pollutants" (POPs), that are resistant to degradation or biodegradation and that can be bioaccumulated into adipose tissue because of their lipotropic properties and great stability [6]. Observational epidemiological studies, carried out on population at high risk of exposure, revealed that POPs may play an important role in the development of a chronic inflammatory state by interfering with pathways associated with essential cellular processes and homeostasis [7]. Acute inflammation represents one of the early responses to injury but, if the causal insult becomes persistent, it may progress with a long chronic phase; although acute inflammation is necessary to rid the organism of

International Journal of
Molecular Sciences

MDPI

Article

STAT3 Post-Translational Modifications Drive Cellular Signaling Pathways in Prostate Cancer Cells

Rossana Cocchiola [1], Elisabetta Rubini [1], Fabio Altieri [1], Silvia Chichiarelli [1], Giuliano Paglia [1], Donatella Romaniello [2], Stefania Carissimi [1], Alessandra Giorgi [1], Flavia Giamogante [1], Alberto Macone [1], Giacomo Perugia [3], Aymone Gurtner [4] and Margherita Eufemi [1,*]

[1] Department of Biochemical Sciences "A. Rossi Fanelli" and Istituto Pasteur-Fondazione Cenci Bolognetti, Sapienza University, P.le A. Moro 5, 00185 Rome, Italy; rossana.cocchiola@uniroma1.it (R.C.); elisabetta.rubini@uniroma1.it (E.R.); fabio.altieri@uniroma1.it (F.A.); silvia.chichiarelli@uniroma1.it (S.C.); giuliano.paglia@uniroma1.it (G.P.); stefania.carissimi@uniroma1.it (S.C.); alessandra.giorgi@uniroma1.it (A.G.); flavia.giamogante@uniroma1.it (F.G.); alberto.macone@uniroma1.it (A.M.)

[2] Department of Biological Regulation, Weizmann Institute of Science, 234 Herzl Street, 7610001 Rehovot, Israel; donatella.romaniello@weizmann.ac.il

[3] Department of Gynecological-Obstretic Science and Urologic Sciences, Sapienza University, V.le Dell'Università, 00185 Rome, Italy; giacomo.perugia@uniroma1.it

[4] Department of Research, Advanced Diagnostics, and Technological Innovation, Translational Research Area, Regina Elena National Cancer Institute; via Elio Chianesi, 53, 00144 Rome, Italy; aymone.gurtner@ifo.gov.it

* Correspondence: margherita.eufemi@uniroma1.it; Tel.: +39-064-991-0598; Fax: +39-064-440-062

Received: 5 March 2019; Accepted: 9 April 2019; Published: 12 April 2019

Abstract: STAT3 is an oncoprotein overexpressed in different types of tumors, including prostate cancer (PCa), and its activity is modulated by a variety of post-translational modifications (PTMs). Prostate cancer represents the most common cancer diagnosed in men, and each phase of tumor progression displays specific cellular conditions: inflammation is predominant in tumor's early stage, whereas oxidative stress is typical of clinically advanced PCa. The aim of this research is to assess the correspondence between the stimulus-specificity of STAT3 PTMs and definite STAT3-mediated transcriptional programs, in order to identify new suitable pharmacological targets for PCa treatment. Experiments were performed on less-aggressive LNCaP and more aggressive DU-145 cell lines, simulating inflammatory and oxidative-stress conditions. Cellular studies confirmed pY705-STAT3 as common denominator of all STAT3-mediated signaling. In addition, acK685-STAT3 was found in response to IL-6, whereas glutC328/542-STAT3 and pS727-STAT3 occurred upon tert-butyl hydroperoxyde (tBHP) treatment. Obtained results also provided evidence of an interplay between STAT3 PTMs and specific protein interactors such as P300 and APE1/Ref-1. In accordance with these outcomes, mRNA levels of STAT3-target genes seemed to follow the differing STAT3 PTMs. These results highlighted the role of STAT3 and its PTMs as drivers in the progression of PCa.

Keywords: STAT3; post translational modification; prostate cancer; transduction signaling

1. Introduction

Prostate cancer (PCa) represents one of the leading causes of morbidity and mortality among adult males in Western countries. It is a multifactorial and biologically heterogeneous disease that could progress to an advanced hormone-refractory stage, which is still considered incurable [1,2].

Prostate cancer is characterized by the dysregulation of several intracellular pathways and its onset and progression are determined by the presence and activation status of the androgen receptor

cells

MDPI

Article

Shmt2: A Stat3 Signaling New Player in Prostate Cancer Energy Metabolism

Ilaria Marrocco [1,†], Fabio Altieri [1], Elisabetta Rubini [1], Giuliano Paglia [1], Silvia Chichiarelli [1], Flavia Giamogante [1], Alberto Macone [1], Giacomo Perugia [2], Fabio Massimo Magliocca [3], Aymone Gurtner [4], Bruno Maras [1], Rino Ragno [5,6], Alexandros Patsilinakos [5,6], Roberto Manganaro [6] and Margherita Eufemi [1,*]

1 Department of Biochemical Sciences "A. Rossi Fanelli" and Istituto Pasteur-Fondazione Cenci Bolognetti, Sapienza University, P.le A. Moro 5, 00185 Rome, Italy
2 Department of Maternal Child and Urologic Sciences, Sapienza University, V.le Dell'Università 33, 00185 Rome, Italy
3 Department of Radiological, Oncological and Pathological Sciences, Sapienza University, V.le del Policlinico 155, 00161 Rome, Italy
4 Department of Research, Advanced Diagnostics, and Technological Innovation, Translational Research Area, Regina Elena National Cancer Institute; via Elio Chianesi 53, 00144 Rome, Italy
5 Rome Center for Molecular Design, Sapienza University, P.le Aldo Moro 5, 00185 Rome, Italy
6 Alchemical Dynamics s.r.l., 00125 Rome, Italy
* Correspondence: margherita.eufemi@uniroma1.it; Tel.: +39-06-4991-0598
† Current Affiliation: Department of Biological Regulation, Weizmann Institute of Science, 234 Herzl Street, Rehovot 7610001, Israel.

Received: 25 July 2019; Accepted: 6 September 2019; Published: 6 September 2019

Abstract: Prostate cancer (PCa) is a multifactorial disease characterized by the aberrant activity of different regulatory pathways. STAT3 protein mediates some of these pathways and its activation is implicated in the modulation of several metabolic enzymes. A bioinformatic analysis indicated a STAT3 binding site in the upstream region of SHMT2 gene. We demonstrated that in LNCaP, PCa cells' SHMT2 expression is upregulated by the JAK2/STAT3 canonical pathway upon IL-6 stimulation. Activation of SHTM2 leads to a decrease in serine levels, pushing PKM2 towards the nuclear compartment where it can activate STAT3 in a non-canonical fashion that in turn promotes a transient shift toward anaerobic metabolism. These results were also confirmed on FFPE prostate tissue sections at different Gleason scores. STAT3/SHMT2/PKM2 loop in LNCaP cells can modulate a metabolic shift in response to inflammation at early stages of cancer progression, whereas a non-canonical STAT3 activation involving the STAT3/HIF-1α/PKM2 loop is responsible for the maintenance of Warburg effect distinctive of more aggressive PCa cells. Chronic inflammation might thus prime the transition of PCa cells towards more advanced stages, and SHMT2 could represent a missing factor to further understand the molecular mechanisms responsible for the transition of prostate cancer towards a more aggressive phenotype.

Keywords: STAT3; SHMT2; prostate cancer; signaling transduction; Warburg effect; cell metabolism

1. Introduction

Prostate cancer (PCa) is a biologically heterogeneous disease, with great differences in its clinical and histological features. The molecular basis of PCa pathogenesis and progression, in fact, is marked by the aberrant activity of alternative regulatory pathways (IL-6, EGF, STAT3, PI3K, PTEN, AKT, mTOR, MAPK) other than the androgen receptors (ARs) signaling [1]. In particular, these pathways are able to interfere with cellular energy metabolism by redirecting glycolysis to lactate production, triggering the

cells

MDPI

Article

Modulation of STAT3 Signaling, Cell Redox Defenses and Cell Cycle Checkpoints by β-Caryophyllene in Cholangiocarcinoma Cells: Possible Mechanisms Accounting for Doxorubicin Chemosensitization and Chemoprevention

Antonella Di Sotto [1,*], Silvia Di Giacomo [1], Elisabetta Rubini [2], Alberto Macone [2], Marco Gulli [1,2], Caterina Loredana Mammola [3], Margherita Eufemi [2], Romina Mancinelli [3] and Gabriela Mazzanti [1]

1 Department of Physiology and Pharmacology "V. Erspamer", Sapienza University of Rome, P.le Aldo Moro 5, 00185 Rome, Italy; silvia.digiacomo@uniroma1.it (S.D.G.); marco.gulli@uniroma1.it (M.G.); gabriela.mazzanti@uniroma1.it (G.M.)

2 Department of Biochemical Science "A. Rossi Fanelli", Sapienza University of Rome, P.le Aldo Moro 5, 00185 Rome, Italy; elisabetta.rubini@uniroma1.it (E.R.); alberto.macone@uniroma1.it (A.M.); margherita.eufemi@uniroma1.it (M.E.)

3 Department of Anatomical, Histological, Forensic and Orthopedic Sciences, Sapienza University of Rome, P.le Aldo Moro 5, 00185 Rome, Italy; caterinaloredana.mammola@uniroma1.it (C.L.M.); romina.mancinelli@uniroma1.it (R.M.)

* Correspondence: antonella.disotto@uniroma1.it; Tel.: +39-06-49912497

Received: 19 February 2020; Accepted: 30 March 2020; Published: 2 April 2020

Abstract: Cholangiocarcinoma (CCA) is an aggressive group of biliary tract cancers, characterized by late diagnosis, low effective chemotherapies, multidrug resistance, and poor outcomes. In the attempt to identify new therapeutic strategies for CCA, we studied the antiproliferative activity of a combination between doxorubicin and the natural sesquiterpene β-caryophyllene in cholangiocarcinoma Mz-ChA-1 cells and nonmalignant H69 cholangiocytes, under both long-term and metronomic schedules. The modulation of STAT3 signaling, oxidative stress, DNA damage response, cell cycle progression and apoptosis was investigated as possible mechanisms of action. β-caryophyllene was able to synergize the cytotoxicity of low dose doxorubicin in Mz-ChA-1 cells, while producing cytoprotective effects in H69 cholangiocytes, mainly after a long-term exposure of 24 h. The mechanistic analysis highlighted that the sesquiterpene induced a cell cycle arrest in G2/M phase along with the doxorubicin-induced accumulation in S phase, reduced the γH2AX and GSH levels without affecting GSSG. ROS amount was partly lowered by the combination in Mz-ChA-1 cells, while increased in H69 cells. A lowered expression of doxorubicin-induced STAT3 activation was found in the presence of β-caryophyllene in both cancer and normal cholangiocytes. These networking effects resulted in an increased apoptosis rate in Mz-ChA-1 cells, despite a lowering in H69 cholangiocytes. This evidence highlighted a possible role of STAT3 as a final effector of a complex network regulated by β-caryophyllene, which leads to an enhanced doxorubicin-sensitivity of cholangiocarcinoma cells and a lowered chemotherapy toxicity in nonmalignant cholangiocytes, thus strengthening the interest for this natural sesquiterpene as a dual-acting chemosensitizing and chemopreventive agent.

Keywords: chemoprevention; genoprotective effects; caryophyllane sesquiterpenes; liver cancer; metronomic schedule; GSH depletion; apoptosis; H2AX phosphorylation; cholangiocytes; cell cycle checkpoint; STAT3 signaling

biomedicines

MDPI

Article

β-Hexachlorocyclohexane: A Small Molecule with a Big Impact on Human Cellular Biochemistry

Elisabetta Rubini [1,2], Giuliano Paglia [1], David Cannella [2], Alberto Macone [1], Antonella Di Sotto [3], Marco Gullì [3], Fabio Altieri [1,†] and Margherita Eufemi [1,*,†]

[1] Department of Biochemical Science "A. Rossi Fanelli", Faculty of Pharmacy and Medicine, Sapienza University of Rome, P.le Aldo Moro 5, 00185 Rome, Italy; elisabetta.rubini@uniroma1.it (E.R.); giuliano.paglia@uniroma1.it (G.P.); alberto.macone@uniroma1.it (A.M.); fabio.altieri@uniroma1.it (F.A.)

[2] PhotoBioCatalysis Unit–Bio-Cat, Interfaculty School of Bioengineers, Université libre de Bruxelles, CP245, Bd du Triomphe, 1050 Brussels, Belgium; david.cannella@ulb.ac.be

[3] Department of Physiology and Pharmacology "V. Erspamer", Faculty of Pharmacy and Medicine, Sapienza University of Rome, P.le Aldo Moro 5, 00185 Rome, Italy; antonella.disotto@uniroma1.it (A.D.S.); marco.gulli@uniroma1.it (M.G.)

* Correspondence: margherita.eufemi@uniroma1.it; Tel.: +39-06-4991-0598

† These authors contributed equally to this work.

Received: 8 September 2020; Accepted: 13 November 2020; Published: 16 November 2020

Abstract: Organochlorine pesticides (OCPs) belong to a heterogeneous class of organic compounds blacklisted by the Stockholm Convention in 2009 due to their harmful impact on human health. Among OCPs, β-hexachlorocyclohexane (β-HCH) is one of the most widespread and, at the same time, poorly studied environmental contaminant. Due to its physicochemical properties, β-HCH is the most hazardous of all HCH isomers; therefore, clarifying the mechanisms underlying its molecular action could provide further elements to draw the biochemical profile of this OCP. For this purpose, LNCaP and HepG2 cell lines were used as models and were subjected to immunoblot, immunofluorescence, and RT-qPCR analysis to follow the expression and mRNA levels, together with the distribution, of key biomolecules involved in the intracellular responses to β-HCH. In parallel, variations in redox homeostasis and cellular bioenergetic profile were monitored to have a complete overview of β-HCH effects. Obtained results strongly support the hypothesis that β-HCH could be an endocrine disrupting chemical as well as an activator of AhR signaling, promoting the establishment of an oxidative stress condition and a cellular metabolic shift toward aerobic glycolysis. In this altered context, β-HCH can also induce DNA damage through H2AX phosphorylation, demonstrating its multifaceted mechanisms of action.

Keywords: β-hexachlorocyclohexane; organochlorine pesticides; endocrine disrupting chemical; aryl hydrocarbon receptor; oxidative stress; DNA damage; energy metabolism; cancer; environmental pollution

1. Introduction

Organochlorine pesticides (OCPs) represent 40% of total environmental pollutants and constitute a significant source of contamination all over the world. OCPs exhibit a related chemical structure characterized by aliphatic or aromatic chlorine-substituted rings and their hazardousness is mostly due to shared physicochemical properties, such as lipophilia and energetic stability, responsible for the persistence and high bioaccumulation potential of these molecules [1].

In recent years, growing attention has been paid to the hexachlorocyclohexane (HCH), a chlorinated cyclic saturated hydrocarbon listed as "POP" (persistent organic pollutant) by the Stockholm Convention and finally banned in 2009 [2].

Bibliography

1. Mostafalou, S. & Abdollahi, M. Pesticides and human chronic diseases: Evidences, mechanisms, and perspectives. *Toxicol. Appl. Pharmacol.* **268**, 157–177 (2013).
2. Gupta, P. K. Pesticide exposure - Indian scene. *Toxicology* **198**, 83–90 (2004).
3. Stockholm Convention on Persistent Organic Pollutants (POPs). in *Encyclopedia of Corporate Social Responsibility* 2336–2336 (Springer Berlin Heidelberg, 2013). doi:10.1007/978-3-642-28036-8_101506
4. Jayaraj, R., Megha, P. & Sreedev, P. Review Article. Organochlorine pesticides, their toxic effects on living organisms and their fate in the environment. *Interdiscip. Toxicol.* **9**, 90–100 (2016).
5. Pimentel, D. Amounts of pesticides reaching target pests: Environmental impacts and ethics. *J. Agric. Environ. Ethics* (1995). doi:10.1007/BF02286399
6. Mnif, W. *et al.* Effect of endocrine disruptor pesticides: A review. *Int. J. Environ. Res. Public Health* **8**, 2265–2303 (2011).
7. Burki, T. K. Regulating endocrine disruptors linked to cancer. *Lancet. Oncol.* **20**, e246 (2019).
8. Demeneix, B. & Slama, R. Endocrine Disruptors : from Scientific Evidence to Human Health Protection. *Endocr. Disruptors from Sci. Evid. to Hum. Heal. Prot.* 128 p. (2019).
9. Soto, A. M. & Sonnenschein, C. Endocrine disruptors: DDT, endocrine disruption and breast cancer. *Nat. Rev. Endocrinol.* **11**, 507–508 (2015).
10. Quagliariello, V. *et al.* Metabolic syndrome, endocrine disruptors and prostate cancer associations: Biochemical and pathophysiological evidences. *Oncotarget* (2017). doi:10.18632/oncotarget.16725
11. Ben-Jonathan, N. Endocrine disrupting chemicals and breast cancer: the saga of bisphenol a. in *Cancer Drug Discovery and Development* (2019). doi:10.1007/978-3-319-99350-8_13
12. Abderrahman, B. & Jordan, V. C. *Steroid receptors in breast cancer*. *The Breast: Comprehensive Management of Benign and Malignant Diseases* (Elsevier Inc., 2018). doi:10.1016/B978-0-323-35955-9.00021-0
13. Tabb, M. M. & Blumberg, B. New modes of action for endocrine-disrupting chemicals. *Mol. Endocrinol.* **20**, 475–482 (2006).

14. Griekspoor, A., Zwart, W., Neefjes, J. & Michalides, R. Visualizing the action of steroid hormone receptors in living cells. *Nucl. Recept. Signal.* **5**, 1–9 (2007).
15. La Merrill, M. A. *et al.* Consensus on the key characteristics of endocrine-disrupting chemicals as a basis for hazard identification. *Nat. Rev. Endocrinol.* **16**, 45–57 (2020).
16. De Coster, S. & Van Larebeke, N. Endocrine-disrupting chemicals: Associated disorders and mechanisms of action. *Journal of Environmental and Public Health* (2012). doi:10.1155/2012/713696
17. Larigot, L., Juricek, L., Dairou, J. & Coumoul, X. AhR signaling pathways and regulatory functions. *Biochim. Open* **7**, 1–9 (2018).
18. Rothhammer, V. & Quintana, F. J. The aryl hydrocarbon receptor: an environmental sensor integrating immune responses in health and disease. *Nat. Rev. Immunol.* **19**, 184–197 (2019).
19. Larigot, L., Juricek, L., Dairou, J. & Coumoul, X. AhR signaling pathways and regulatory functions. *Biochimie Open* (2018). doi:10.1016/j.biopen.2018.05.001
20. Marroqui, L. *et al.* Mitochondria as target of endocrine-disrupting chemicals: Implications for type 2 diabetes. *J. Endocrinol.* **239**, R27–R45 (2018).
21. Poljšak, B. & Fink, R. The protective role of antioxidants in the defence against ROS/RNS-mediated environmental pollution. *Oxid. Med. Cell. Longev.* **2014**, (2014).
22. Narayanan, K. B. *et al.* Disruptive environmental chemicals and cellular mechanisms that confer resistance to cell death. *Carcinogenesis* (2015). doi:10.1093/carcin/bgv032
23. Horvath, C. M. STAT proteins and transcriptional responses to extracellular signals. *Trends in Biochemical Sciences* (2000). doi:10.1016/S0968-0004(00)01624-8
24. Peyser, N. D. & Grandis, J. R. Critical analysis of the potential for targeting STAT3 in human malignancy. *Onco. Targets. Ther.* **6**, 999–1010 (2013).
25. Calò, V. *et al.* STAT Proteins: From Normal Control of Cellular Events to Tumorigenesis. *J. Cell. Physiol.* **197**, 157–168 (2003).
26. Takeda, K. & Akira, S. STAT family of transcription factors in cytokine-mediated biological responses. *Cytokine Growth Factor Rev.* **11**, 199–207 (2000).
27. Yu, H. & Jove, R. The stats of cancer - New molecular targets come of age. *Nat. Rev. Cancer* **4**, 97–105 (2004).
28. Ma, J. H., Qin, L. & Li, X. Role of STAT3 signaling pathway in breast cancer. *Cell Communication and Signaling* (2020). doi:10.1186/s12964-020-0527-z
29. Dimri, S., Sukanya & De, A. Approaching non-canonical STAT3 signaling to redefine

cancer therapeutic strategy. *Integr. Mol. Med.* (2017). doi:10.15761/imm.1000268

30. Avalle, L. & Poli, V. Nucleus, mitochondrion, or reticulum? STAT3 à la carte. *International Journal of Molecular Sciences* (2018). doi:10.3390/ijms19092820
31. Rincon, M. & Pereira, F. V. A new perspective: Mitochondrial stat3 as a regulator for lymphocyte function. *International Journal of Molecular Sciences* (2018). doi:10.3390/ijms19061656
32. Yang, R. & Rincon, M. Mitochondrial Stat3, the need for design thinking. *International Journal of Biological Sciences* (2016). doi:10.7150/ijbs.15153
33. Ardito, F., Giuliani, M., Perrone, D., Troiano, G. & Muzio, L. Lo. The crucial role of protein phosphorylation in cell signalingand its use as targeted therapy (Review). *International Journal of Molecular Medicine* (2017). doi:10.3892/ijmm.2017.3036
34. Narita, T., Weinert, B. T. & Choudhary, C. Functions and mechanisms of non-histone protein acetylation. *Nature Reviews Molecular Cell Biology* (2019). doi:10.1038/s41580-018-0081-3
35. Townsend, D. M. S-glutathionylation: Indicator of cell stress and regulator of the unfolded protein response. *Molecular Interventions* (2008). doi:10.1124/mi.7.6.7
36. Harhous, Z., Booz, G. W., Ovize, M., Bidaux, G. & Kurdi, M. An Update on the Multifaceted Roles of STAT3 in the Heart. *Frontiers in Cardiovascular Medicine* (2019). doi:10.3389/fcvm.2019.00150
37. Xie, Y., Kole, S., Precht, P., Pazin, M. J. & Bernier, M. S-Glutathionylation impairs signal transducer and activator of transcription 3 activation and signaling. *Endocrinology* (2009). doi:10.1210/en.2008-1241
38. Lee, H., Jeong, A. J. & Ye, S. K. Highlighted STAT3 as a potential drug target for cancer therapy. *BMB Reports* (2019). doi:10.5483/BMBRep.2019.52.7.152
39. Sikka, S. *et al.* Targeting the STAT3 signaling pathway in cancer: Role of synthetic and natural inhibitors. *Biochimica et Biophysica Acta - Reviews on Cancer* (2014). doi:10.1016/j.bbcan.2013.12.005
40. Demaria, M. & Poli, V. PKM2, STAT3 and HIF-1α: The Warburg's vicious circle. *JAK-STAT* (2012). doi:10.4161/jkst.20662
41. Poli, V. & Camporeale, A. STAT3-mediated metabolic reprograming in cellular transformation and implications for drug resistance. *Frontiers in Oncology* (2015). doi:10.3389/fonc.2015.00121
42. Vijgen, J. The Legacy of Lindane HCH Isomer Production. *Int. HCH Pestic. Assoc.*

22 (2006).

43. Vijgen, J., de Borst, B., Weber, R., Stobiecki, T. & Forter, M. HCH and lindane contaminated sites: European and global need for a permanent solution for a long-time neglected issue. *Environ. Pollut.* **248**, 696–705 (2019).
44. UNEP, U. *Report of the Conference of the Parties of the Stockholm Convention on Persistent Organic Pollutants on the work of its fourth meeting*. *United Nations Environment Programme: Stockholm Convention on Persistent Organic Pollutants. Geneva* (2009). doi:10.1007/s11745-004-1250-2
45. Vijgen, J. *et al.* Hexachlorocyclohexane (HCH) as new Stockholm Convention POPs-a global perspective on the management of Lindane and its waste isomers. *Environ. Sci. Pollut. Res.* **18**, 152–162 (2011).
46. Porta, D. *et al.* A biomonitoring study on blood levels of beta-hexachlorocyclohexane among people living close to an industrial area. *Environ. Heal. A Glob. Access Sci. Source* **12**, 1–10 (2013).
47. Vega, M., Romano, D. & Uotila, E. El lindano (contaminante orgánico persistente) en la UE. *PE 571.398. Dep. Temático C Derechos los Ciudad. y Asuntos Const. Parlam. Eur. B-1047 Bruselas* (2016).
48. Narduzzi, S. *et al.* Predictors of Beta-Hexachlorocyclohexane blood levels among people living close to a chemical plant and an illegal dumping site. *Environ. Heal. A Glob. Access Sci. Source* **19**, 1–9 (2020).
49. Rani, M. & Shanker, U. Degradation of traditional and new emerging pesticides in water by nanomaterials: recent trends and future recommendations. *International Journal of Environmental Science and Technology* (2018). doi:10.1007/s13762-017-1512-y
50. WHO. Reducing Global Health Risks. *Through mitigation of short-lived climate pollutants* (2015).
51. Kalita, E. & Baruah, J. Environmental remediation. in *Colloidal Metal Oxide Nanoparticles* (2020). doi:10.1016/b978-0-12-813357-6.00014-0
52. Lo, I. M. C. Innovative waste containment barriers for subsurface pollution control. *Pract. Period. Hazardous, Toxic, Radioact. Waste Manag.* (2003). doi:10.1061/(ASCE)1090-025X(2003)7:1(37)
53. Kumar, A., Joshi, V., Dhewa, T. & Bisht, B. Review on bioremediation of polluted environment: A management tool. *Int. J. Environ. Sci.* (2011).

54. Reichenauer, T. G. & Germida, J. J. Phytoremediation of organic contaminants in soil and groundwater. in *ChemSusChem* (2008). doi:10.1002/cssc.200800125

55. Araújo, S. C. da S. *et al.* MBSP1: a biosurfactant protein derived from a metagenomic library with activity in oil degradation. *Sci. Rep.* (2020). doi:10.1038/s41598-020-58330-x

56. Kujawinski, E. B. *et al.* Fate of dispersants associated with the Deepwater Horizon oil spill. *Environ. Sci. Technol.* (2011). doi:10.1021/es103838p

57. Patel, S., Homaei, A., Patil, S. & Daverey, A. Microbial biosurfactants for oil spill remediation: pitfalls and potentials. *Applied Microbiology and Biotechnology* (2019). doi:10.1007/s00253-018-9434-2

58. Mascarelli, A. Deepwater Horizon dispersants lingered in the deep. *Nature* (2011). doi:10.1038/news.2011.54

59. Koul, B. & Taak, P. Biotechnological strategies for effective remediation of polluted soils. *Biotechnol. Strateg. Eff. Remediat. Polluted Soils* 1–240 (2018). doi:10.1007/978-981-13-2420-8

60. Gan, S., Lau, E. V. & Ng, H. K. Remediation of soils contaminated with polycyclic aromatic hydrocarbons (PAHs). *Journal of Hazardous Materials* (2009). doi:10.1016/j.jhazmat.2009.07.118

61. Bradl, H. & Xenidis, A. Chapter 3 Remediation techniques. *Interface Sci. Technol.* (2005). doi:10.1016/S1573-4285(05)80022-5

62. Khan, F. I., Husain, T. & Hejazi, R. An overview and analysis of site remediation technologies. *J. Environ. Manage.* (2004). doi:10.1016/j.jenvman.2004.02.003

63. Phillips, T. M., Seech, A. G., Lee, H. & Trevors, J. T. Biodegradation of hexachlorocyclohexane (HCH) by microorganisms. *Biodegradation* (2005). doi:10.1007/s10532-004-2413-6

64. Camacho-Pérez, B., Ríos-Leal, E., Rinderknecht-Seijas, N. & Poggi-Varaldo, H. M. Enzymes involved in the biodegradation of hexachlorocyclohexane: A mini review. *Journal of Environmental Management* (2012). doi:10.1016/j.jenvman.2011.06.047

65. Lal, R. *et al.* Biochemistry of Microbial Degradation of Hexachlorocyclohexane and Prospects for Bioremediation. *Microbiol. Mol. Biol. Rev.* (2010). doi:10.1128/mmbr.00029-09

66. Nagata, Y., Endo, R., Ito, M., Ohtsubo, Y. & Tsuda, M. Aerobic degradation of lindane (γ-hexachlorocyclohexane) in bacteria and its biochemical and molecular basis.

Applied Microbiology and Biotechnology (2007). doi:10.1007/s00253-007-1066-x

67. Zhang, W., Lin, Z., Pang, S., Bhatt, P. & Chen, S. Insights Into the Biodegradation of Lindane (γ-Hexachlorocyclohexane) Using a Microbial System. *Frontiers in Microbiology* (2020). doi:10.3389/fmicb.2020.00522
68. Kumar, D. & Pannu, R. Perspectives of lindane (γ-hexachlorocyclohexane) biodegradation from the environment: a review. *Bioresources and Bioprocessing* (2018). doi:10.1186/s40643-018-0213-9
69. Maqbool, Z. *et al.* Perspectives of using fungi as bioresource for bioremediation of pesticides in the environment: a critical review. *Environ. Sci. Pollut. Res.* (2016). doi:10.1007/s11356-016-7003-8
70. Ulčnik, A., Kralj Cigić, I. & Pohleven, F. Degradation of lindane and endosulfan by fungi, fungal and bacterial laccases. *World J. Microbiol. Biotechnol.* (2013). doi:10.1007/s11274-013-1389-y
71. Nitoi, I., Oncescu, T. & Oancea, P. Mechanism and kinetic study for the degradation of lindane by photo-Fenton process. *J. Ind. Eng. Chem.* (2013). doi:10.1016/j.jiec.2012.08.016
72. Pignatello, J. J., Oliveros, E. & MacKay, A. Advanced oxidation processes for organic contaminant destruction based on the fenton reaction and related chemistry. *Crit. Rev. Environ. Sci. Technol.* **36**, 1–84 (2006).
73. Neyens, E. & Baeyens, J. A review of classic Fenton's peroxidation as an advanced oxidation technique. *J. Hazard. Mater.* (2003). doi:10.1016/S0304-3894(02)00282-0
74. Yuan, S., Gou, N., Alshawabkeh, A. N. & Gu, A. Z. Efficient degradation of contaminants of emerging concerns by a new electro-Fenton process with Ti/MMO cathode. *Chemosphere* **93**, 2796–2804 (2013).
75. Wang, N., Zheng, T., Zhang, G. & Wang, P. A review on Fenton-like processes for organic wastewater treatment. *Journal of Environmental Chemical Engineering* (2016). doi:10.1016/j.jece.2015.12.016
76. Bokare, A. D. & Choi, W. *Review of iron-free Fenton-like systems for activating H2O2 in advanced oxidation processes*. *Journal of Hazardous Materials* **275**, (Elsevier B.V., 2014).
77. Malato, S., Fernández-Ibáñez, P., Maldonado, M. I., Blanco, J. & Gernjak, W. Decontamination and disinfection of water by solar photocatalysis: Recent overview and trends. *Catalysis Today* (2009). doi:10.1016/j.cattod.2009.06.018

78. Goi, A. & Trapido, M. Hydrogen peroxide photolysis, Fenton reagent and photo-Fenton for the degradation of nitrophenols: A comparative study. *Chemosphere* (2002). doi:10.1016/S0045-6535(01)00203-X

79. Kruid, J., Fogel, R. & Limson, J. L. Quantitative methylene blue decolourisation assays as rapid screening tools for assessing the efficiency of catalytic reactions. *Chemosphere* (2017). doi:10.1016/j.chemosphere.2017.02.051

80. Yap, C. L., Gan, S. & Ng, H. K. Fenton based remediation of polycyclic aromatic hydrocarbons-contaminated soils. *Chemosphere* (2011). doi:10.1016/j.chemosphere.2011.01.026

81. Begum, A., Agnihotri, P., Mahindrakar, A. B. & Gautam, S. K. Degradation of endosulfan and lindane using Fenton's reagent. *Appl. Water Sci.* (2017). doi:10.1007/s13201-014-0237-z

82. Services, H. AND DELTA-HEXACHLOROCYCLOHEXANE. (2005).

83. Loomis, D. *et al.* Carcinogenicity of lindane, DDT, and 2,4-dichlorophenoxyacetic acid. *Lancet Oncol.* (2015). doi:10.1016/S1470-2045(15)00081-9

84. Traina, M. E. *et al.* Long-lasting effects of lindane on mouse spermatogenesis induced by in utero exposure. *Reprod. Toxicol.* (2003). doi:10.1016/S0890-6238(02)00101-6

85. Olivero-Verbel, J., Guerrero-Castilla, A. & Ramos, N. R. Biochemical effects induced by the hexachlorocyclohexanes. *Rev. Environ. Contam. Toxicol.* (2011). doi:10.1007/978-1-4419-8453-1_1

86. Richardson, J. R. *et al.* β-Hexachlorocyclohexane levels in serum and risk of Parkinson's disease. *Neurotoxicology* (2011). doi:10.1016/j.neuro.2011.04.002

87. Tomczak, S., Baumann, K. & Lehnert, G. Occupational exposure to hexachlorocyclohexane - IV. Sex Hormone Alterations in HCH-exposed Workers. *Int. Arch. Occup. Environ. Health* (1981). doi:10.1007/BF00405615

88. Sharma, H., Zhang, P., Barber, D. S. & Liu, B. Organochlorine pesticides dieldrin and lindane induce cooperative toxicity in dopaminergic neurons: Role of oxidative stress. *Neurotoxicology* (2010). doi:10.1016/j.neuro.2009.12.007

89. Rubini, E. *et al.* STAT3, a hub protein of cellular signaling pathways, is triggered by β-hexaclorocyclohexane. *Int. J. Mol. Sci.* (2018). doi:10.3390/ijms19072108

90. Crawford, E. D. *et al.* Androgen Receptor Targeted Treatments of Prostate Cancer: 35 Years of Progress with Antiandrogens. *Journal of Urology* (2018). doi:10.1016/j.juro.2018.04.083

91. Duffy, M. J. Biomarkers for prostate cancer: Prostate-specific antigen and beyond. *Clinical Chemistry and Laboratory Medicine* (2020). doi:10.1515/cclm-2019-0693

92. Zhao, B., DeGroot, D. E., Hayashi, A., He, G. & Denison, M. S. Ch223191 is a ligand-selective antagonist of the Ah (dioxin) receptor. *Toxicol. Sci.* (2010). doi:10.1093/toxsci/kfq217

93. Shah, H. K., Sharma, T. & Banerjee, B. D. Organochlorine pesticides induce inflammation, ROS production, and DNA damage in human epithelial ovary cells: An in vitro study. *Chemosphere* (2020). doi:10.1016/j.chemosphere.2019.125691

94. Marrocco, I., Altieri, F. & Peluso, I. Measurement and Clinical Significance of Biomarkers of Oxidative Stress in Humans. *Oxidative Medicine and Cellular Longevity* (2017). doi:10.1155/2017/6501046

95. Gwangwa, M. V., Joubert, A. M. & Visagie, M. H. Crosstalk between the Warburg effect, redox regulation and autophagy induction in tumourigenesis. *Cellular and Molecular Biology Letters* (2018). doi:10.1186/s11658-018-0088-y

96. Dong, H. *et al.* Polychlorinated biphenyl quinone-induced genotoxicity, oxidative DNA damage and γ-H2AX formation in HepG2 cells. *Chem. Biol. Interact.* (2014). doi:10.1016/j.cbi.2014.01.016

97. Lushchak, V. I., Matviishyn, T. M., Husak, V. V., Storey, J. M. & Storey, K. B. Pesticide toxicity: A mechanistic approach. *EXCLI Journal* (2018). doi:10.17179/excli2018-1710

98. Mah, L. J., El-Osta, A. & Karagiannis, T. C. γh2AX: A sensitive molecular marker of DNA damage and repair. *Leukemia* (2010). doi:10.1038/leu.2010.6

99. Macip, S., Kosoy, A., Lee, S. W., O'Connell, M. J. & Aaronson, S. A. Oxidative stress induces a prolonged but reversible arrest in p53-null cancer cells, involving a Chk1-dependent G2 checkpoint. *Oncogene* (2006). doi:10.1038/sj.onc.1209629

100. Rubini, E. *et al.* β-Hexachlorocyclohexane: A Small Molecule with a Big Impact on Human Cellular Biochemistry. *Biomedicines* **8**, 1–17 (2020).

101. Blackadar, C. B. Historical review of the causes of cancer. *World Journal of Clinical Oncology* (2016). doi:10.5306/wjco.v7.i1.54

102. Yamagiwa, K. & Ichikawa, K. Experimental study of the pathogenesis of carcinoma. *J. Cancer Res.* (1918). doi:10.1158/jcr.1918.1

103. Loomis, D. IARC Evaluation of the Carcinogenicity of Pesticides: Epidemiological Evidence. 1–19 (2014).

104. Satelli, A. & Li, S. Vimentin in cancer and its potential as a molecular target for cancer therapy. *Cellular and Molecular Life Sciences* (2011). doi:10.1007/s00018-011-0735-1

105. Their, J. P. Epithelial-mesenchymal transitions in tumor progression. *Nature Reviews Cancer* (2002). doi:10.1038/nrc822

106. Correia, I., Chu, D., Chou, Y. H., Goldman, R. D. & Matsudaira, P. Integrating the actin and vimentin cytoskeletons: Adhesion-dependent formation of fimbrin-vimentin complexes in macrophages. *J. Cell Biol.* (1999). doi:10.1083/jcb.146.4.831

107. Kim, J. *et al.* Vimentin filaments regulate integrin-ligand interactions by binding to the cytoplasmic tail of integrin β3. *J. Cell Sci.* (2016). doi:10.1242/jcs.180315

108. Sasaki, T., Hiroki, K. & Yamashita, Y. The role of epidermal growth factor receptor in cancer metastasis and microenvironment. *BioMed Research International* (2013). doi:10.1155/2013/546318

109. Morris, E. J. & Geller, H. M. Induction of neuronal apoptosis by camptothecin, an inhibitor of DNA topoisomerase-I: Evidence for cell cycle-independent toxicity. *J. Cell Biol.* (1996). doi:10.1083/jcb.134.3.757

110. Hanahan, D. & Weinberg, R. A. Hallmarks of cancer: The next generation. *Cell* (2011). doi:10.1016/j.cell.2011.02.013

111. Dasika, G. K. *et al.* DNA damage-induced cell cycle checkpoints and DNA strand break repair in development and tumorigenesis. *Oncogene* (1999). doi:10.1038/sj.onc.1203283

112. Øya, E. *et al.* DNA damage and DNA damage response in human bronchial epithelial BEAS-2B cells following exposure to 2-nitrobenzanthrone and 3-nitrobenzanthrone: Role in apoptosis. *Mutagenesis* (2011). doi:10.1093/mutage/ger035

113. Fernandez-Capetillo, O. *et al.* DNA damage-induced G2-M checkpoint activation by histone H2AX and 53BP1. *Nat. Cell Biol.* (2002). doi:10.1038/ncb884

114. Li, L. T., Jiang, G., Chen, Q. & Zheng, J. N. Predic Ki67 is a promising molecular target in the diagnosis of cancer (Review). *Molecular Medicine Reports* (2015). doi:10.3892/mmr.2014.2914

115. Dzobo, K. *et al.* Chemoresistance to cancer treatment: Benzo-α-pyrene as friend or foe? *Molecules* **23**, 1–23 (2018).

116. Sève, P. & Dumontet, C. Chemoresistance in non-small cell lung cancer. *Current Medicinal Chemistry - Anti-Cancer Agents* (2005). doi:10.2174/1568011053352604

117. Moy, B., Kirkpatrick, P., Kar, S. & Goss, P. Lapatinib. *Nat. Rev. Drug Discov.* (2007). doi:10.1038/nrd2332

118. Siddiquee, K. *et al.* Selective chemical probe inhibitor of Stat3, identified through structure-based virtual screening, induces antitumor activity. *Proc. Natl. Acad. Sci. U. S. A.* (2007). doi:10.1073/pnas.0609757104

119. Liu, L. F. *et al.* Mechanism of action of camptothecin. in *Annals of the New York Academy of Sciences* (2000). doi:10.1111/j.1749-6632.2000.tb07020.x

120. Spencer, C. M. & Faulds, D. Paclitaxel: A Review of its Pharmacodynamic and Pharmacokinetic Properties and Therapeutic Potential in the Treatment of Cancer. *Drugs* (1994). doi:10.2165/00003495-199448050-00009

121. Dasari, S. & Bernard Tchounwou, P. Cisplatin in cancer therapy: Molecular mechanisms of action. *European Journal of Pharmacology* (2014). doi:10.1016/j.ejphar.2014.07.025

122. Cocchiola, R. *et al.* STAT3 post-translational modifications drive cellular signaling pathways in prostate cancer cells. *Int. J. Mol. Sci.* **20**, (2019).

123. Marrocco, I. *et al.* Shmt2: A Stat3 Signaling New Player in Prostate Cancer Energy Metabolism. *Cells* **8**, (2019).

124. Paik, Cho, Kim, Kim, Choi & Lee, G. Simultaneous clinical monitoring of lactic acid, pyruvic acid and ketone bodies in plasma as methoxime/tert- butyldimethylsilyl derivatives by gas chromatography– mass spectrometry in selected ion monitoring mode. *Biomed. Chromatogr.* **288**, 278–288 (2008).

125. Service, U. P. H. Toxicological profiles for alpha-, beta-, and gamma-, and delta-hexachlorocyclohexane. *Agency Toxic Subst. Dis. Regist. US ...* 173–176 (2005).

126. Naidu, N. V, Smith-Baker, C. & Yakubu, M. A. Analysis of lindane and metabolites by HPLC-UV-Vis and MALDI-TOF . *FASEB J.* (2012).

127. Lunn, G. *HPLC Methods for Recently Approved Pharmaceuticals*. *HPLC Methods for Recently Approved Pharmaceuticals* (2005). doi:10.1002/0471711683

128. Cannella, D. *et al.* Light-driven oxidation of polysaccharides by photosynthetic pigments and a metalloenzyme. *Nat. Commun.* (2016). doi:10.1038/ncomms11134

129. Morozova, O. V., Shumakovich, G. P., Shleev, S. V. & Yaropolov, Y. I. Laccase-mediator systems and their applications: A review. *Appl. Biochem. Microbiol.* (2007). doi:10.1134/S0003683807050055

130. Christopher, L. P., Yao, B. & Ji, Y. Lignin biodegradation with laccase-mediator

systems. *Frontiers in Energy Research* (2014). doi:10.3389/fenrg.2014.00012

131. Rybak, A. P., Bristow, R. G. & Kapoor, A. Prostate cancer stem cells: Deciphering the origins and pathways involved in prostate tumorigenesis and aggression. *Oncotarget* (2015). doi:10.18632/oncotarget.2953

132. Bishop, J. L., Thaper, D. & Zoubeidi, A. The multifaceted roles of STAT3 signaling in the progression of prostate cancer. *Cancers* (2014). doi:10.3390/cancers6020829

133. Guanizo, A. C., Fernando, C. D., Garama, D. J. & Gough, D. J. STAT3: a multifaceted oncoprotein. *Growth Factors* (2018). doi:10.1080/08977194.2018.1473393

134. Cocchiola, R. *et al.* Analysis of STAT3 post-translational modifications (PTMs) in human prostate cancer with different Gleason Score. *Oncotarget* (2017). doi:10.18632/oncotarget.17245

135. Gordetsky, J. & Epstein, J. Grading of prostatic adenocarcinoma: Current state and prognostic implications. *Diagnostic Pathology* (2016). doi:10.1186/s13000-016-0478-2

136. Yu, L., Chen, X., Wang, L. & Chen, S. The sweet trap in tumors: Aerobic glycolysis and potential targets for therapy. *Oncotarget* (2016). doi:10.18632/oncotarget.7676

137. Gentric, G., Mieulet, V. & Mechta-Grigoriou, F. Heterogeneity in Cancer Metabolism: New Concepts in an Old Field. *Antioxidants and Redox Signaling* (2017). doi:10.1089/ars.2016.6750

138. Movafagh, S., Crook, S. & Vo, K. Regulation of hypoxia-inducible Factor-1a by reactive oxygen species: New developments in an old debate. *Journal of Cellular Biochemistry* (2015). doi:10.1002/jcb.25074

139. Dayton, T. L., Jacks, T. & Vander Heiden, M. G. PKM 2, cancer metabolism, and the road ahead . *EMBO Rep.* (2016). doi:10.15252/embr.201643300

140. Gui, D. Y., Lewis, C. A. & Vander Heiden, M. G. Allosteric Regulation of PKM2 Allows Cellular Adaptation to Different Physiological States. *Sci. Signal.* (2013). doi:10.1126/scisignal.2003925

141. Ubonprasert, S. *et al.* A flap motif in human serine hydroxymethyltransferase is important for structural stabilization, ligand binding, and control of product release. *J. Biol. Chem.* (2019). doi:10.1074/jbc.RA119.007454